

Antenna Reduction Techniques in MIMO Systems and Ad-Hoc Networks

A thesis submitted to the University of
Manchester for the degree of PhD in the
Faculty of Engineering and Physical
Sciences

September 2012

GEORGIOS SPYRIDAKIS
SCHOOL of ELECTRICAL AND ELECTRONIC
ENGINEERING

Table of Contents

Table of Contents.....	2
Table of Figures	5
List of Tables.....	8
List of abbreviations	9
List of Notations and Operators	11
Abstract.....	13
Declaration of Originality	15
Copyright Statement	16
Acknowledgement.....	17
Chapter 1	18
Introduction	18
1.1 Motivation	18
1.2 Aims and Objectives	19
1.2 Structure of this thesis	21
Chapter 2	22
Background Material	22
2.1 Channel Characterisation	24
2.1.1 AWGN channel	24
2.1.2 Rayleigh channel	25
2.1.3 Multipath channel.....	25
2.2 Multiple Access Schemes.....	28
2.2.1 Duplex Systems	28
2.2.2 Frequency Division Multiple Access Scheme (FDMA)	29
2.2.3 Time Division Multiple Access Scheme (TDMA)	30
2.2.4 Hybrid TDMA-FDMA	31
2.2.5 Code Division Multiple Access Scheme (CDMA)	32
2.3 Spatial Modulation	33
2.3.1 System Model	34
2.4 Simultaneous Spatial Modulation	36
2.4.1 System Model	38
2.5 Dual Polarised Antennas	40
2.5.1 Channel Model.....	41
2.5.2 ML Detector	42
2.5.3 Linear Least Squares Estimation (LLSE) Detector	43
2.5.4 Inverse Channel Detector (ICD).....	44
2.6 Precoding Techniques.....	44
2.6.1 Channel Inversion Precoding.....	46
2.6.2 Selective Channel Inversion Precoding	46
2.7 Cooperative Communication	50
2.7.1 Cooperative Transmission Protocols	52
Chapter 3	56
Code Shift Keying Modulation.....	56
3.1 Introduction.....	57
3.2 Spatial Modulation	59
3.3 Code Shift Keying Modulation in a SISO system.....	61
3.3.1 Code Index Estimation.....	62

3.3.2 Example: 3 bits Space Shift Keying Modulation using 1x1 antenna configuration and 4 orthogonal spreading codes	63
3.4 Improved Code Shift Keying Modulation in a SISO system.....	66
3.4.1 Code Index Estimation.....	67
3.4.2 Example: 3 bits Space Shift Keying Modulation using 1x1 antenna configuration and 2 orthogonal spreading codes and 2-ASK modulation.....	68
3.5 Complexity Estimation	70
3.6 Code Shift Keying Modulation and Improved Code Shift Keying Modulation in a SIMO system.....	71
3.7 Analytical SER Calculation for Code Shift Keying Modulation and Improved Code Shift Keying Modulation	72
3.7.1 Analytical SER of the Transmitted Symbol Estimation Process.....	73
3.7.2 Analytical Error Calculation of the Orthogonal Spreading Code Estimation Process in Code Shift Keying Modulation	73
3.7.3 Analytical Error Calculation of the Orthogonal Spreading Code Estimation Process in Improved Code Shift Keying Modulation	77
3.8 Numerical Simulation.....	79
3.9 Summary	93
Chapter 4	95
Polarization Assisted Space Shift Keying Modulation	95
4.1 Introduction.....	96
4.2 Basics of the PASSK Technique	97
4.2.1 Polarisation Index Estimation.....	98
4.2.2 Case study	100
4.3 Complexity Estimation.....	102
4.4 Numerical Simulation.....	103
4.5 Summary	110
Chapter 5	111
Precoded Polarization Assisted SSK	111
5.1 Introduction.....	112
5.2 The PPASSK Technique	113
5.2.1 Polarisation Index Estimation.....	114
5.2.2 Example: 3 bits Elimination of Cross Polarisation Effects in PPASSK	117
5.2.3 Example: 3 bits Exploitation of Cross Polarisation Effects	119
5.3 Complexity Estimation	121
5.4 SINR of Precoded PASSK.....	122
5.4.1 SINR for Elimination of Cross Polarisation Effects in Precoded Polarisation Assisted Space Shift Keying Modulation.....	122
5.4.2 SINR for Exploitation of Cross Polarisation Effects in Precoded Polarisation Assisted Space Shift Keying Modulation.....	123
5.5 Numerical Simulation.....	125
5.6 Summary	135
Chapter 6	137
Network Coding Techniques and Code Shift Keying Modulation	137
6.1 Introduction.....	138
6.2 Collaborative Codes	141
6.3 Existing Network Coding Technique and Proposed Modification	143
6.3.1 Loop Coding Scheme	143
6.3.2 Proposed Approach based on Collaborative Codes	145

6.4 Outage analysis.....	148
6.4.1 Outage Analysis of three users without network coding.....	148
6.4.2 Outage Analysis of three users with network coding	150
6.5 Network Coding and Code Shift Keying Modulation.....	153
6.5.1 Example of four Orthogonal Spreading Codes in three bits Transmission rate.	155
6.6 Numerical Simulation.....	157
6.7 Summary	163
Chapter 7	164
Conclusions and Future work	164
7.1 Conclusions.....	164
7.2 Future Work.....	165
A.1 Gray Coding.....	176
A.2 Useful Distributions	177
A.2.1 The Gaussian Distribution	177
A.2.2 The Rayleigh Distribution	178
A.3. The Q Function	179
A.4 Bit Error Rate Analysis	180
A.4.1 Bit Error Rate Analysis for BPSK modulation in AWGN	180
A.4.2 Bit Error Rate Analysis for BPSK modulation in Rayleigh.....	183
A.4.3 Monte Carlo Simulation of Communication Systems.....	184

Table of Figures

Fig. 2.1: Frequency Division Multiplexing System.....	30
Fig. 2.2: Time Division Multiplexing System.....	31
Fig. 2.3: Hybrid Time and Frequency Division Multiplexing	32
Fig. 2.4: Code Division Multiplexing System	32
Fig. 2.5 Areas (red striped one) that the received symbol should lie in for the interference to be constructive.	49
Fig. 2.6 Cooperative Transmission at the Base Station	51
Fig. 3.1 Spatial Modulation in a MIMO 4x4 system.	60
Fig. 3.2 Received vector \mathbf{g}	65
Fig. 3.3 Received vector \mathbf{g}	69
Fig. 3.4 Order statistics pdfs for four random variables when SNR is 15 dB..	76
Fig. 3.5 Order statistics pdfs for three random variables in Improved Code Shift Keying Modulation when SNR is 15dB.	78
Fig. 3.6 Comparison between Analytical and Simulation BER of CSK over AWGN in 3 bits transmission rate and 4 spreading codes available	80
Fig. 3.7 Comparison between Analytical and Simulation BER of Improved CSK over AWGN in 3 bits transmission rate and 2 spreading codes available	81
Fig. 3.8 Performance comparison between CSK in a SIMO system and the conventional Spatial Modulation, MMRC and V-BLAST MMSE	82
Fig. 3.9 Performance comparison between the proposed and spatial	83
modulation when transmission rate is 5 bits per period of interest.....	83
Fig. 3.10 Performance comparison in Code Shift Keying Modulation when the number of available codes varies and the transmission rate remains the same (5 bits per time slot) in an ideal channel scenario.	84
Fig. 3.13 Performance comparison between the Improved and the conventional CSK when transmission rate is 3 bits per period of interest.....	87
Fig. 3.14 Performance comparison in Code Shift Keying Modulation when the number of available codes varies and the transmission rate remains the same in an ideal channel scenario.....	88
Fig. 3.15 Performance comparison between the Improved and the conventional CSK when transmission rate is 4 bits per period of interest. Net spreading level of the Improved CSK scheme is half the size of the conventional CSK scheme.	89
Fig. 3.16 Performance comparison between the Improved and the conventional CSK when transmission rate is 4 bits per period of interest. Number of receive antennas is one in both systems.....	90
Fig. 3.17 Performance comparison between the Improved and the conventional CSK when transmission rate is 4 bits per period of interest....	91
Fig. 3.18 Throughput results in CSK modulation when the number of available spreading codes is four and eight respectively in an ideal channel scenario .	92
Fig. 3.19 Throughput results in CSK and Improved CSK modulation when the number of available spreading codes is 4 and 2 respectively in a flat Rayleigh fading channel scenario.	93
Fig. 4.1 2x2 MIMO system consisted of one dual polarised transmitter antenna and one dual polarised receiver antenna (H: horizontally, V: vertically polarised)	99

Fig. 4.2 Performance comparison between the proposed and SM when transmission rate is 3 bits per symbol.....	104
Fig. 4.3 Performance comparison in PASSK when the number of available polarisations is 2 and the transmission rate varies in a Flat Rayleigh fading channel scenario.....	105
Fig. 4.4 Performance comparison in PASSK when the transmission bit rate number varies and the available polarisations are 2 in a Ricean channel scenario and $K=10$	106
Fig. 4.5 Performance comparison between PASSK when the transmission rate varies and the available polarisations are 2 in a ricean channel scenario when the k-factor is 20.....	107
Fig. 4.6 Performance comparison between the PASSK and Spatial Modulation at different levels of cross-polarisation effects and when transmission rate is 3 bits per period of interest. The system is MIMO 2x4 in all cases	108
Fig. 4.7 Throughput results in PASSK modulation in three and four bit transmission rate when the channel is Ricean ($K=20$)	109
Fig. 5.1 Performance comparison between Precoded PASSK, PASSK, the conventional SM, MMRC and V-BLAST MMSE when the number of available polarisations is 2 and the transmission rate is 3 bits, in a Flat Rayleigh fading channel scenario. The MIMO system is 2x4 in all cases.....	126
Fig. 5.2 Performance comparison between PPASSK and PASSK when α is 0.9 and 0.1 respectively.	127
Fig. 5.3 Performance comparison between PPASSK when transmission rate is 3 and 5 bits respectively in a Flat Rayleigh Fading Channel. Cross-polarisation effects are eliminated.....	128
Fig. 5.4 Performance comparison between the proposed scheme and PASSK as well as the conventional SM, MMRC and V-BLAST MMSE. Transmission rate is 3 bits.....	129
Fig. 5.5 Performance comparison between the proposed scheme when cross polarisation effects are either eliminated or exploited. Transmission rate is 3 bits	130
Fig. 5.6 Performance comparison of PPASSK for several values of the alpha factor.....	131
Fig. 5.7 Performance comparison between the proposed scheme and PASSK when the transmission rate is 3 bits.	131
Fig. 5.8 Performance comparison of the proposed scheme when transmission rate is 3 and 5 bits respectively in a Flat Rayleigh Fading Channel.	132
Fig. 5.9 Throughput results in Precoded PASSK modulation when the cross polarisation effects are either eliminated or exploited	133
Fig. 5.10 SINR per received symbol in Precoded PASSK when cross polarisation effects are eliminated.....	134
Fig. 5.11 SINR per received symbol in Precoded PASSK when cross polarisation effects are exploited.....	135
Fig. 6.1 Network coding when 3 users are attempting to access the relay. .	144
Fig. 6.2 When 3 users are trying to access the relay using network coding. No other communication path exists but through the relay station	150
Fig. 6.3 Network Coding and Code Shift Keying Modulation in an Ad-Hoc Network of two users and a relay antenna.....	154

Fig. 6.4 Outage Probability when 3 users are trying to access the relay using network coding as well as using no network coding. No other communication path exists but through the relay station	157
Fig. 6.5 Performance comparison using BPSK modulation	158
Fig. 6.6 Performance comparison using BPSK modulation of 3 and 5 users respectively that are managing to access the relay station.....	160
Fig. 6.7 Performance comparison using BPSK modulation of 3 users for Amplify and Forward as well as Decode and Forward Transmission protocol.	161
Fig. 6.8 Performance comparison of Network Coding CSK scheme with the simple CSK scheme that is employed at the relay station so as to forward the bits to the destinations.	162
Fig. A.1 Gaussian Distribution for various values of mean and variance.	178
Fig. A.2 Rayleigh Distribution for various values of variance.	179
Fig. A.3 The Q function	180
Fig. A.4 BPSK symbols and conditional probability in the existence of AWGN	182

List of Tables

Table 1 Mapping table for Spatial Modulation	35
Table 2 Mapping table for Simultaneous Spatial Modulation	37
Table 3 Mapping table for Simultaneous Spatial Modulation	38
Table 4 Mapping table for Simultaneous Spatial Modulation	48
Table 5 Mapping table for Code Shift Keying Modulation	62
Table 6 Mapping table for Improved Code Shift Keying Modulation	67
Table 7 Mapping table for Polarisation Assisted Shift Keying Modulation.....	98
Table 8 Mapping Table for Precoded Polarisation Assisted Shift Keying Modulation	114
Table 9 Polarisation index estimation in Precoded Polarisation Assisted Shift Keying Modulation	117
Table 10 Codewords of three-code CCMA system	142
Table 11 Three user CCMA scheme.....	143
Table 12 Throughput for various numbers of users	147
Table 13 Time slots consumed for various numbers of users when relay forwards information at the destination	147
Table 14 Three user CCMA scheme.....	151

List of abbreviations

AAF	Amplify and Forward
ASK	Amplitude Shift Keying
AWGN	Additive White Gaussian Noise
BER	Bit Error Rate
BLAST	Bell Laboratories Layered Space Time
BLER	Block Error Rate
BPSK	Binary Phase Shift Keying
BS	Base Station
CCMA	Collaborative Coding Multiple Access
CDMA	Code Division Multiple Access
CI	Channel Inversion
CRC	Cyclic Redundancy Check
CSI	Channel State Information
CSK	Code Shift Keying
DAF	Decode and Forward
DPC	Dirty Paper Coding
DS-CDMA	Direct Sequence CDMA
FDMA	Frequency Division Multiple Access
FH-CDMA	Frequency Hopping CDMA
GSM	Global System for Mobile communications
ICD	Inverse Channel Detector
ICI	Inter Channel Interference
ISI	Inter Symbol Interference
LLSE	Linear Least Square Error
LOS	Line of Sight
MIMO	Multiple Input Multiple Output
ML	Maximum Likelihood
MLD	Maximum Likelihood Detector
MMSE	Minimum Mean Square Error
MMRC	Maximal Ratio Receiver Combining
MU	Mobile Unit
OFDMA	Orthogonal Frequency Division Multiple Access
PASSK	Polarisation Assisted Space Shift Keying
PDC	Personal Digital Cellular
PDF	Probability Density Function

PPASSK	Precoded Polarisation Assisted Space Shift Keying
PSK	Phase Shift Keying
QPSK	Quadrature Phase Shift Keying
QAM	Quadrature Amplitude Modulation
RCI	Regularised Channel Inversion
RSCI	Regularised Selective Channel Inversion
SCI	Selective Channel Inversion
SD	Sphere Decoding
SER	Symbol Error Rate
SINR	Signal to Interference Noise Ratio
SM	Spatial Modulation
SNR	Signal to Noise Ratio
SSM	Simultaneous Spatial Modulation
STC	Space Time Coding
TDMA	Time Division Multiple Access
USDC	United States Digital Communications
V-BLAST	Vertical-Bell Laboratories Layered Space-Time
XOR	Exclusive Or Logical Operation
ZF	Zero Forcing

List of Notations and Operators

Matrix Notations

\mathbf{XY}	Matrix multiplication
$\mathbf{X} \circ \mathbf{Y}$	Element-wise matrix multiplication
\mathbf{X}^T	Transpose of matrix \mathbf{X}
\mathbf{X}^H	Hermitian of matrix \mathbf{X}
$\text{Re}\{\mathbf{X}\}$	Real part of matrix \mathbf{X} with complex elements
$\text{Im}\{\mathbf{X}\}$	Imaginary part of matrix \mathbf{X} with complex elements
$[\mathbf{X}]_k$	Column k of matrix \mathbf{X}
$[\mathbf{X}]_{k,u}$	Element of u -th row and k -th column of matrix \mathbf{X}
$\text{diag}(\mathbf{X})$	Diagonal of matrix \mathbf{X} / Matrix containing the elements of vector \mathbf{X} on its diagonal and zeros elsewhere
$\text{sum}(\mathbf{X})$	Sum of the elements of each column of matrix \mathbf{X} / Sum of the elements of vector \mathbf{X}
\mathbf{X}^{-1}	Inverse matrix of matrix \mathbf{X}
$\ \mathbf{X}\ ^2$	Norm of matrix \mathbf{X}
$\det(\mathbf{X})$	Determinant of matrix \mathbf{X}

Scalar/Function/Variable Notations

$\text{Re}\{x\}$	Real part of complex number x
$\text{Im}\{x\}$	Imaginary part of complex number x
x^*	Conjugate of complex number x

$E_{p,q}\{x(p,q\dots)\}$	Expectation of x with respect to (w.r.t.) p,q
$var(x)$	Variance of x
$P(x)$	Probability density function (pdf) of x
$p(x)$	Probability of x
$ x $	Absolute value of x
$x!$	Factorial of x
$\log_2(x)$	Logarithm of x with base 2
$\text{mod}_\tau(x)$	Modulo of x with base τ
\bar{x}	Average of x
$x[t]$	Discrete sampled function x
$x(t)$	Continuous function x

Abstract

In this thesis, an antenna reduction technique in Multiple Input Multiple Output (MIMO) systems, which is called Code Shift Keying (CSK) Modulation, is introduced. With the use of Walsh Hadamard orthogonal spreading codes, we overcome the biggest drawback of conventional Spatial Modulation (SM) which is the antenna index estimation errors due to channel correlation. Also SM fails to perform in non normalised channel conditions. The combination of orthogonal spreading codes and antenna devices, as a means to convey information at the receiver, results in a remarkable performance improvement at the receiver.

Moreover, an improved scheme that uses half the amount of spreading codes so as to represent the total number of information bits has been introduced leading to an important reduction in bandwidth usage. By maintaining the net spreading levels of the system we attain remarkable performance improvements.

A technique called Polarisation Assisted Space Shift Keying Modulation (PASSK) has also been proposed which manages to exploit the polarisation domain and it is able to outperform the conventional SM technique as well as the Maximal Ratio Receiver Combine (MRRC) and Vertical-Bell Laboratories Layered Space-Time (V-BLAST) schemes. A new precoding scheme that manages to either eliminate or exploit the cross polarisation effects has also been proposed as a complementary study of the PASSK scheme.

As modern and future communications show a rising demand for higher data transmission rates, network coding is increasingly incorporated in wireless communication standards. In harmonisation with this trend, this thesis discusses the main state-of-art network coding schemes. The contribution here includes a number of innovative schemes that are able to further increase throughput. Finally, the employment of network coding is discussed in conjunction with CSK Modulation resulting to further improvement in terms of throughput as well as Bit Error Rate (BER) performance at the cost of increased bandwidth usage.

Declaration of Originality

I hereby declare that no portion of the work referred to in the thesis has been submitted in support of an application for another degree or qualification of this or any other university or other institute of learning.

Georgios Spyridakis

Copyright Statement

The author of this thesis (including any appendices and/or schedules to this thesis) owns any copyright in it (the “Copyright”) and he has given The University of Manchester the right to use such Copyright for any administrative, promotional, educational and/or teaching purposes.

Copies of this thesis, either in full or in extracts, may be made only in accordance with the regulations of the John Rylands University Library of Manchester. Details of these regulations may be obtained from the Librarian. This page must form part of any such copies made.

The ownership of any patents, designs, trade marks and any and all other intellectual property rights except for the Copyright (the “Intellectual Property Rights”) and any reproductions of copyright works, for example graphs and tables (“Reproductions”), which may be described in this thesis, may not be owned by the author and may be owned by third parties. Such Intellectual Property Rights and Reproductions cannot and must not be made available for use without the prior written permission of the owner(s) of the relevant Intellectual Property Rights and/or Reproductions.

Further information on the conditions under which disclosure, publication and exploitation of this thesis, the Copyright and any Intellectual Property Rights and/or Reproductions described in it may take place is available from the Head of School of Electrical and Electronic Engineering (or the Vice-President).

Acknowledgement

I would like to express my thanks to my supervisor Dr Emad Alsusa for his valuable guidance and observations. I would also like to thank my parents for their continued support and endless love through my life.

Chapter 1

Introduction

1.1 Motivation

Robust communication as well as increased throughput over fading channels has always been a challenge for the designers of digital communication systems. Therefore, a new generation of cellular standards has appeared approximately every decade since 1G systems were introduced in 1981/1982. Each generation is characterised by new frequency bands, higher data rates and non backwards compatible transmission technology. The available frequencies for these systems amid increasingly demands of modern applications are remarkably limited, and thus it would be appropriate to be exploited at an optimal level.

A promising and efficient approach would be the exploitation of spatial diversity by using more than one antenna at the receiver and transmitter so as to forward the desired information at the destination using the same frequency bands. It is shown that a great number of theoretical capacities could be achieved in a wireless channel when multiple antennas are used both at the source and destination. It would be a remiss not to mention that performance is better in MIMO systems than in systems that employ only one antenna device. However, simultaneous transmission on the same frequency from multiple transmitting antennas causes high Inter Channel Interference (ICI). In

order to mitigate this problem, high complexity algorithms need to be applied at the receiver so as to recover the signal in a robust way. Thus, high amounts of energy need to be consumed so as to process the received signal and considering the case of Mobile Units (MU) (power limited devices), this is a big burden. It is, therefore, necessary to investigate and develop different approaches on how to use multiple antenna transmission without losing the basic advantages of MIMO techniques. SM is a well promising technique for attaining this goal.

Another approach that could help achieve exploitation of frequencies is Network Coding. Since it was introduced [1], it has encouraged great research efforts in the computer networking and communication communities.

As such both approaches have recently attracted significant attention, since there has been a plethora of different algorithms that have been utilised throughout the last decade. Near future tends to be quite promising for further enhancement in the performance of the existing schemes. Moreover, this area tends to be somewhat challenging because of the continual developments in data transferring in contrast to the available limited bandwidth that is being provided.

1.2 Aims and Objectives

The ultimate aim of this research has been to develop new techniques for the improvement of the BER performance of modern cellular wireless communications and specifically MIMO systems and ad-hoc networks. The focus has been on error rate reduction schemes towards improving the quality

of service in wireless communications, along with the increase in throughput of the overall system.

The approach adopted throughout this research project followed a path of intermediate objectives mainly consisting of

- Reviewing the existing literature on SM, Dual Polarised Antennas and Network Coding attaining a good understanding of the main detection techniques, their function and weaknesses.
- Find ways to increase capacity in a system, which uses a distributed antenna system as the exclusive way for the sources to communicate amongst them. The existing Network Coding scheme is able to accommodate only two sources.
- Outage analysis of a system that uses Network Coding and a system that does not use any Network Coding scheme.
- Attempt to overcome the main weaknesses of conventional SM, which are the antennas index estimation due to channel correlation and failure to function in non normalised channel conditions.
- Investigating and evaluating the cross polarization effects inherent in dual Polarised Antennas, analysing these effects and establishing ways to either eliminate or exploit so as to contribute to the useful signal
- Designing innovative transmitter-based MIMO methods for uplink and downlink communications towards the simplification of MU that can outperform existing schemes.

1.2 Structure of this thesis

In this thesis, Chapter 2 introduces SM, dual polarised antennas, various types of detectors and the most important precoding techniques at the transmitter. It also presents the basics of network coding, Collaborative Codes and Cooperative Communication. Chapter 3 proposes a novel approach that stems its existence from SM, but this time orthogonal spreading codes and not the antennas carry information along with the transmitted signal. This new technique is called CSK Modulation. Chapter 4 introduces Polarization Assisted Space Shift Keying Modulation. Chapter 5 discusses the elimination and exploitation of cross polarization effects that are experienced in dual polarised antennas. Chapter 6 proposes how Network Coding can be combined with CSK Modulation in an ad-hoc network. Finally, Chapter 7 summarises and concludes the proposed schemes.

Chapter 2

Background Material

It is well known that high spectral efficiency can be attained by the use of multiple antenna techniques. However, simultaneous transmission on the same frequency from multiple transmitting antennas causes high Interchannel Interference (ICI). In order to mitigate this problem, high complexity algorithms need to be applied at the receiver so as to fully recover the signal. Thus, high amounts of energy need to be used, so as to process the received signal and considering the case of MU (power limited devices), this is a big burden. It is, therefore, necessary to investigate and develop different approaches on how to use multiple antenna transmission without losing the basic advantages of MIMO techniques.

SM is a recently developed approach that manipulates this problem and is able to attain zero levels of ICI. Besides that, the need of synchronisation between antennas is avoided since only one antenna transmits at any time instant. The antenna index is employed as source of information as well as the transmitted signal. In more details, a single valued signal, for example, a pure sinusoidal frequency carrier signal transmitted from an antenna of an antenna array conveys actual information, provided that the receiver can detect where the actual signal originated from. Thus, the detection process, in the case of more complex signals, requires two different steps. The first one is

the transmit antenna estimation and the second one is the transmit symbol estimation.

The employment of dual-polarised antennas would be a promising cost- and space-effective technique and would help improving the above approach in SM by making more than one antenna to send information at the same time without increasing the levels of ICI since antennas transmit in two different orthogonal polarizations. Although, in practice there are still some levels of interference but by precoding at the transmitter (Base Station), this type of interference can be exploited. It is known that the current trend is to maintain a simple architecture at the MU for reasons of manufacturing cost.

Dual-polarised antennas are mainly preferred when large antenna spacing, that is required to achieve significant multiplexing gain, is not desirable by the size of the transmitter and receiver devices. Therefore, two spatially separated uni-polarised antennas are replaced by a single antenna structure employing orthogonal polarizations. The richness of scattering is also an important factor that contributes to the performance of a MIMO system and dual polarised antennas are mainly preferred when the channel is not rich enough.

This chapter is organised as follows: Channel Characterisation, Multiple Access Schemes, SM as well as Simultaneous SM Section provides a brief and concise synopsis of the important concepts. Dual polarised antennas are introduced as well as precoding schemes at the transmitter so as to exploit the existing levels of ICI. Finally, the basics of Network Coding, Collaborative Codes and Cooperative Communication will be discussed in this chapter.

2.1 Channel Characterisation

The channel, which is available for the transmission of bits, can be classified as the most significant part of a communication system. Signal is distorted and its power is degraded because of the channel characteristics and based on these characteristics we can determine all the standards and conditions in communications.

In effect, the existence of the channel and its properties is the motivation for the existing research so as to optimise communication between a source and a destination. If the signal could have been forwarded in a way such that no distortion or degradation could occur, then there would be no reason to try and come up with strategies to enhance the communication link.

2.1.1 AWGN channel

The only distortion that is experienced in this channel is due to thermal noise that degrades the signal due to receiver circuitry. The received signal can be expressed as follows

$$r = x + n \quad (2.1)$$

where r is the received signal, x is the signal prior to transmission and n is a Gaussian random variable [2].

2.1.2 Rayleigh channel

Rayleigh fading is a statistical model for the effect of propagation environment on a radio signal, such as that used by wireless devices. Rayleigh fading models assume that the magnitude of a signal that has passed through such a communications channel will vary randomly, or fade, according to a Rayleigh distribution (see Appendix A.2.2) — the radial component of the sum of two uncorrelated Gaussian random variables.

Rayleigh fading is viewed as a reasonable model for tropospheric and ionospheric signal propagation as well as the effect of heavily built-up urban environments on radio signals. Rayleigh fading is most applicable when there is no dominant propagation along a line of sight between the transmitter and receiver. If there is a dominant line of sight, Rician fading may be more applicable [3].

2.1.3 Multipath channel

In the case of wireless channels, the signal can be propagated through variable paths that are created from reflection occurring on surfaces, and dissipation through physical obstacles namely trees, buildings or ions in the ionospheric layers of the atmosphere when propagation between satellites happens. Because of these phenomena the signal is attenuated, phase shifted and dispersed. All these replicas of the useful signal that arrive at the destination act as interference and they cannot assist to recover the signal in

a more robust way. Therefore, it should be important to identify all the effects that happen during communication, so as to be able to detect the various paths and based on that knowledge to enhance the received signal once the levels of distortion will be familiar and thus easily compensated.

Each different path of the channel delays and attenuates the signal in its own way. Eventually these effects leave a fraction of the channel at the receiver. In mathematical terms the effects are represented by a complex number in which the amplitude denotes the amplitude attenuation of the signal and the phase of the complex number indicates the phase shifting of the desired signal.

The following equation depicts signal g that is propagated through the multipath channel.

$$r(t) = \sum_{p=1}^P (g(t - \tau_p) h_p(t)) + n \quad (2.2)$$

where P is the number of paths and h_p is the complex number that represents attenuation and phase shift that characterises each path. Finally, n is Additive White Gaussian Noise (AWGN) and τ_p is the time delay of the signal.

Five parameters characterise a communication channel.

1. Multipath Delay Spread T_m is the time difference between the first and the last ray of the multipath received signal
2. Coherence Bandwidth B_c is the maximum frequency difference where the signals are highly correlated. Practically speaking the signal in this frequency band experiences the same levels of distortion.

3. Channel Fading Rate R_c is the rate that the channel changes and it is mostly related to relative motion of the transmitter and the receiver.
4. Coherence Time T_c is the time in which channel remains constant and it is reciprocal to R_c .
5. Doppler Spread B_d is the signal bandwidth spread due to relative motion between the transmitter and receiver.

Considering the above parameters, communication channels can be classified as follows [3]

1. Flat Fading Channel is the case where $B_c > B_s$ where B_s is the signal bandwidth. Intuitively, all the spectral components face the same levels of distortion.
2. Frequency Selective Channel is the channel for which $B_c < B_s$ and thus the signal experiences different levels of distortion. In this scenario signal is corrupted by ISI and the latter one increases when the number of paths of the multipath increases.
3. Slow Fading Channel is the channel in which $T_c > T_s$, where T_s is the signal period and it means that signal faces constant distortion.
4. Fast Fading Channel is the channel in which $T_c < T_s$ and this means that the channel changes in less than a symbol period and thus the signal experiences different distortion.

2.2 Multiple Access Schemes

2.2.1 Duplex Systems

Duplex systems enable simultaneous transmission between Base Station (BS) and mobile station. Many communication networks make use of duplex systems so as to provide either a two-way path between the source and destination or to control a remote device in the field. There are some broadcast systems that do not employ this duplex capability since the source sends information and the destination eventually just receives it.

In a half-duplex system communication occurs in both ways not simultaneously but at two different time slots. In other words, when one of the devices is due for reception it starts receiving and it has to wait for the transmitter to stop sending information before responding back.

On the other hand in a full-duplex system communication happens at the same time with no collisions or other problems that might exist during simultaneous transmission and reception. Land-line telephone networks are full-duplex, since they allow both callers to speak and be heard at the same time.

When a communication system is employing a full-duplex system can be improved in various aspects. Firstly, there is no waste of time since no collisions do exist and thus no frames need to be sent again. Secondly, the two paths for transmission and reception are well separated and hence the full

capacity is achieved. Moreover, the various nodes can send and receive at any time slot without having to wait other nodes to finish transmission.

2.2.1.1 Emulation of full-duplex in shared physical data

The channel access methods that are bound to divide the physical medium for forward and reverse transmission are called as duplexing methods and these are:

- Frequency Division Duplexing: There exist two different frequency bands (simplex channels) for each user.
- Time Division Multiplexing: Forward and reverse channels are transmitted on the same frequency, but not the same time. Although, half-duplex in theory (two-way transmission, single direction at any one time), in practise it is perceived as full duplex due to the very high switching rate.

2.2.2 Frequency Division Multiple Access Scheme (FDMA)

In FDMA the total spectrum is divided into narrow channels L (see Fig. 2.1).

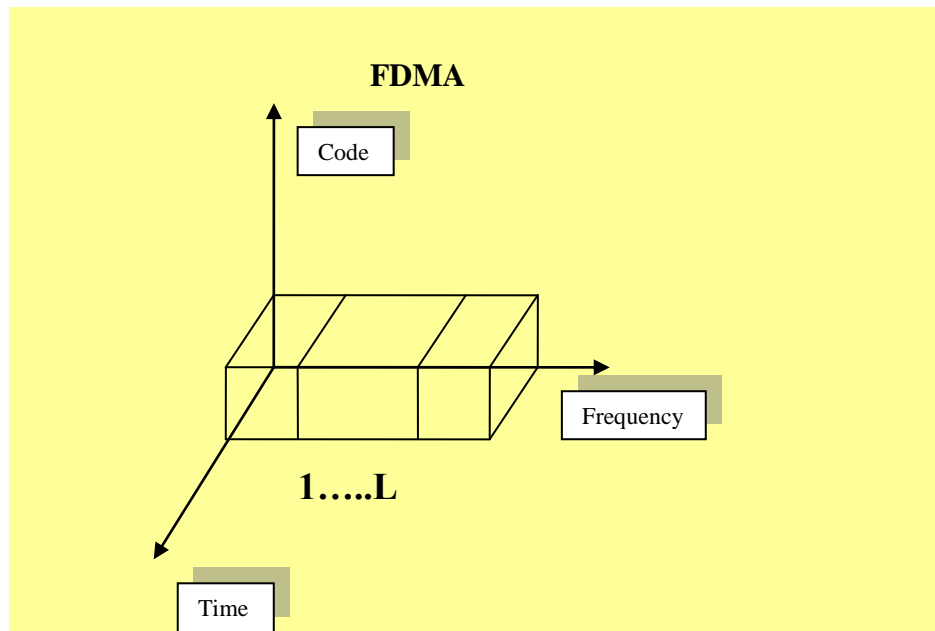


Fig. 2.1: Frequency Division Multiplexing System

Channels are temporarily allocated to users during transmission and they are used in traditional analogue systems. Moreover, they are characterised by simplicity as simple hardware is employed with band pass filters to isolate users. Finally, no timing or synchronisation is necessary and narrow bands imply flat fading and hence equalisers are not needed.

2.2.3 Time Division Multiple Access Scheme (TDMA)

In TDMA data is transmitted in L time slots (see Fig.2.2), which make up frames.

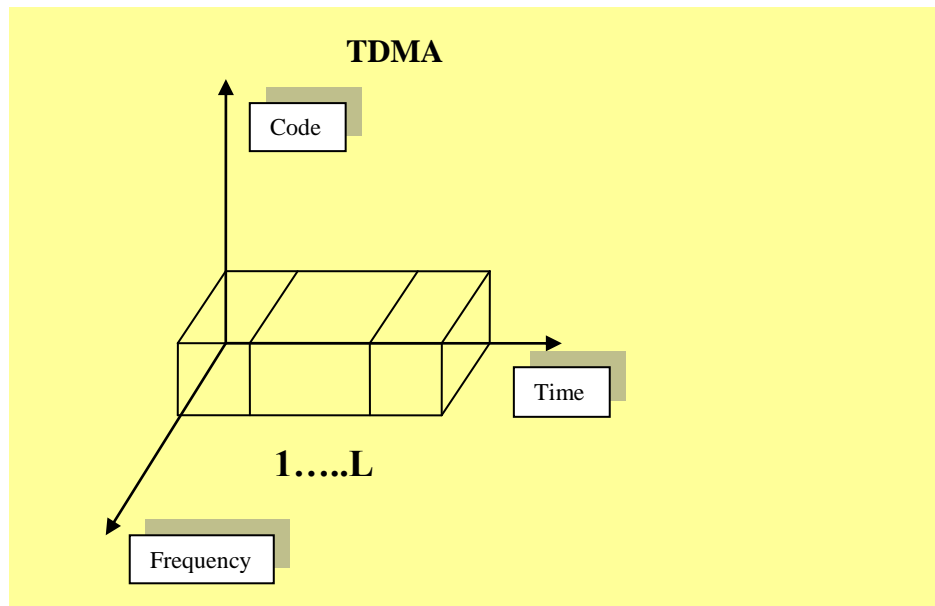


Fig. 2.2: Time Division Multiplexing System

At each different slot a guard time is added so as to cater for time inaccuracies due to clock instability, Delay Spread and Propagation Delay. This technique is bandwidth efficient once guards are not required between the channels. Nevertheless, time guards and synchronisation require large overheads and the flexible data rate that can be utilised, sometimes requires equalisation [2].

2.2.4 Hybrid TDMA-FDMA

In Hybrid TDMA-FDMA transmission occurs in bursts (see Fig.2.3), whereby each user is allocated part of the signal bandwidth for the duration of a burst. It can straightforwardly be concluded that capacity is highly increased because of the involvement of more users as both time and frequency are exploited simultaneously. Finally it is currently used in North American Digital Cellular (USDC), Global System for mobile communications (GSM) and Personal Digital Cellular (PDC).

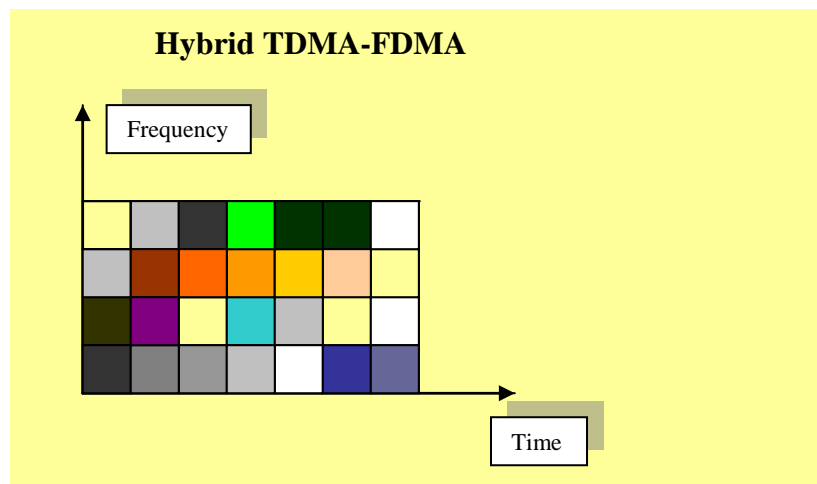


Fig 2.3: Hybrid Time and Frequency Division Multiplexing

2.2.5 Code Division Multiple Access Scheme (CDMA)

CDMA (see Fig. 2.4) was first used for military applications since spread spectrum is difficult to jam and detect [2],

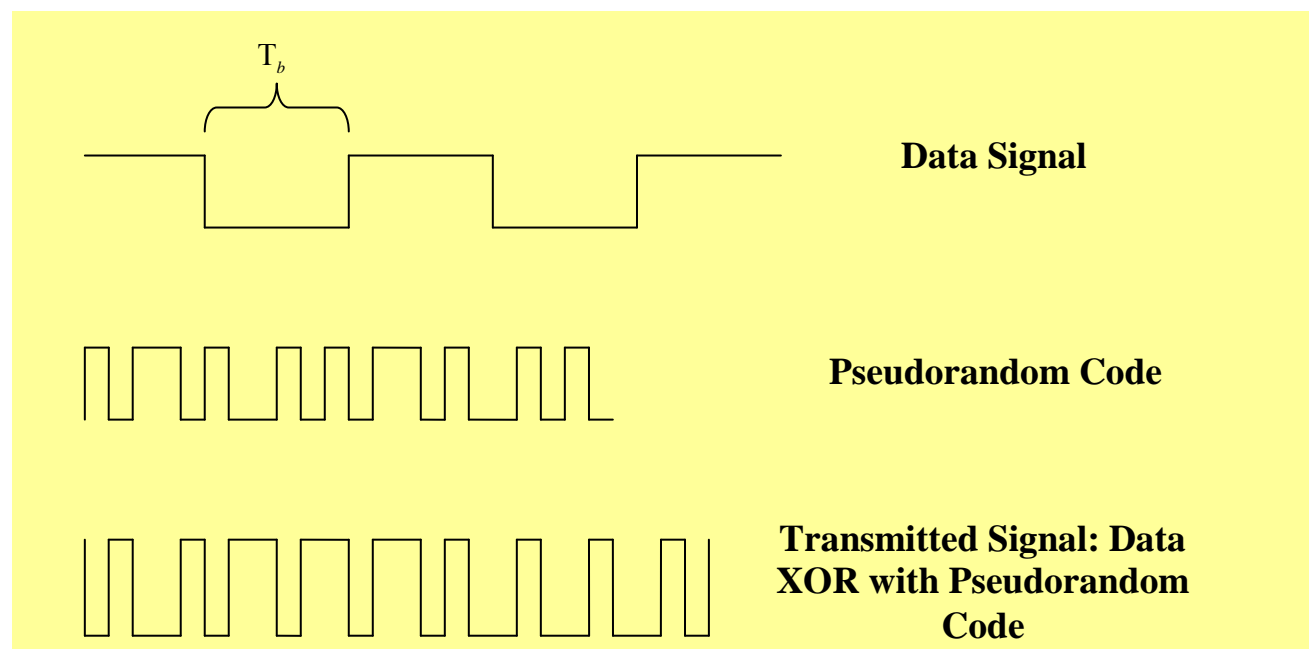


Fig. 2.4: Code Division Multiplexing System

where T_b is the signal period.

There are two different CDMA schemes.

- Frequency-Hopping CDMA (FH-CDMA): The spectrum is divided into a number of frequency bands. In this technique a channel is assigned upon demand by assigning each user a unique frequency-hopping sequence such that each segment of information is transmitted on a different frequency to the previous segment. Finally, no two users transmit using the same band at the same time along with the fact that the capacity of the system is a function of the number of unique hopping sequences that can be used.
- Direct Sequence CDMA (DS-CDMA): In this scheme the allocated frequency band is shared between multiple users at the same time. Although, users are separated by modulating their information by unique high bit rate code sequences. Codes are essentially uncorrelated (orthogonal). In this thesis we will mainly focus on this technique which is more popular in our nowadays systems compared to FH-CDMA.

2.3 Spatial Modulation

The rationale behind SM is that spatial domain is exploited as well as the information signal. In more details, multiple antennas are deployed as information carrying units along with the symbol designated to each antenna device. This symbol is derived from a constellation diagram. When multiple antennas are used it is well known that higher spectral efficiency is achieved

at the overall system. Receiver's complexity sharply falls when compared to Vertical-Bell Laboratories Layered Space-Time scheme (V-BLAST) [4].

Apart from the ICI, that deteriorates performance and thus it has to be traded-off with higher complexity at the receiver's side, there are other impediments encountered in the development of multiple antenna transmission schemes [5] - [8]. The source of these problems is the several transmit antennas that are applied, among which the following are:

- Synchronisation of transmit antennas is a difficult task and adds on system's complexity.
- For acceptable levels of performance in V-BLAST techniques it is required that the number of transmit antennas has to be at least the same as the number of receive antennas.

SM is a scheme that deals with these kinds of problems [6]-[10]. Firstly, one antenna transmits at a time. The antenna index partly contributes so as for the signal to be retrieved correctly at the receiver.

2.3.1 System Model

In this section, it will be attempted to illustrate how SM works. TABLE 1 will facilitate the illustration of this method.

TABLE 1 MAPPING TABLE FOR SPATIAL MODULATION

Input Bits	2 , 8QAM		4 , 4QAM		8 , BPSK	
	Antenna Number	Transmit Symbol	Antenna Number	Transmit Symbol	Antenna Number	Transmit Symbol
0000	1	j	1	1+j	1	1
0001	1	1+j	1	1-j	1	-1
0010	1	-1+j	1	-1+j	2	1
0011	1	1	1	-1-j	2	-1
0100	1	-1-j	2	1+j	3	1
0101	1	-j	2	1-j	3	-1
0110	1	-1	2	-1+j	4	1
0111	1	1-j	2	-1-j	4	-1
1000	2	j	3	1+j	5	1
1001	2	1+j	3	1-j	5	-1
1010	2	-1+j	3	-1+j	6	1
1011	2	1	3	-1-j	6	-1
1100	2	-1-j	4	1+j	7	1
1101	2	-j	4	1-j	7	-1
1110	2	-1	4	-1+j	8	1
1111	2	1-j	4	-1-j	8	-1

We have all the possible cases of 4 bits transmission. When one antenna is employed then a 16-Quadrature Amplitude Modulation (16-QAM) constellation signal will be used so as to map bits into symbols. In the case now that 2 antennas are deployed each antenna will be designated to transmit a lower constellation signal namely an 8-QAM. The map of bits to constellation symbols in the simulations follows the Gray coding (see Appendix A.1). When the number of antennas increases, the constellation order decreases. Thus, there is a trade-off between the number of antennas and the constellation

signal used. Apparently, any number of antennas can be used with any constellation signal.

As denoted in a previous subchapter the index of the antennas along with the signal will assist so as for the bits to be recovered at the destination. Therefore, there tends to appear two distinct sources of errors. The first one is when the antenna index is identified and the second is when the signal that this specific antenna has transmitted.

The only disadvantage of this method is the transmission rates that attains, when a large number of antennas and a high order constellation signal are applied, compared to V-BLAST. However, it is prohibitively complicated when a large amount of antennas is used according to the current standards in technology.

2.4 Simultaneous Spatial Modulation

Simultaneous SM [11] is a modification of the conventional SM which allows two antennas instead of one [4] to transmit at the same time. This leads to higher data rates and the fact that both antennas transmit simultaneously does not spoil the initial property of SM in which the antenna index as well as the signal transmitted carry information.

TABLE 2 would ease facilitation of this alternative technique that is called Simultaneous SM.

TABLE 2 MAPPING TABLE FOR SIMULTANEOUS SPATIAL
MODULATION

Input Bits	Antenna1	Antenna2
0000	1+j	0
0001	-1+j	0
0010	j	1
0011	j	-1
0100	1-j	0
0101	-1-j	0
0110	-j	1
0111	-j	-1
1000	1	j
1001	-1	j
1010	0	1+j
1011	0	-1+j
1100	1	-j
1101	-1	-j
1110	0	1-j
1111	0	-1-j

As can be seen, in this example each antenna is designated for the transmission of two of the 4 possible pairs of bits

$$Antenna1 = \left\{ \begin{pmatrix} 0 & 0 \\ 0 & 1 \end{pmatrix} \right\}$$

$$Antenna2 = \left\{ \begin{pmatrix} 1 & 0 \\ 1 & 1 \end{pmatrix} \right\}.$$

In the following subchapter we will explain in more details why this mapping is opted for.

Although, in this example by employing two antennas as information carrying units we can manage to send BPSK signal from each one when 4

bits rate per transmission takes place. In the conventional SM each of the two antennas would send an 8-QAM signal constellation and thus the modified technique shows performance superiority against the conventional one.

2.4.1 System Model

In this section we will discuss the mathematical system model of the SSM in the case of two transmitter and two receiver antennas and when two bits per transmission is employed. TABLE 3 explains the mapping process for the case of 2 bits rate transmission.

TABLE 3 MAPPING TABLE FOR SIMULTANEOUS SPATIAL MODULATION

Symbol	Antenna1	Antenna2
0 0	0	$1+j$
0 1	1	j
1 0	j	1
1 1	$1+j$	0

Based on the above mapping antenna number 2 will send the first bit from the first and second case and antenna number 1 will send the first bit from the third and fourth case of this table. In more details, the imaginary and the real domain are exploited and based on the symbols transmitted we realise which antenna has sent the respective bits so as to be recovered properly. The same happens in TABLE 7 where 4 bits rate transmission is used.

To elaborate on this more, it would be necessary to propose the mathematical model that lies behind this technique. Therefore the received signal at the destination is as follows:

$$\mathbf{r} = [A_1 \quad A_2] \mathbf{H} + \mathbf{n} \quad (2.3)$$

where A_1, A_2, \mathbf{H} and \mathbf{n} are the symbol for antenna number 1, symbol from antenna number 2, channel matrix and AWGN noise that has zero mean and σ^2 variance.

$$\mathbf{r} = [A_1 \quad A_2] \begin{bmatrix} h_{11} & h_{12} \\ h_{21} & h_{22} \end{bmatrix} + [n_1 \quad n_2]. \quad (2.4)$$

At the receiver we multiply the received signal with the conjugate of the channel

$$\begin{aligned} \mathbf{d} = \mathbf{r} \begin{bmatrix} h_{11} & h_{12} \\ h_{21} & h_{22} \end{bmatrix}^H &= [A_1(|h_{11}|^2 + |h_{12}|^2) + A_2(h_{21}h_{11}^* + h_{22}h_{12}^*) + N_1, \\ A_1(h_{11}h_{21}^* + h_{12}h_{22}^*) + A_2(|h_{21}|^2 + |h_{22}|^2) + N_2]. \end{aligned} \quad (2.5)$$

Based on these two elements, we are able to retrieve the antenna index as well as the symbol transmitted, as we can detect which antenna has sent the Imaginary symbols and which antenna has sent the Real ones. Throughout this thesis, the notation $(.)^H$ denotes Hermitian of a vector or a matrix respectively. The one that has sent the imaginary is transmitting the first bit and the other one is transmitting the second bit. As can be seen, there is some ICI once both antennas share the same bandwidth along with time slot.

It is easily conclusive that the correct detection of the signal is dependent on the correlation of the channels (ICI levels) and the noise element.

2.5 Dual Polarised Antennas

Space limitations are a significant factor that is considered when a MIMO system is designed. It is known that in order to achieve high multiplexing or diversity gain large antenna spacings are often necessary [12]. Moreover, the performance of these techniques relies on MIMO channel characteristics and these characteristics are dependent on the antenna height, spacing and the richness of scattering.

Dual polarised antennas devices are a means that would assist to overcome some of these characteristics of MIMO systems which deteriorate performance of physical antennas. Besides that, two physical antenna structures can be replaced by one dual polarised antenna that uses orthogonal polarisations and overcomes the necessity of large spacings when they are unattainable especially in small mobile devices. It is shown in [12] that in the case of spatial multiplexing dual antennas are preferred when scattering is not rich enough and they can achieve enhancements in terms of BER up to an order of magnitude. In the case of transmit diversity physical antennas are mainly preferred [12].

2.5.1 Channel Model

It is assumed a system with one dual polarised antenna at the transmitter and one dual polarised antenna at the receiver without loss of generality. The following equation represents the model of dual polarised antennas.

$$\mathbf{r} = \mathbf{x}\mathbf{H} + \mathbf{n} \quad (2.6)$$

where $\mathbf{x} = [x_1, x_2]$ is the transmitted symbol, $\mathbf{r} = [r_1, r_2]$ is the received signal, \mathbf{n} is the zero mean complex Gaussian noise and $\mathbf{H} = \begin{bmatrix} h_{11} & h_{12} \\ h_{21} & h_{22} \end{bmatrix}$ is the channel matrix.

In this matrix h_{ij} is the path that connects the i -th transmitter with the j -th receiver antenna. Practically speaking, two polarisation schemes are mostly used: horizontal/vertical ($0^\circ / 90^\circ$) or slanted ($45^\circ / -45^\circ$). It is also worth mentioning that symbols x_1 and x_2 are forwarded on the two different polarisations and r_1 , r_2 are the symbols received on the corresponding ones.

In this thesis we assume that $E\{|h_{11}|^2\} = E\{|h_{22}|^2\} = 1$, where h_{11} and h_{22} are the main paths that connect the antennas of the same polarisation and $E\{|h_{21}|^2\} = E\{|h_{12}|^2\} = a$, where h_{21} and h_{12} are the cross-polarised paths that have power $0 \leq a \leq 1$. This a denotes the separation of orthogonal polarisations and thus a small value of a leads to a good discrimination

between them. Ideally $a = 0$, but because of the level of scattering this value may change because of the coupling of the two polarisations.

It would be a remiss not to mention the level of scattering and if scattering is poor then paths will be highly correlated and vice-versa. Thus

$$t = \frac{E\{h_{11}h_{12}^*\}}{\sqrt{a}} = \frac{E\{h_{21}h_{22}^*\}}{\sqrt{a}} \quad (2.7)$$

and

$$z = \frac{E\{h_{11}h_{21}^*\}}{\sqrt{a}} = \frac{E\{h_{12}h_{22}^*\}}{\sqrt{a}} \quad (2.8)$$

where t and z are the transmit and receive correlation coefficients and these coefficients denote the richness of scattering of the channel environment.

Higher levels of enhancement performance are achieved with high levels of transmit correlation [12]. Therefore, in this thesis we will mainly deal with this level of correlation. It could be easily explained that in poor environments the cross-polarised paths do not offer any extra levels of diversity order once they are highly correlated with the auto polarised ones. Although, they cause ICI and this ICI tends to be eliminated when dual polarised antennas are deployed.

Moreover, when a line of sight path exists dual antennas can achieve even greater enhancements in terms of Symbol Error Rate (SER) regardless the richness of scattering.

2.5.2 Maximum Likelihood (ML) Detector

The ML Detector is the optimum detector once the probability of error is minimised. The noise terms at the receiving antennas are statistically

independent, identically distributed, zero mean Gaussian and therefore, joint conditional probability density function $P(y/s)$ is Gaussian. Hence, the detector opts for the symbol vector that minimises the Euclidean distance metric [2]

$$\mu(s) = \sum_{m=1}^{N_r} |y_m - \sum_{n=1}^{N_t} h_{nm} s_n|^2 \quad (2.9)$$

where N_r is the number of receive antennas and N_t is the number of transmit antennas.

2.5.3 Linear Least Squares Estimation (LLSE) Detector

This detector outputs the estimate

$$\hat{a} = Q(\hat{a}_{LLSE}) \quad (2.10)$$

where \hat{a}_{LLSE} is a linear estimator that is given by

$$\hat{a}_{LLSE} = \mathbf{W}\mathbf{r} \quad (2.11)$$

where \mathbf{W} is chosen to minimise the following

$$E\{\|\mathbf{W}\mathbf{r} - \mathbf{a}\|^2\} \quad (2.12)$$

Therefore, the LLSE estimator matrix is given by [13]

$$\mathbf{W} = \frac{\rho}{M} \mathbf{H}^* \left(\frac{\rho}{M} \mathbf{H}\mathbf{H}^* + N_o \mathbf{I}_N \right)^{-1} \quad (2.13)$$

where $\frac{\rho}{M}$ is the average received energy per bit at each receiver antenna, \mathbf{H}^* is the Hermitian Transpose of the channel matrix \mathbf{H} and \mathbf{I}_N is an $N \times N$ identity matrix.

2.5.4 Inverse Channel Detector (ICD)

This detector is a low complexity linear one that outputs

$$a = Q(\hat{a}_{ICD}) \quad (2.14)$$

where $\hat{a}_{ICD} = \mathbf{H}^+ \mathbf{r}$ (2.15)

and \mathbf{H}^+ denotes the Moore-Pseudoinverse of channel matrix \mathbf{H} which is a generalised inverse that exists even if \mathbf{H} is rank-deficient [13].

2.6 Precoding Techniques

In terms of signal enhancement schemes we could classify these methods based on the processing that takes place at the receiver, transmitter or both respectively. Hence, there are three main categories:

- MIMO detection schemes: In this category all the processing occurs at the receiver. The signal quality afterwards is enhanced as regards noise and interference has been remarkably mitigated. Zero Forcing (ZF) and Minimum Mean Square Error (MMSE)

linear detection, ML, Sphere Decoding (SD) and BLAST detection are the main involved ones in this category.

- MIMO precoding schemes: All the processing takes place at the transmitter. There are two main classes in this approach:

1. Linear Schemes: In this group we mainly have the Channel Inversion (CI) precoding, Selective Channel Inversion (SCI) precoding as well as the regularised Channel Inversion and regularised Selective Channel Inversion precoding.

2. Non linear Schemes: The Dirty Paper Coding (DPC) is the main scheme that falls in this group.

- MIMO schemes which require processing both at the transmitter and the receiver. These involve beam forming techniques and Space Time Coding (STC) schemes.

There is another categorisation of MIMO which would worth to refer and that is associated with their dependency on Channel State Information (CSI) availability.

- MIMO schemes based on CSI at the receiver. These involve MIMO detection techniques and space time coding.
- MIMO schemes based on the CSI at the transmitter (precoding schemes)
- MIMO schemes based on CSI at both the transmitter and receiver (beam forming schemes).

In this thesis we primarily focus on MIMO precoding techniques namely CI and SCI precoding. The latter one will contribute to take advantage of the existing ICI in our dual-polarised antenna system.

2.6.1 Channel Inversion Precoding

The main advantage of this group of techniques is the transferring of the computational burden from the MU to the BS. Thus signal is processed prior to transmission. CI precoding technique, first introduced in [14], multiplies the signal b prior to transmission with the inverse of the channel matrix \mathbf{H}

$$x = f\mathbf{H}^H(\mathbf{H}\mathbf{H}^H)^{-1}b \quad (2.16)$$

Symbols as can be seen are pre-distorted with the channel effects so as to compensate for the channel fading. The component $\mathbf{H}^H(\mathbf{H}\mathbf{H}^H)^{-1}$ is the pseudo inverse of the channel matrix and f is a scaling factor that maintains the signal power at the levels of the power of the signal without precoding.

$$f = \frac{1}{(\mathbf{b}^H(\mathbf{H}\mathbf{H}^H)^{-1}\mathbf{b})} \quad (2.17)$$

It should be noted that signal at the receiver is interference free.

2.6.2 Selective Channel Inversion Precoding

This technique is a modification of CI precoding and first proposed in [15]. The rationale that lies behind this method is attempting to exploit constructive ICI that occurs in the system as well as eliminate destructive ICI. Therefore

channel is partially inversed and according to this the signal is constructively corrupted so as to fall even further away from the decision thresholds. By doing so, the effective SINR delivered to MU is enhanced, without the need to invest in additional transmitted signal power at the BS.

Without loss of generality, it will be presented the ICI characterisation in a 2x2 dual polarised antennas environment. In the noiseless case we have as follows:

$$\mathbf{r} = \mathbf{x}\mathbf{H}\mathbf{H}^H \quad (2.18)$$

$$\begin{bmatrix} r_1 & r_2 \end{bmatrix} = \begin{bmatrix} x_1 & x_2 \end{bmatrix} \begin{bmatrix} h_{11} & h_{12} \\ h_{21} & h_{22} \end{bmatrix} \begin{bmatrix} h_{11}^* & h_{21}^* \\ h_{12}^* & h_{22}^* \end{bmatrix} \quad (2.19)$$

$$\begin{bmatrix} r_1 & r_2 \end{bmatrix} = \begin{bmatrix} x_1 & x_2 \end{bmatrix} \begin{bmatrix} |h_{11}|^2 + |h_{12}|^2 & h_{11}h_{21}^* + h_{12}h_{22}^* \\ h_{21}h_{11}^* + h_{22}h_{12}^* & |h_{21}|^2 + |h_{22}|^2 \end{bmatrix} \quad (2.20)$$

$$\begin{bmatrix} r_1 & r_2 \end{bmatrix} = \begin{bmatrix} x_1 & x_2 \end{bmatrix} \begin{bmatrix} \rho_{11} & \rho_{12} \\ \rho_{21} & \rho_{22} \end{bmatrix} = [x_1\rho_{11} + x_2\rho_{21}, x_1\rho_{12} + x_2\rho_{22}] \quad (2.21)$$

where x_1, x_2 are the transmitted symbols from antenna 1 and 2 respectively,

r_1, r_2 are the received symbols at receiver antenna 1 and 2, \mathbf{H} is the channel matrix, h_{ij} is the path connecting transmitter antenna i with receiver antenna j .

The elements ρ_{11} and ρ_{22} improve the energy of the signal at the receiver, as they represent the autocorrelation of the channel paths. On the other hand, the elements ρ_{12} and ρ_{21} degrade the quality of the signal at the receiver.

The component $\mathbf{H}\mathbf{H}^H$ is the autocorrelation channel matrix and the received signal has still some ICI regardless of the fact that dual polarised antennas have been used. In more details, in the component $r_l = x_1\rho_{1l} + x_2\rho_{2l}$, the product $x_2\rho_{2l}$ is the interference that occurs because of cross-polarisation effects from antenna 2 to antenna 1 during simultaneous transmission.

In order to classify interference as constructive and destructive it is required to make an analysis based on the symbols transmitted from the two antennas at the same time. TABLE 4 shows all the four possible cases, when two bits per time slot rate is applied.

TABLE 4 MAPPING TABLE FOR SIMULTANEOUS SPATIAL MODULATION

Symbol	Antenna1	Antenna2
0 0	1	-j
0 1	-1	j
1 0	j	-1
1 1	-j	1

Based on this symbol information we can easily apply the characterisation of ICI. Fig 2.5 depicts the area of the Cartesian level that ICI is constructive for each symbol that each is designated to send through the channel.

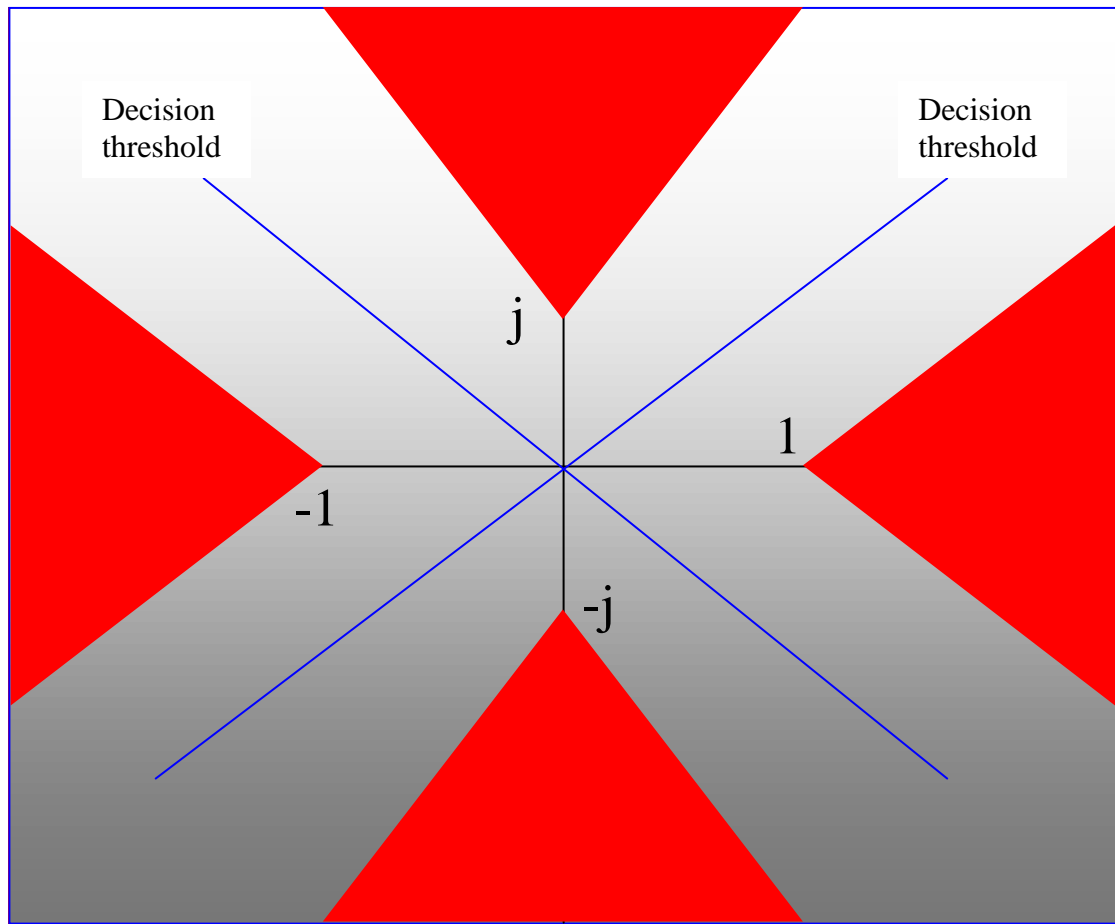


Fig. 2.5 Areas (red ones) that the received symbol should lie in for the interference to be constructive.

Therefore, the received signal must fall within the red areas so as to experience constructive levels of interference. By observing the signal prior transmission at each time slot we could easily determine the elements of the $\mathbf{R} = \mathbf{H}\mathbf{H}^H$ matrix that need to be eliminated and retain those that can provide constructive levels of interference. Subsequently, instead of the conventional precoding matrix $\mathbf{T} = \mathbf{H}^H(\mathbf{H}\mathbf{H}^H)^{-1}$, the modified selective precoding matrix could be used

$$\mathbf{T}^c = \mathbf{H}^H(\mathbf{H}\mathbf{H}^H)^{-1}\mathbf{R}^c \quad (2.22)$$

where \mathbf{R}^c is the matrix that contains the elements that provide constructive levels of interference.

It would be a remiss not to mention that due to this adaptive part of the precoding processing this method is dynamic and therefore has higher complexity than conventional CI. However, in the case of fast fading that precoding has to be adapted on a symbol-by-symbol base even for conventional CI, this burden is remarkably reduced. Based on this technique the received symbols are

$$\mathbf{r} = \mathbf{R}^c \mathbf{b} + \mathbf{n} \quad (2.23)$$

where the transmitted symbols because of the matrix \mathbf{R}^c are corrupted with constructive ICI. With the conventional CI this amount of ICI is wasted once full orthogonalisation of the symbols takes place.

2.7 Cooperative Communication

In this section we will briefly refer to cooperative communication and the basic protocols that are applied in this area of communications. Spatial diversity can be attained by employing various approaches. For instance, multiple antennas are a remarkable pledge so as to increase capacity and performance via the increased diversity that occurs. On the other hand, size limitations are a big factor, which is strongly considered so as to deploy MIMO systems. An interesting contribution for resolving this problem is to create a virtual MIMO system by making users cooperating with each other [16], [17]. A

simple example that could facilitate explanation could be the case where a source sends a signal to the destination through a direct link and at the same time a relay station is listening to that transmission (see Fig 2.6).

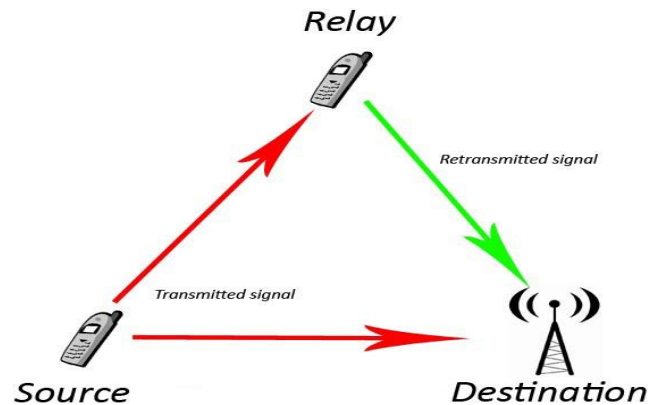


Fig. 2.6 Cooperative Transmission at the Base Station

Eventually, the relay transmits the data after a process that has taken place on it. The relay channel is made up of three nodes:

- The transmitter: a node that transmits information
- The relay: a node, that can be idle or not, which receives and transmits information to enhance communication between the source and the destination.
- The receiver: the BS that receives information.

The transmitter can benefit from the relay user in its proximity, by letting the relay retransmit its data to the destination (BS). The goal of the relay is thus to help the transmitter communicate with the BS. Since the information is transmitted through two independent wireless links, a diversity gain is achieved which is the main rationale of this technique. This new type of

diversity is called User Cooperation Diversity. For the two different transmissions orthogonal channels have been used [18].

2.7.1 Cooperative Transmission Protocols

Several transmission protocols are to be employed for retransmission to occur. Employment of these protocols explains how data that have been received by the relay are processed before the relay operation takes place. The main protocols that are briefly discussed are Amplify and Forward (AAF), Decode and Forward (DAF) and Coded Cooperation Protocol.

2.7.1.1 Amplify and Forward

In this type of protocol the signal received by the relay station is attenuated [19]. Therefore, an amplification process would be desired before retransmission. Although, during enhancement of the signal power, noise power is highly improved and it is worth mentioning that this is the greatest impediment of this technique. Amplification of the signal is either block wise or bitwise. The incoming power is

$$E[|y_r|^2] = E[|h_{s,r}|^2]E[|x_s|^2] + E[|n_{s,r}|^2] = |h_{s,r}|^2 x + 2s_{s,r}^2 \quad (2.24),$$

where y_r is the received signal at the relay station, $h_{s,r}$ is the channel path that connects the source with the relay station, x_s is the transmitted symbol from the source, $n_{s,r}$ is the noise at the relay station, ξ is the transmitted

signal energy, $\sigma_{s,r}^2$ is the noise variance at the relay station, s is the source and r is the relay station.

In order to retain the power of the signal at the relay station the gain factor has to be

$$\beta = \sqrt{\frac{x}{|h_{s,r}|^2 x + 2\sigma_{s,r}^2}} \quad (2.25)$$

AAF can be applied in the case where computing power or time has to be minimised when the relay is attempting to decode and re encode the message. It is quite obvious that when an analogue signal is employed for transmission a DAF transmission protocol cannot be utilised [19].

2.7.1.2 Decode and Forward

The trend of applying digital signals and the increase in available power has led to significant usage of the DAF transmission protocol [19]. In order to elaborate more on this, the signal received is first decoded and then re encoded. Hence, there is no enhanced noise at the relay after process of the useful signal. There tend to be made two assumptions with regard to the relay process that occurs at the relay before re transmission.

The original message can be fully retrieved. Although, substantial amount of computing time is required. When the error correction codes are incorporated into the bit sequence, errors might be eliminated at the relay. On the other hand, a checksum is applied so as to detect any erroneous transmission. A checksum is a fixed size datum computed from an arbitrary block of digital data for the purpose of detecting accidental errors that they

may have been introduced during its transmission or storage [20]. Any time data is received; the checksum of them is calculated and compared to the original one. If the checksums are different, then data was certainly modified (either on purpose or accidentally). The better the algorithm the more likely the two checksums not to match when the data is corrupted; on the other hand, the more likely the checksums to match if the data are free of accidental errors.

In the case that the original message cannot be fully recovered, an error correction or a checksum cannot be implemented. This occurs when the time required during decoding and processing the message is not acceptable or when there are capacity limitations at the relay.

Under the assumption of perfect error detection, in this thesis a Cyclic Redundancy Checksum has not been applied and therefore for purposes of limitation in space the reader can advise bibliography associated to that [21].

2.7.1.3. Coded Cooperation

When Coded Cooperation is used cooperation and channel coding are combined. The rationale is that each user's bits are split and send to the destination through two different fading channels [17], [22], [23], [24]. Each partner receives incremental redundancy from its intended user, under the assumption that this is done properly. In case not, users do not cooperate with each other. The basic advantage is that all this is achieved through code design, thus no feedback is essential among the users and their partners.

By taking advantage of the properties of Cyclic Redundancy Codes (CRC), each user enciphers K source bits using a concatenation of CRC codes [17].

The total code rate is $R = \frac{K}{N}$ where N is the total number of bits of the source block. The whole source block is separated into two frames using puncturing. Thus the first frame is consisted of $N_1 = \frac{K}{R_1}$ bits and the remaining $N_2 = N - N_1$ are the punctured bits.

Cooperation is accomplished by initially sending the first frame of N_1 bits and the proposed users detect and decode what has been sent. Under the assumption that bits are correctly detected and decoded, partners using the properties of CRC codes are attempting to calculate the remaining N_2 bits of the source block. If bits are not properly decoded then no cooperation can be completed and users revert back to the non-cooperative mode.

Eventually a total of N bits are transmitted and the level of cooperation can be named as $\frac{N_2}{N}$. With Coded Cooperation incorrect data are thwarted from being send leading to significant performance enhancement. Moreover, during the second frame users are surely independent from each other, requiring no knowledge of whether their own data was successfully decoded by their partner.

Chapter 3

Code Shift Keying Modulation

In conventional SM antenna index estimation is a potential source of errors and therefore increased diversity at the receiver is required to minimise this problem. Moreover, the conventional SM method is unable to perform unless the channel is normalised, a condition that may not be satisfied, since the channel power instantaneously is not always 1 but only the expectation of it. In this chapter we consider two alternatives in the form of orthogonal sequence shift keying. Similar to SM each orthogonal code is dedicated to a specific small subset of information bits. These alternative techniques eliminate the need to estimate the antenna index and do not require as much receiver diversity to achieve improved performance. It will be shown that this alternative approach not only outperforms the conventional SM technique, MRRC and V-BLAST MMSE in the low SNR region but also its complexity is also lower. Finally hybrid CSK systems are investigated and are shown to achieve significant performance improvements relative to the above techniques.

3.1 Introduction

Exploiting the spatial domain has become a popular method for meeting the high data rate requirements of today's and tomorrow's applications [11]. MIMO systems are widely known to benefit from spatial diversity and spatial multiplexing. A MIMO system experiences transmitter diversity when all transmitting antennas forward the same symbol to the destination. Likewise, a MIMO system experiences receiver diversity, when there are more than one receiver antennas to receive the data. Alamouti's scheme [25] is the most common MIMO technique that provides a full diversity order. On the other hand, a MIMO system experiences spatial multiplexing when each transmitter antenna is employed to forward different data streams simultaneously. This leads to increased throughput at the receiver but receiver complexity increases. V-BLAST [26] technique is a good receiver example of spatial multiplexing.

Spatial multiplexing techniques are found to be prone to ICI due to the simultaneous transmission of different symbols over the same frequency band triggering the need to use advanced receivers which tend to be complex. This is often perceived as a disadvantage of MIMO.

SM [10], is a recently developed approach that eliminates this type of interference, by only transmitting from one antenna at a time. The rationale behind this technique is that the number of information bits depends on the used constellation diagram and the available number of transmit antennas.

Each antenna is dedicated to a small subset of data bits. While the receiver associated with the original technique could only perform under a specific set of conditions, the optimal SM detector that is able to outperform V-BLAST has been presented [27]. The major disadvantage with this technique however is its susceptibility to antenna index estimation errors and strong reliance on receiver diversity.

This chapter introduces two schemes, in which the antenna index estimation is not needed and also high receiver diversity order is not essential to achieve a good performance. Also in this approach we overcome SM's biggest drawback, which is its inability to perform in conventional channel conditions. These methods are referred as CSK Modulation and Improved CSK Modulation. One code is available at each time slot. Similar to SM, the total block of bits is represented by one spreading code as well as a symbol from a constellation diagram. During reception the system exploits the property that codes are orthogonal; so as to eventually estimate the code index along with the symbol transmitted. We show that the proposed schemes perform better over a significant range of SNR values. It would be a remiss not to mention that CSK and Improved CSK are shown to have lower complexity compared to conventional SM. Finally, two multiple antenna scenarios, where orthogonal spreading codes are deployed in SIMO systems, have also been introduced. For the purpose of fair comparisons the net-spreading level of the systems is kept unchanged. These systems can offer remarkable performance improvements relative to the other two methods as will be shown.

The proposed schemes stem their idea from [28] where the Walsh Hadamard matrix is used to generate M-ary orthogonal symbols, in order to create a unipolar non-coherent M-ary orthogonal keying (NC-MOK) for an OFDM system that does not require channel estimation. Its performance is compared with that of bipolar Coherent MOK where for the latter phase information is obtained via pilot-based channel estimation. Each orthogonal symbol is a row from the $M \times M$ matrix, where M is the total bit rate. The total block of information bits was represented by one row in the Walsh matrix. At the receiver the signal is retrieved via the correlation of each of the received orthogonal symbol with all the possible M Walsh symbols.

The rest of the chapter is organised as follows, in Section 3.2 the conventional SM technique is briefly introduced. In Section 3.3 and 3.4 the CSK Modulation and Improved CSK technique, in a Single Input Single Output (SISO) system, are illustrated in details. This is followed by a complexity analysis of the proposed schemes in Section 3.5. In Section 3.6 the proposed approaches are discussed in a Single Input Multiple Output (SIMO) system by retaining the net spreading level of the overall system. Finally, in Section 3.7 and 3.8 simulation results and summarisation are presented, respectively.

3.2 Spatial Modulation

We assume a 4×4 MIMO (see Fig. 3.1) system and, without loss of generality, the signal at the receiver is

$$\mathbf{r} = \mathbf{h}_{ij}x + \mathbf{n} \quad (3.1)$$

where \mathbf{h}_{ij} are the channel paths between transmitter i and receiver j and \mathbf{n} AWGN noise. Normally the \mathbf{h}_{ij} term is a vector, when only one transmitter antenna is active at each time period (black solid lines in Fig. 3.1).

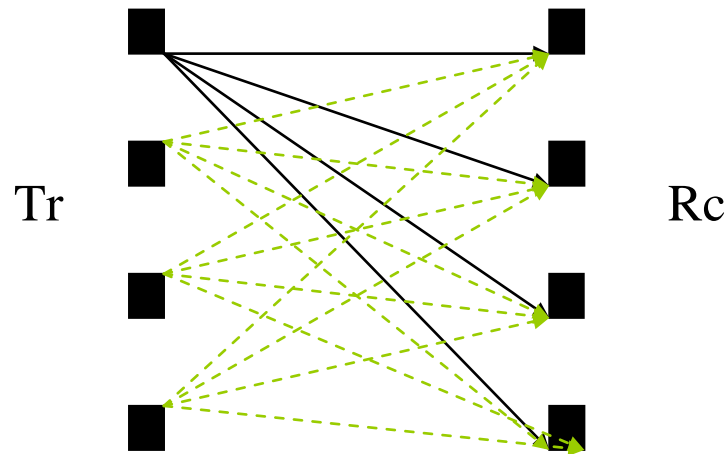


Fig. 3.1 SM in a MIMO 4x4 system.

At the receiver there are two detection processes that can be invoked [27].
 1) The transmit antenna number is estimated and 2) the transmitted symbol is estimated. The received signal \mathbf{r} is iteratively multiplied by the channel path gains that are assumed to be known at the receiver as

$$\mathbf{g}_k = \mathbf{h}_k^H \mathbf{r} = \mathbf{h}_k^H \mathbf{h}_j \mathbf{x} + \mathbf{n} \mathbf{h}_k^H \quad (3.2)$$

where \mathbf{h}_k is the path vector that connects transmitter antenna k with all the receiver antennas. This algorithm works for every possible transmitter antenna k and then the signal g_k , where $k=j$, will be chosen as it is going to be

the one with the greatest power once the channel paths best match (best correlation).

As mentioned in Chapter 2, SM is an approach that entirely avoids ICI, which is a common burden in spatial multiplexing MIMO systems [10]. In addition to this, SM produces no correlation between the transmit antennas and requires no synchronisation at the transmitter. However, two significant drawbacks of conventional SM are that there is no transmit diversity and only performs under normalised channel conditions. On the other hand, the system benefits from diversity at the receiver.

Although, cross correlation between different channel paths is not instantaneously zero it remains a burden during the antenna index estimation process. To mitigate this, increased diversity at the receiver is required.

3.3 Code Shift Keying Modulation in a SISO system

In this section we describe the new technique that employs orthogonal spreading codes to convey information at the receiver. This method is named CSK Modulation. The system consists of one transmitter antenna and one receiver antenna. The total bit rate is distributed over the spreading codes and the symbol that is chosen from a constellation signal. This can occur in two different ways-either by changing the constellation signal and/or the number of available orthogonal codes. For example, when the transmission rate is three bits and the number of available spreading codes is four, the system employs BPSK modulation (see TABLE 5). Alternatively, using two spreading codes instead of four, three bits used to be sent if the modulation technique is

changed to Quadrature Phase Shift Keying (QPSK). At the receiver the code index along with the transmitted symbol will determine the total number of bits.

TABLE 5 MAPPING TABLE FOR CODE SHIFT KEYING
MODULATION

Input Bits	4 Codes , BPSK	
	Orthogonal Codes	Trans. Symbol
000	1 st	1
001	1 st	-1
010	2 nd	1
011	2 nd	-1
100	3 rd	1
101	3 rd	-1
110	4 th	1
111	4 th	-1

3.3.1 Code Index Estimation

In this section we discuss how to detect the active orthogonal spreading code. Therefore a code selection algorithm is introduced in the following. The received signal is described as:

$$\mathbf{r} = \mathbf{h}x\mathbf{c}_j + \mathbf{n} \quad (3.3)$$

where \mathbf{h} is the channel path, x is the transmitted symbol, \mathbf{c}_j is the corresponding spreading code and finally \mathbf{n} is AWGN noise. This signal is

then multiplied with all the available codes and the output is given as follows

$$g_k = \mathbf{h}^H \mathbf{r} \mathbf{c}_k^* = \mathbf{h}^H \mathbf{h} x \mathbf{c}_j \mathbf{c}_k^* + \mathbf{h}^H \mathbf{n} \mathbf{c}_k^* \quad (3.4)$$

$$\mathbf{g} = [g_1 \quad g_2 \dots g_{N_c}] \quad (3.5)$$

where \mathbf{g} is the vector that contains all the possible outputs and \mathbf{c}_k^* are the conjugate values of all the possible spreading codes. In view of the fact that codes are orthogonal, the output with the greatest power, where $k=j$, is chosen to be the actual received signal. Eventually, combining the result from this selection algorithm along with the estimated transmitted symbol the total number of information bits is acquired.

3.3.2 Example: 3 bits Space Shift Keying Modulation using 1x1 antenna configuration and 4 orthogonal spreading codes

The mapping table for 3 bits transmission using four orthogonal spreading codes and BPSK modulation in a SISO system [2] is shown in TABLE 5. The four spreading codes are $\mathbf{c}_1 = [1, 1, 1, 1]$, $\mathbf{c}_2 = [1, -1, 1, -1]$, $\mathbf{c}_3 = [1, 1, -1, -1]$ and $\mathbf{c}_4 = [1, -1, -1, 1]$.

Assuming that the bits to be transmitted are $\mathbf{q}(k) = [1, 0, 0]$, from the mapping table we can map this sequence to $x = 1$ and $\mathbf{c}_3 = [1, 1, -1, -1]$. The SISO channel configuration will be a one path fading channel $h = [-0.2326 - 0.6590j]$. The Signal to Noise Ratio (SNR) in this example is 8

dB. Thus the spread symbol will be forwarded through the channel h at the destination and the received signal will be the following

$$\mathbf{r} = [-0.0282 - 0.5589j, -0.0939 - 0.4006j, 0.1942 + 0.3603j, 0.0654 + 0.6086j].$$

The code index estimation algorithm is considered in the following and the channel is assumed to be known at the receiver. Applying the estimation algorithm to the received vector results in

$$\mathbf{g} = [0.1425 - 0.0543j, -0.2678 + 0.0283j, 0.8096 + 0.1494j, 0.2974 - 0.2411j].$$

By observing the vector \mathbf{g} in Fig. 3.2, we see that $\mathbf{g}(3)$ is the element with the greatest power. From this element we are able to estimate that $\mathbf{c}_3 = [1, 1, -1, -1]$ and BPSK symbol $\bar{x} = 1$ have been employed. From the estimated code and symbol we can retrieve the initial sequence of bits $\bar{\mathbf{q}}(k) = [1, 0, 0]$, which exactly corresponds to the transmitted bits.

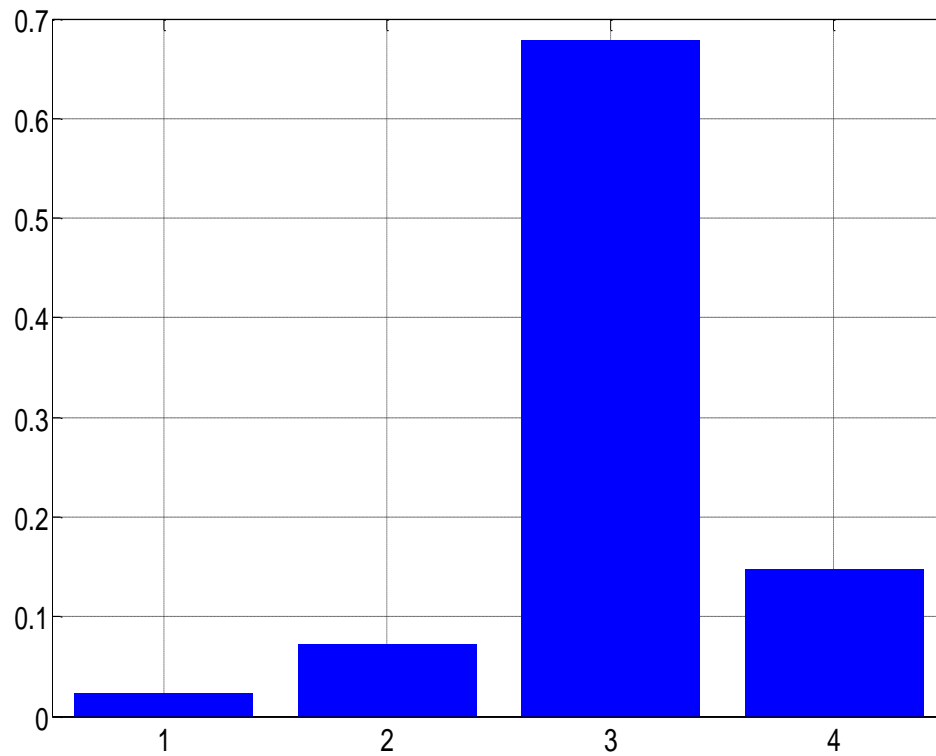


Fig. 3.2 Received vector g .

The estimation of the transmitted bits is based on the cross correlation of the orthogonal codes and not the cross correlation of the different channels like in conventional SM. It should be noted that orthogonal codes' cross correlation is instantaneously zero [2] and thus only noise will affect the performance of the code index estimation algorithm. This is deemed an important feature- especially for uplink transmission, where a multiple number of transmit antennas would be prohibitive option especially in small mobile devices.

3.4 Improved Code Shift Keying Modulation in a SISO system

We introduce an improved CSK scheme that uses half the amount of spreading codes by exploiting the real and imaginary domain of the Cartesian plane and employing ASK modulation. This technique uses much less bandwidth than conventional CSK modulation. By keeping the net spreading level of the systems the same, it is shown that the proposed still significantly outperforms the conventional SM, CSK modulation technique, MRRC and V-BLAST MMSE [37].

The system consists of one transmitter antenna and one receiver antenna. As in conventional CSK, the total bit rate is distributed over the spreading codes and the symbol that is chosen from a constellation signal (see TABLE 6). At the receiver the code index along with the transmitted symbol will determine the total number of bits.

TABLE 6 MAPPING TABLE FOR IMPROVED CODE SHIFT KEYING
MODULATION

Input Bits	2 Distinct Codes , 2-ASK	
	Orthogonal Codes	Transmitted Symbol
000	$\mathbf{c}_1 = \mathbf{c}_1$	1
001	$\mathbf{c}_1 = \mathbf{c}_1$	-1
010	$\mathbf{c}_2 = \mathbf{j}\mathbf{c}_1$	1
011	$\mathbf{c}_2 = \mathbf{j}\mathbf{c}_1$	-1
100	$\mathbf{c}_3 = \mathbf{c}_2$	1
101	$\mathbf{c}_3 = \mathbf{c}_2$	-1
110	$\mathbf{c}_4 = \mathbf{j}\mathbf{c}_2$	1
111	$\mathbf{c}_4 = \mathbf{j}\mathbf{c}_2$	-1

3.4.1 Code Index Estimation

In a SISO system, where the Improved CSK Modulation has been applied, the corresponding code that has been active needs to be identified. The received signal is described as in Eq. (3.3). This signal is then multiplied with all the available codes and all the possible outputs are given as in Equation 3.4 and all the possible outputs are stored in vector \mathbf{g} (see Eq. 3.5). In view of the fact that codes are orthogonal amongst each other along with the signal employed is ASK [2], the real part of the output with the greatest power, where

$k=j$, is chosen to be the actual received signal. Eventually, combining the result from this selection algorithm along with the estimated transmitted symbol the total number of information bits is acquired.

3.4.2 Example: 3 bits Space Shift Keying Modulation using 1x1 antenna configuration and 2 orthogonal spreading codes and 2-ASK modulation

The mapping table for 3 bits transmission using two distinct orthogonal spreading codes and 2-ASK modulation in a SISO system is shown in TABLE 5. The four spreading codes (two of them are distinct) will be the following $\mathbf{c}_1 = [1, 1]$, $\mathbf{c}_2 = j\mathbf{c}_1$, $\mathbf{c}_3 = [1, -1]$ and $\mathbf{c}_4 = j\mathbf{c}_3$.

Assuming that the bits to be transmitted are $\mathbf{q}(k) = [1, 0, 0]$, from the mapping table we can map this sequence to $x = 1$ and $\mathbf{c}_3 = [1, -1]$. The SISO channel configuration will be a one path fading channel $h = [0.8409 - 0.0266j]$. The Signal to Noise Ratio (SNR) in this example is 8dB. Thus the spreading symbol will be forwarded through the channel h at the destination and the received signal will be the following

$$\mathbf{r} = [0.6478 + 0.0115j, -0.5662 - 0.0991j].$$

The code index estimation algorithm is considered in the following and the channel is assumed to be known at the receiver. Applying the estimation algorithm to the received vector results in

$$\mathbf{g} = [0.0709 - 0.0714i, -0.0714 - 0.0709i, 1.0169 + 0.1252i, 0.1252 - 1.0169i].$$

By observing the vector \mathbf{g} in Fig. 3.3, we see that $\mathbf{g}(3)$ is the element with the real part that has the greatest power. From this element we are able to estimate that $\mathbf{c}_3 = [1, -1]$ and ASK symbol $x = 1$ have been employed. From the estimated code and symbol we can retrieve the initial sequence of bits $\mathbf{q}(k) = [1, 0, 0]$, which exactly corresponds to the transmitted bits.

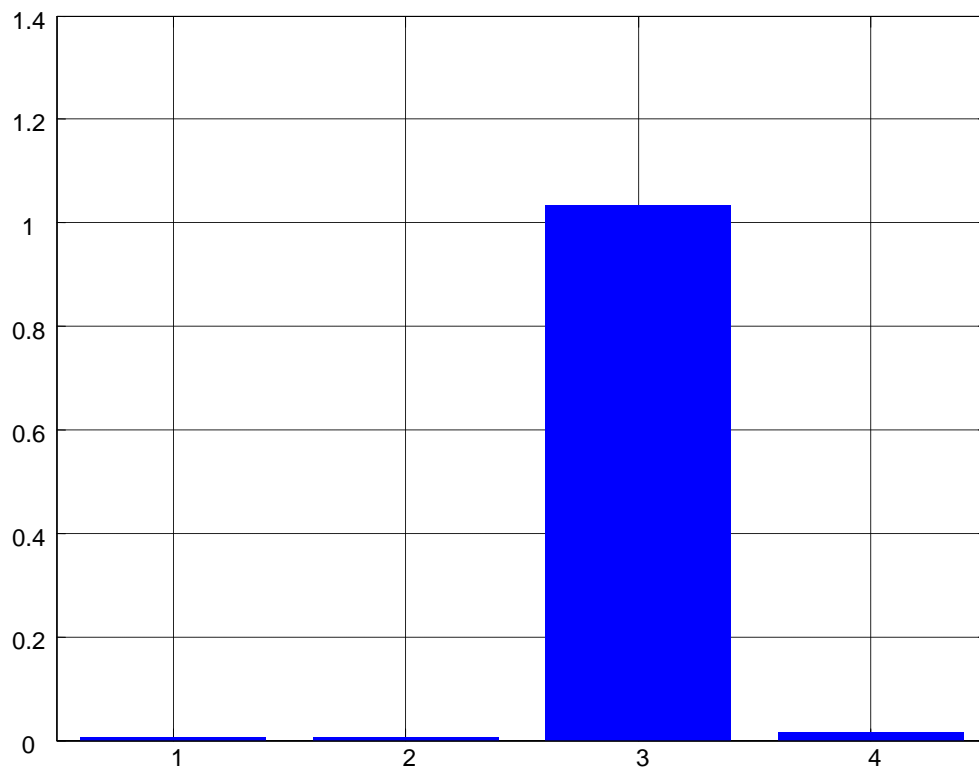


Fig. 3.3 Received vector \mathbf{g} .

The estimation of the transmitted bits is based on the cross correlation of the orthogonal codes and not the cross correlation of the different channels like in conventional SM. It should be noted that orthogonal codes' cross

correlation is instantaneously zero and thus only noise will affect the performance of the code index estimation algorithm.

3.5 Complexity Estimation

In this section the complexities of the proposed algorithms in a SISO system are discussed and compared with the conventional SM technique. The number of multiplications when the system uses conventional SM [27] is

$$\delta_{SM} = 2N_r N_t + N_t \quad (3.6)$$

where N_r is the number of receive antennas and N_t is the number of transmit antennas.

In CSK we can likewise view that from Eq. (3.3) we have N_c multiplications and from Eq. (3.4) we have N_c^2 multiplications, since the algorithm correlates the received signal with all the possible orthogonal spreading codes. N_c is the number of orthogonal spreading codes. Finally, we have N_c comparisons, so as to detect the signal with the greatest power. Therefore the total number of multiplications is

$$\delta_{CSK} = N_c N_c + 2N_c \quad (3.7)$$

where N_c is the number of the available orthogonal codes as well as the length of each spreading code. Assuming that the net-spreading levels of the systems remain the same, we can see that in an 8x8 MIMO system we have

136 calculations and in the alternative SISO system, that employs the CSK Modulation with eight orthogonal spreading codes available, we have only 82 calculations. This leads to a remarkable reduction in system's complexity.

In Improved CSK, where the number of available distinct spreading codes is $N_c/2$, we can view that from Eq. (3.3) we have $N_c/2$ multiplications and from Eq. (3.4) we have $N_c^2/4$ multiplications, since the algorithm correlates the received signal with all the possible orthogonal spreading codes. Finally we have N_c comparisons, so as to detect the signal with the greatest power. Therefore the total number of multiplications is

$$\delta_{\text{improvedCSK}} = \frac{N_c^2}{4} + \frac{3}{2} N_c. \quad (3.8)$$

3.6 Code Shift Keying Modulation and Improved Code Shift Keying Modulation in a SIMO system

As mentioned previously, in the proposed techniques high receive diversity order is not required to obtain acceptable levels of performance. Although, in conventional SM high receive diversity order is experienced, which potentially boosts performance of the system at high SNR values. Therefore, a system that would benefit from both the orthogonality of the spreading codes, as well as increased diversity at the receiver would promisingly offer even better performance.

However, such a system should maintain its net spreading levels so as to obtain a fair comparison with the proposed SISO system that employs CSK as

well as the conventional SM technique. By keeping the same level of overall net system we swap each antenna element with one orthogonal spreading code. Therefore, we firstly introduce a SIMO system that employs two orthogonal spreading codes (length two each) and four receiver antennas. Finally, we could propose a similar scenario where the number of receiver antennas is two. It would be a remiss not to mention that the latter system's net-spreading level is half the size of the other systems.

3.7 Analytical SER Calculation for Code Shift Keying Modulation and Improved Code Shift Keying Modulation

In CSK Modulation as well as Improved CSK Modulation two estimation processes are involved: 1.) Estimation of the Orthogonal Spreading Code and 2.) Estimation of the transmitted symbol. Therefore in order to calculate the probability of error P_{err} , it is required the estimation of the probability that the orthogonal spreading code is incorrect as well as the probability that the transmitted symbol is incorrect. Let P_c and P_s denote the two probabilities respectively.

At the receiver the bits are correct only if the code index estimate and the transmitted symbol estimate are correct.

$$P_{cor} = (1 - P_c)(1 - P_s) \quad (3.9)$$

Thus the probability of error is

$$P_{err} = 1 - P_{cor} \quad (3.10)$$

$$P_{err} = P_c + P_s - P_c P_s. \quad (3.11)$$

In Sections 3.7.1, 3.7.2 and 3.7.3 we consider the estimation of the two estimation processes for both techniques.

3.7.1 Analytical SER of the Transmitted Symbol Estimation Process

The analytical estimation of the transmitted symbol for any M-PSK is 1x1 MRRC detection in a SISO system. The estimation is identical for both methods. The conditional SER for M-PSK [29] is as,

$$P_s(\{\gamma_l\}_{l=1}^M) = \frac{1}{\pi} \int_0^{\frac{(M-1)\pi}{M}} \exp\left(-\frac{g_{psk}\gamma_l}{\sin^2\varphi}\right) d\varphi \quad (3.12)$$

where $g_{psk} = \sin^2(\frac{\pi}{M})$ and γ_l is the average SNR at each receive antenna.

3.7.2 Analytical Error Calculation of the Orthogonal Spreading Code Estimation Process in Code Shift Keying Modulation

For simplicity and without loss of generality, a SISO system with 4 orthogonal spreading codes is considered for the calculation. The result is, later, generalised to any number of spreading codes. The code estimate is the position of the maximum absolute value of all elements in the vector \mathbf{g}_i

$$\hat{l} = \arg \max_{\forall i} | \mathbf{g}_i |. \quad (3.13)$$

Under the assumption that a sequence of bits is mapped to symbol s_2 , from a BPSK constellation, and to the second available spreading code \mathbf{c}_2 , the received signal will be

$$y = hs_2\mathbf{c}_2 + \mathbf{n}. \quad (3.14)$$

By multiplying with all the available codes the vector \mathbf{g} is created

$$\mathbf{g} = \begin{bmatrix} |h|^2 s_2 \mathbf{c}_2 \mathbf{c}_1^* + h^* \mathbf{n} \mathbf{c}_1^* \\ |h|^2 s_2 \mathbf{c}_2 \mathbf{c}_2^* + h^* \mathbf{n} \mathbf{c}_2^* \\ |h|^2 s_2 \mathbf{c}_2 \mathbf{c}_3^* + h^* \mathbf{n} \mathbf{c}_3^* \\ |h|^2 s_2 \mathbf{c}_2 \mathbf{c}_4^* + h^* \mathbf{n} \mathbf{c}_4^* \end{bmatrix}. \quad (3.15)$$

From Eq. (3.15) we can view that three out of the four elements have zero mean and σ_n^2 variance. The other element has mean $|h|^2 s_2$ and σ_n^2 variance. Assuming AWGN channel conditions we have as follows. The BPSK signal is one phase modulated signal which is either positive real value or negative.

Only the real value is considered for the calculation. Assume that μ_i is the absolute value of the real part of the transmitted symbol s_2 . Then $\boldsymbol{\mu}$ is a vector of length $c = 2^{(m/2-2)}$ which contains the absolute real elements of the constellation diagram.

Let $p(\mu_i)$ denote the probability that the code number estimate is incorrect when transmitting μ_i . Thus, the average overall Probability of error for the transmitted spreading code is

$$P_C = P_{avg} = \frac{1}{c} \sum_{i=1}^c p(\mu_i). \quad (3.16)$$

According to the detection process of the transmitted code from Eq. (3.13) we introduce $x = |u|$, where u is a random variable that follows a Gaussian distribution with mean μ_i and variance σ_n^2 . Thus, the probability density function for x is

$$P_X(x | \mu_i, \sigma_n^2) = \frac{1}{\sigma_n \sqrt{2\pi}} \left(\exp^{-\frac{(x-\mu_i)^2}{2\sigma_n^2}} + \exp^{-\frac{(x+\mu_i)^2}{2\sigma_n^2}} \right). \quad (3.17)$$

In order to estimate the code index it is necessary to find the element in the vector \mathbf{g} with the maximum absolute value. Each element of the vector \mathbf{g} is a sample from a random variable N_t with pdfs as shown in Eq. (3.17). Each distinct pdf has a different mean value. This problem can be treated with order statistics [30].

We assume that $X_{(1)}, \dots, X_{(N_c)}$ are random samples from a continuous population with a cumulative distribution function $F_X(x / \mu_i, \sigma_n^2)$ and a pdf $P_X(x / \mu_i, \sigma_n^2)$ where $X_{(N_c)} > X_{(N_c-1)} \dots X_{(j)}$. The pdf of $X_{(j)}$ [5] is

$$P_{X_{(j)}}(x / \mu_i, \sigma_n^2) = \frac{n!}{(j-1)!(N_c - j)!} P_X(x / \mu_i, \sigma_n^2) [F_X(x / \mu_i, \sigma_n^2)]^{j-1} [1 - F_X(x / \mu_i, \sigma_n^2)]^{N_c - j}. \quad (3.18)$$

In the case of four orthogonal spreading codes in Fig. 3.4 is presented the order statistics pdfs of the four random variables.

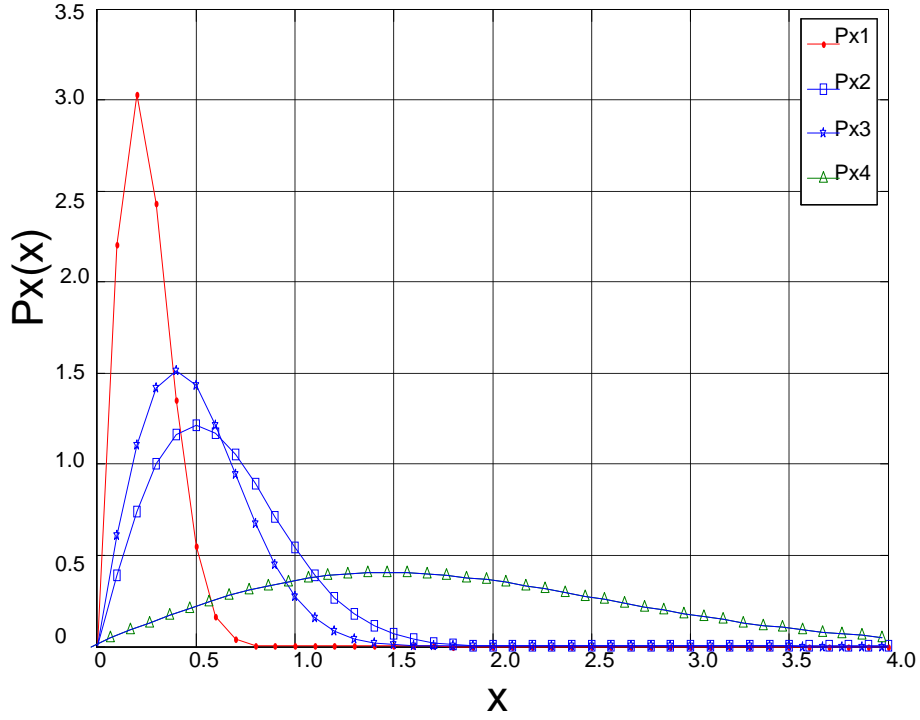


Fig. 3.4 Order statistics pdfs for four random variables when SNR is 15 dB.

Considering that the pdfs are statistically independent, the probability that the code index estimation is incorrect can be found by numerically integrating the intersection areas of $P_{X_{(4)}}(x/\mu_i, \sigma_n^2)$ (see Fig. 3.4) with all the other distributions.

Therefore, if x_3, x_2, x_1 denote the intersection points between $P_{X_{(4)}}(x/\mu_i, \sigma_n^2)$ and $P_{X_{(3)}}(x/\mu_i, \sigma_n^2)$, $P_{X_{(2)}}(x/\mu_i, \sigma_n^2)$ and $P_{X_{(1)}}(x/\mu_i, \sigma_n^2)$ respectively, then the probability of error for each μ_i is given as follows

$$p(\mu_i) = \frac{1}{3} \left(\int_0^{x_3} P_{X_{(4)}}(x/\mu_i, \sigma_n^2) dx + \int_0^{x_2} P_{X_{(4)}}(x/\mu_i, \sigma_n^2) dx + \int_0^{x_1} P_{X_{(4)}}(x/\mu_i, \sigma_n^2) dx \right). \quad (3.19)$$

For any number of spreading codes is written as

$$p(\mu_i) = \frac{1}{N_c - 1} \left(\sum_{i=1}^{N_c-1} \int_0^{x_i} P_{X_{(N_c)}}(x / \mu_i, \sigma_n^2) dx \right). \quad (3.20)$$

Knowing $p(\mu_i)$, we can calculate P_{avg} and P_c from Eq. (3.16). Both P_c and P_s are used to calculate the overall probability of error.

3.7.3 Analytical Error Calculation of the Orthogonal Spreading Code Estimation Process in Improved Code Shift Keying Modulation

Under the same assumptions as in Section 3.7.2 and if the available spreading codes are $\mathbf{c}_1 = \mathbf{c}_1, \mathbf{c}_2 = j\mathbf{c}_1, \mathbf{c}_3 = \mathbf{c}_3, \mathbf{c}_4 = j\mathbf{c}_3$ we have as follows.

A sequence of bits is mapped to symbol s_2 , from a BPSK constellation, and to the second available spreading code \mathbf{c}_2 , the received signal will be

$$\mathbf{y} = h s_2 \mathbf{c}_2 + \mathbf{n} = h s_2 (j\mathbf{c}_1) + \mathbf{n}. \quad (3.21)$$

By multiplying with all the available codes the vector \mathbf{g} is created:

$$\mathbf{g} = \begin{bmatrix} |h|^2 s_2 (j\mathbf{c}_1) \mathbf{c}_1^* + h^* \mathbf{n} \mathbf{c}_1^* \\ |h|^2 s_2 (j\mathbf{c}_1) (j\mathbf{c}_1)^* + h^* \mathbf{n} (j\mathbf{c}_1)^* \\ |h|^2 s_2 (j\mathbf{c}_1) \mathbf{c}_2^* + h^* \mathbf{n} \mathbf{c}_2^* \\ |h|^2 s_2 (j\mathbf{c}_1) (j\mathbf{c}_2)^* + h^* \mathbf{n} (j\mathbf{c}_2)^* \end{bmatrix}. \quad (3.22)$$

From Eq. (3.22) we can view that two out of the four elements have zero mean and σ_n^2 variance. The other element has mean $j|h|^2 s_2$ and σ_n^2

variance. The second element has $|h|^2 s_2$ and σ_n^2 . Assuming AWGN channel conditions we have as follows.

As in Section 3.7.2 the problem is treated with order statistics. Only the elements with real mean value or zero mean value are considered for the calculation. Therefore during the estimation process the receiver has to choose between three (and not four) elements in order to identify the code transmitted. This leads to performance improvement at the receiver. Fig. 3.5 presents the order statistics Probability Density Functions (PDFs) of the three random variables when four orthogonal spreading codes (two of them are distinct) are employed.

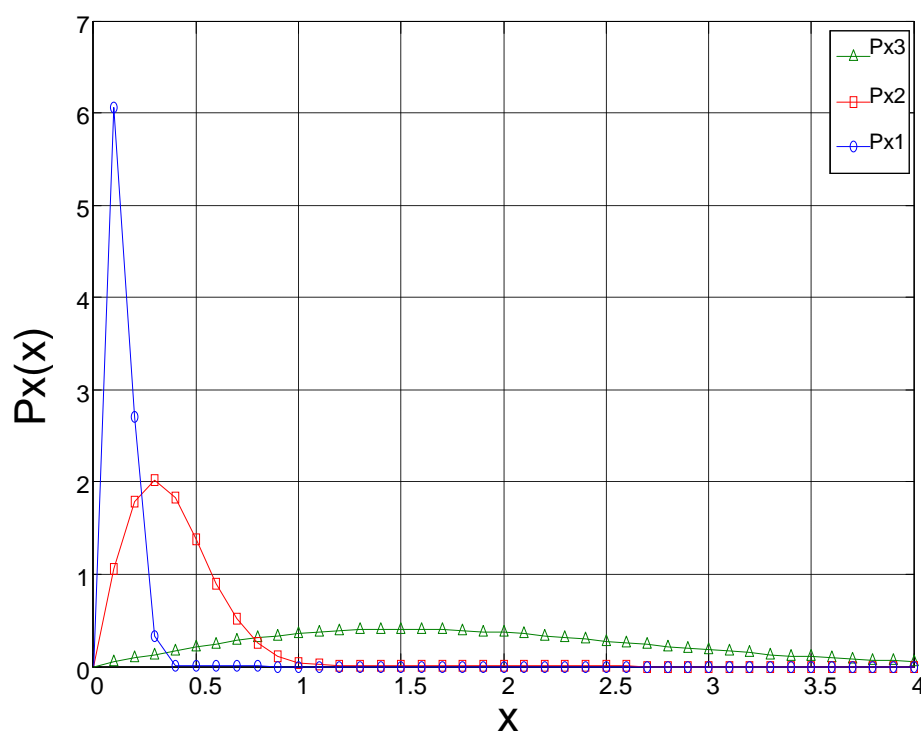


Fig. 3.5 Order statistics pdfs for three random variables in Improved CSK Modulation when SNR is 15dB.

Considering that the PDFs are statistically independent, the probability that the code index estimation is incorrect can be found by numerically integrating the intersection areas of $P_{X_{(3)}}(x/\mu_i, \sigma_n^2)$ with the other two distributions.

Therefore, if x_2, x_1 denote the intersection points between $P_{X_{(3)}}(x/\mu_i, \sigma_n^2)$ and $P_{X_{(2)}}(x/\mu_i, \sigma_n^2)$, and $P_{X_{(1)}}(x/\mu_i, \sigma_n^2)$ respectively, then the probability of error for each μ_i is

$$p(\mu_i) = \frac{1}{2} \left(\int_0^{x_2} P_{X_{(3)}}(x/\mu_i, \sigma_n^2) dx + \int_0^{x_1} P_{X_{(3)}}(x/\mu_i, \sigma_n^2) dx \right). \quad (3.23)$$

For any number of spreading codes is written as Eq. (3.20).

Knowing $p(\mu_i)$, we can calculate P_{avg} and P_c from Eq. (3.16). Both P_c and P_s are used to calculate the overall probability of error as in Section 3.7.2

3.8 Numerical Simulation

In this section we validate the proposed approach by means of simulation results for various scenarios. In the simulations the channel is either flat Rayleigh fading, Rician fading or AWGN (see Appendix A.2). The channel is assumed to be known at the receiver. The Monte Carlo technique (see Appendix A.4.3) is applied for the estimation of the Bit Error Rate. The SNR is defined as P/σ^2 , where P is the total transmitted power and σ^2 is the noise variance. Finally the variance of the fading channel paths is 1.

We next consider the simulation and analytical BER of CSK Modulation and Improved CSK Modulation over AWGN channel conditions (see Fig. 3.6 and Fig. 3.7). The transmission rate is 3 bits per period of interest and the number of the available orthogonal spreading codes is four. As can be seen in both Fig. 3.6 and 3.7 the analytical and simulation results are in close agreement.

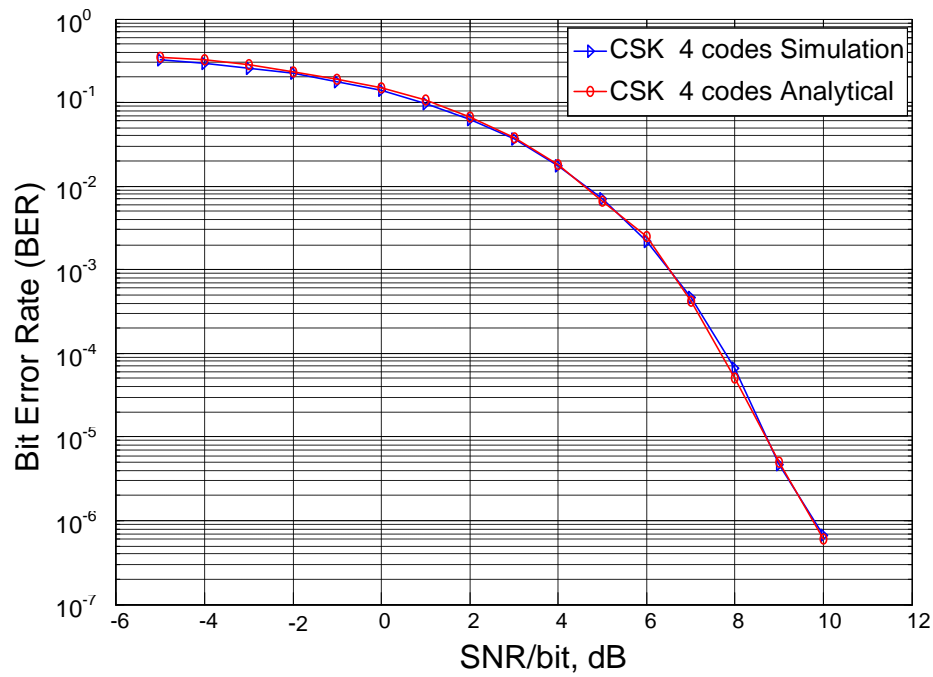


Fig. 3.6 Comparison between Analytical and Simulation BER of CSK over AWGN in 3 bits transmission rate and 4 spreading codes available

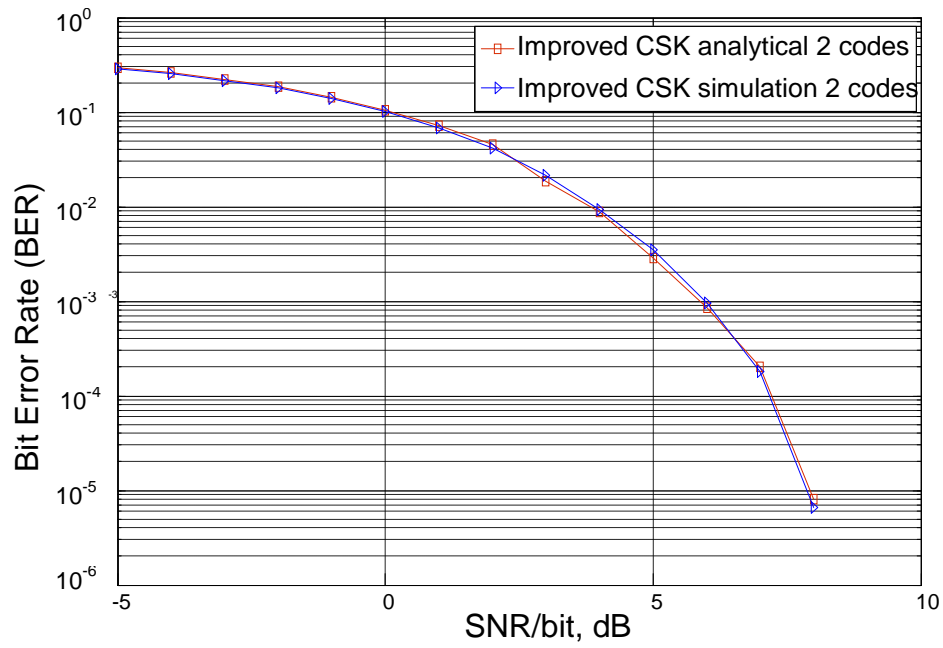


Fig. 3.7 Comparison between Analytical and Simulation BER of Improved CSK over AWGN in 3 bits transmission rate and 2 spreading codes available

Fig. 3.8 depicts the performance of CSK in the two SIMO systems scenario that have been discussed in Section 3.5. The first SIMO system employs 2 receiver antennas, 2 orthogonal codes (length 2 each). The second system employs 4 receiver antennas, 2 orthogonal codes (length 2 each). The channel is flat Rayleigh fading.

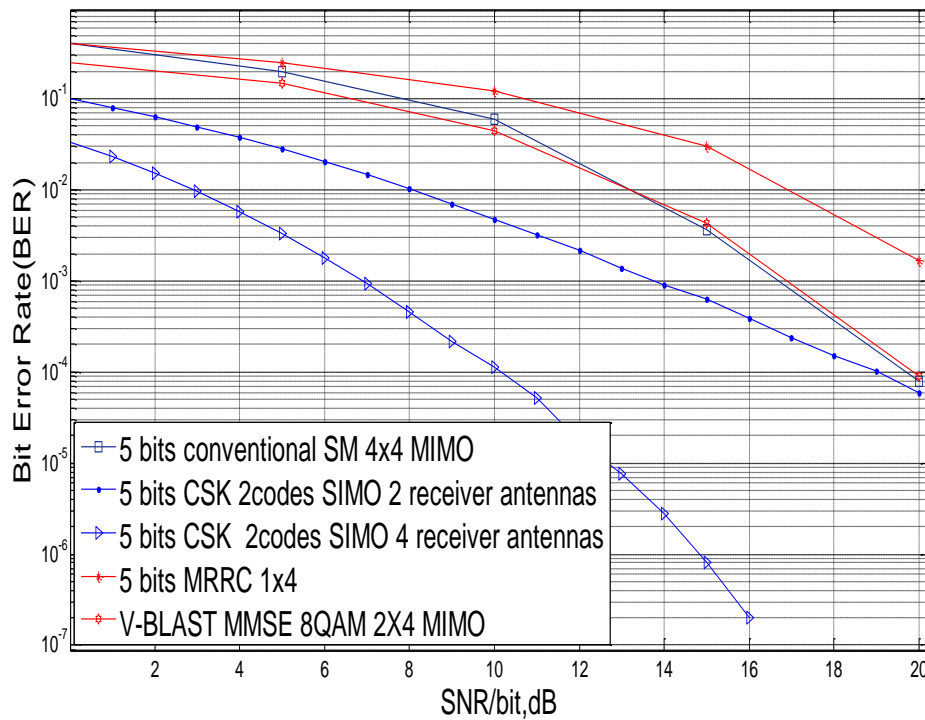


Fig. 3.8 Performance comparison between CSK in a SIMO system and the conventional SM, MRRC and V-BLAST MMSE

It can be seen that even the system with the 2 receiver antennas, which has half the size of the net-spreading level compared to the other ones, outperforms the conventional SM, MRRC and V-BLAST MMSE. Both systems have increased receive diversity order and thus performance is boosted for all SNR values. However, at SNR values above 20 dB the performance of the proposed scheme with the two receive antennas cannot manage to overcome the performance of the other schemes. This is purely attributed to the high receive diversity experienced in the other techniques. It is worth mentioning that the system uses a significant smaller number of antennas at the cost of increased bandwidth.

Fig. 3.9 introduces the performance (BER) of the CSK technique in flat Rayleigh fading channel coefficients. Transmission rate is 5 bits and 4

spreading codes are available. Moreover, Fig. 3.9 also plots the conventional SM, the MRRC and the V-BLAST MMSE scheme in a 4x4 MIMO system.

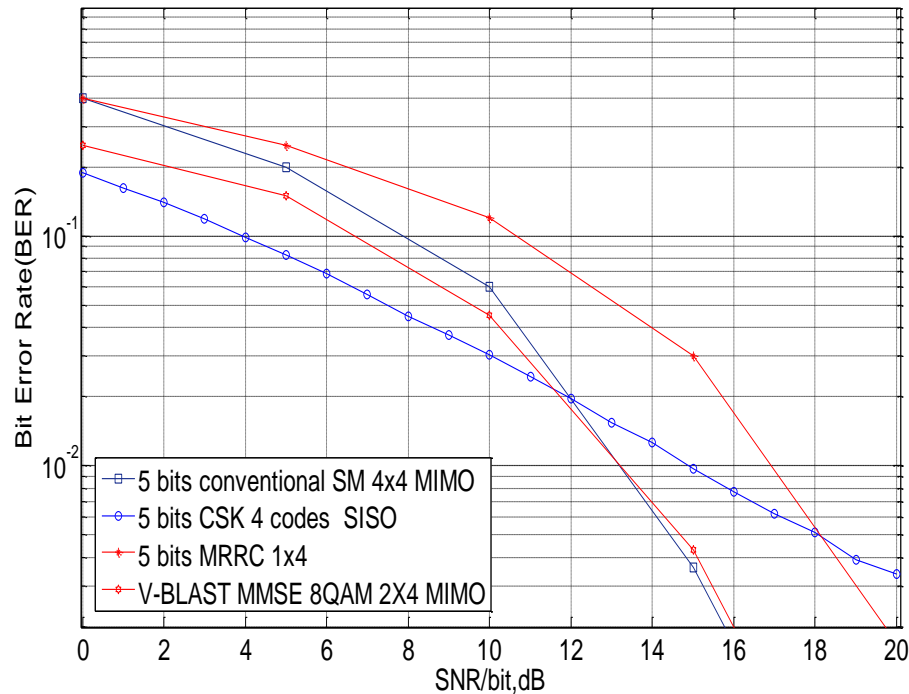


Fig. 3.9 Performance comparison between the proposed and spatial modulation when transmission rate is 5 bits per period of interest

The system does not benefit from receive diversity although it outperforms SM, MRRC and V-BLAST MMSE over a significant range of SNR values. Codes are instantaneously orthogonal [2] as opposed to the uncorrelated channel paths in the MIMO system. The above property affects the performance of the code index estimation algorithm at the destination. After 12dB SNR, SM performs better because of the increased diversity order which is experienced at the receiver (see Fig. 3.9).

In Fig. 3.10 it is attempted to compare the performance of the CSK scheme for various numbers of available spreading codes in an ideal channel scenario. Namely, the transmission rate is 5 bits and the number of codes is 4

and 8 respectively. In the case of 4 codes, each code will forward an 8-QAM symbol and when the available codes are 8 then each code will forward a QPSK symbol.

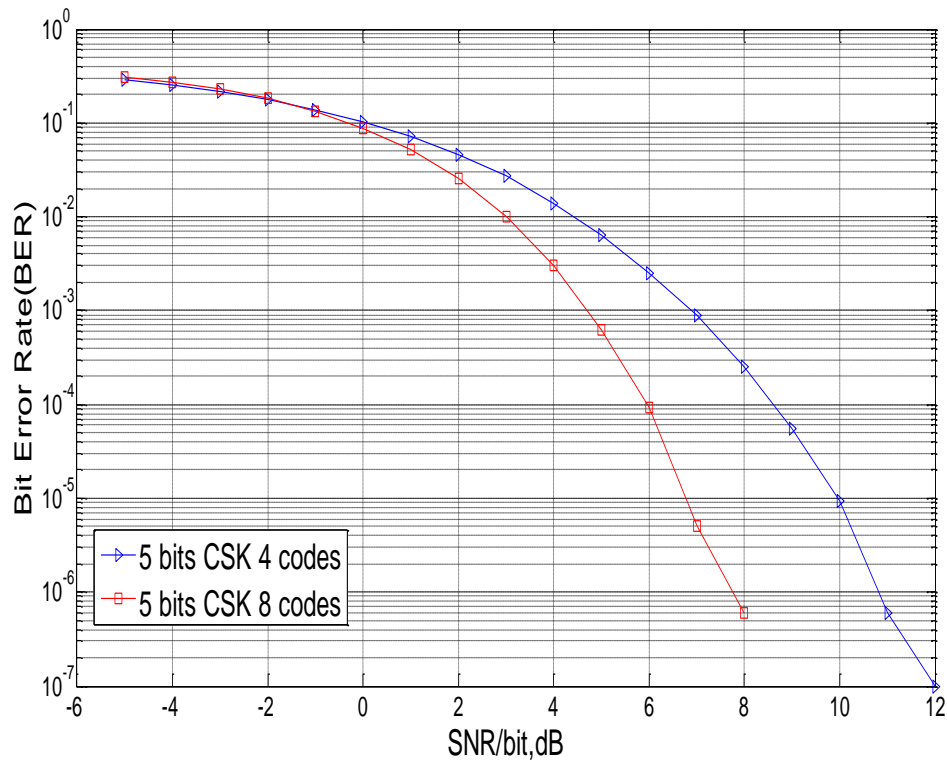


Fig. 3.10 Performance comparison in CSK Modulation when the number of available codes varies and the transmission rate remains the same (5 bits per time slot) in an ideal channel scenario.

It is easily noticeable from Fig. 3.10 that the system with the 8 codes performs better than the corresponding one with the 4 codes. When 8 codes are employed, the system uses QPSK modulation, whereas in the case of 4 codes the system employs 8-QAM modulation. It is well known [11] that BER performance of signals that use 8-QAM modulation is worse than those signals in which QPSK modulation is applied.

When SNR values are below 0 dB we can see that the two plots cross each other and the system in which four codes are available performs slightly better. This is attributed to the fact that the selection algorithm detects the

signal with the greatest power and in such a noisy environment the estimation is more likely to be erroneous. When 8 codes are available then, it is less likely to opt for the right one.

Fig. 3.11 depicts the same scenario as in Fig. 3.10 apart from the fact that the channel paths are now Rayleigh slow fading.

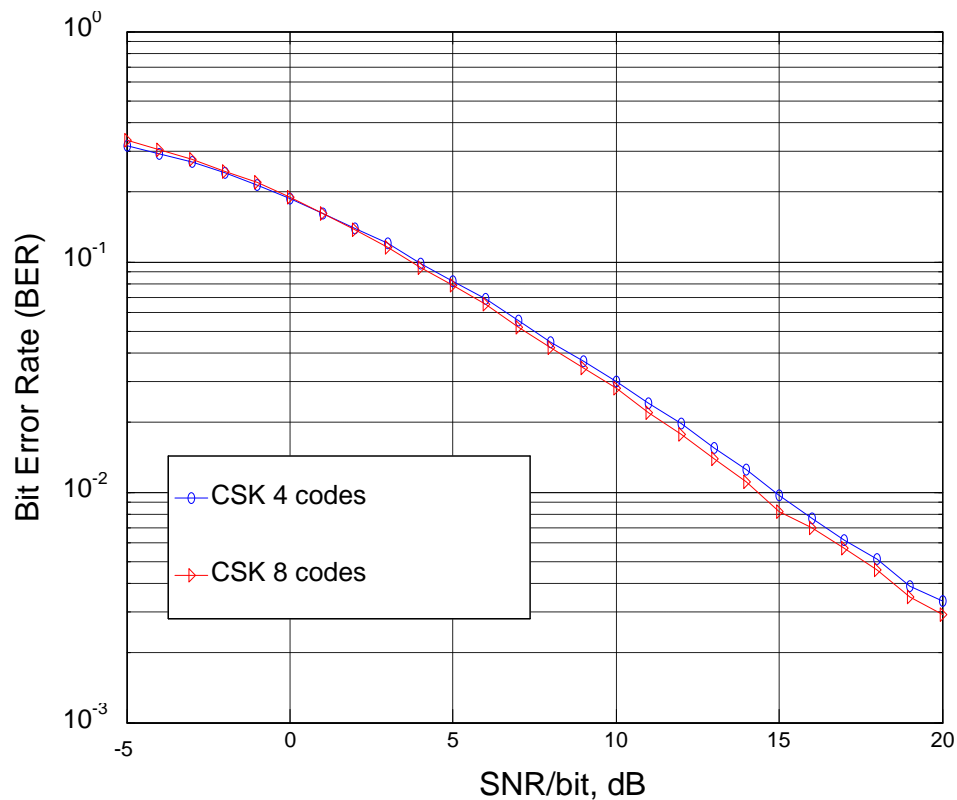


Fig. 3.11 Performance comparison in CSK Modulation when the number of available codes varies and the transmission rate remains the same in a Rayleigh slow fading channel scenario.

Although, there is still enhancement in performance, this is not as significant as in an AWGN channel case. This is because of the existence of channel imperfections that make transmission less robust. It is also worth referring that below 0 dB SNR the system with the 4 codes performs slightly better than the system with the 8 codes as already seen in Fig. 3.10.

Fig. 3.12 depicts the performance of Improved CSK in a SIMO system that employs four receiver antennas, two orthogonal codes (length two each) and 8-ASK modulation. For fair comparisons, the systems that use the conventional CSK technique as well as the conventional SM technique are also plotted in the same figure. All systems have the same net spreading level. Transmission rate is five bits per symbol. In the case of conventional CSK, where four orthogonal codes are available in a SISO system, each code will transmit an 8-QAM symbol.

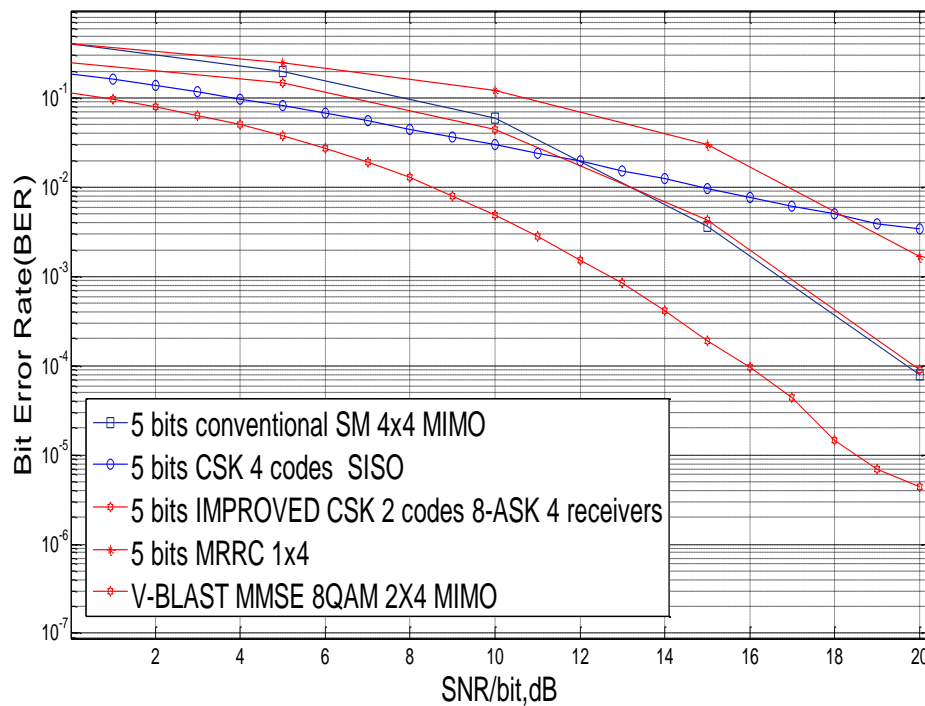


Fig. 3.12 Performance comparison between the improved CSK and the conventional SM, MRRC and V-BLAST MMSE scheme.

Likewise in the case of conventional SM, where a 4x4 MIMO system is employed, each transmit antenna will use an 8-QAM symbol. It can be seen that the Improved CSK, although it employs 8-ASK modulation, outperforms conventional CSK, SM, MMRC and V-BLAST MMSE schemes at about 5 dB. Using a smaller amount of spreading codes allows us to employ more receive

antennas so as to boost performance due to spatial diversity at the receiver. We always make sure that the net-spreading level of the systems remains the same.

Fig. 3.13 introduces the BER performance of the Improved CSK technique in Flat Rayleigh fading channel coefficients. Transmission rate is three bits and two spreading codes are available. Moreover, in Fig. 3.13 is also plotted the conventional CSK scheme in a SISO system when four codes are available.

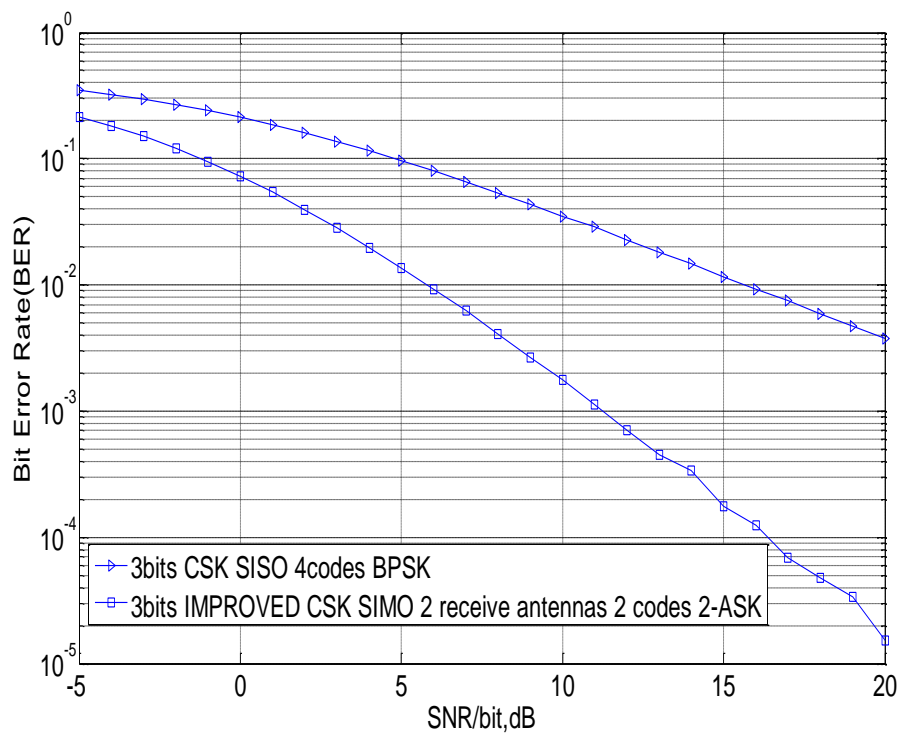


Fig. 3.13 Performance comparison between the Improved and the conventional CSK when transmission rate is 3 bits per period of interest

The net spreading level of the proposed system is half the size of the one that employs the conventional CSK, although it manages to provide much better performance at the receiver.

In Fig. 3.14 the performance of the Improved CSK in three bits transmission rate in a SISO system is compared with the one that uses the conventional CSK. The conventional scheme employs four spreading codes whereas the Improved CSK employs only two codes. The number of receive antennas in both systems is one. However, the net spreading level of the proposed scheme is 75% smaller than in the conventional one.

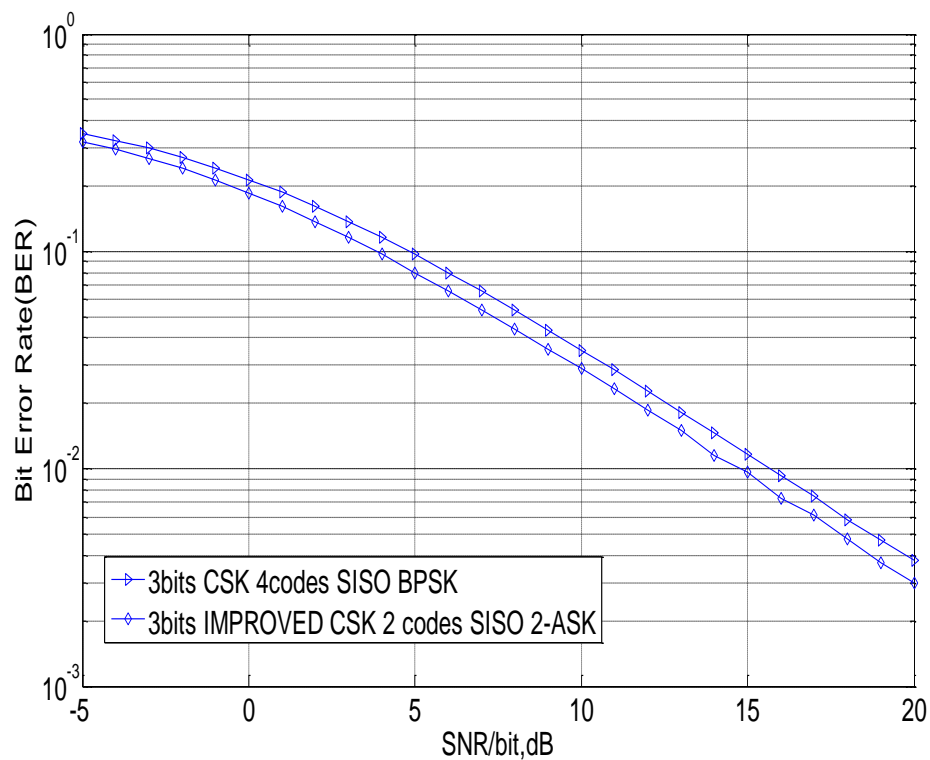


Fig. 3.14 Performance comparison in CSK Modulation when the number of available codes varies and the transmission rate remains the same in an ideal channel scenario

It is easily noticeable from Fig. 3.14 that the Improved CSK provides slightly better performance. This is attributed to the fact that the code index estimation algorithm has to identify less spreading codes and also that the constellation symbols used in this scenario are 2-ASK which provide the same performance as the BPSK symbols.

Fig. 3.15 plots the conventional CSK SISO system when eight codes are available as well as the Improved CSK scheme in the same transmission rate when four codes are available and the number of receive antennas is two. The net spreading level of the proposed scheme is half the size of the level of the conventional CSK, once only four codes (length four each) are available and thus we can employ two receive antennas so as to boost the performance of the receiver detection algorithm.

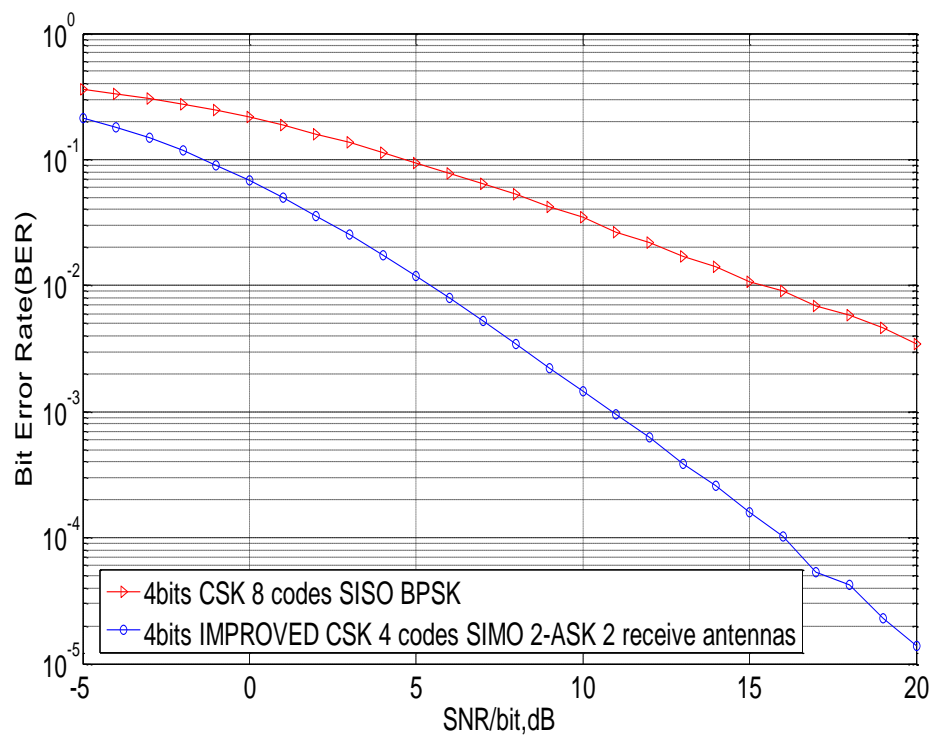


Fig. 3.15 Performance comparison between the Improved and the conventional CSK when transmission rate is 4 bits per period of interest. Net spreading level of the Improved CSK scheme is half the size of the conventional CSK scheme.

Fig. 3.16 depicts the Improved CSK scheme in a SISO configuration when two codes are available and each code will forward 4-ASK symbols at the destination. It is also plotted the conventional CSK SISO system when 8 codes are employed and each code employs BPSK modulation. Transmission

rate is four bits per period of interest. The net spreading level of the proposed system is remarkably smaller (about 87.5%) than the one in the conventional CSK once only two spreading codes are available.

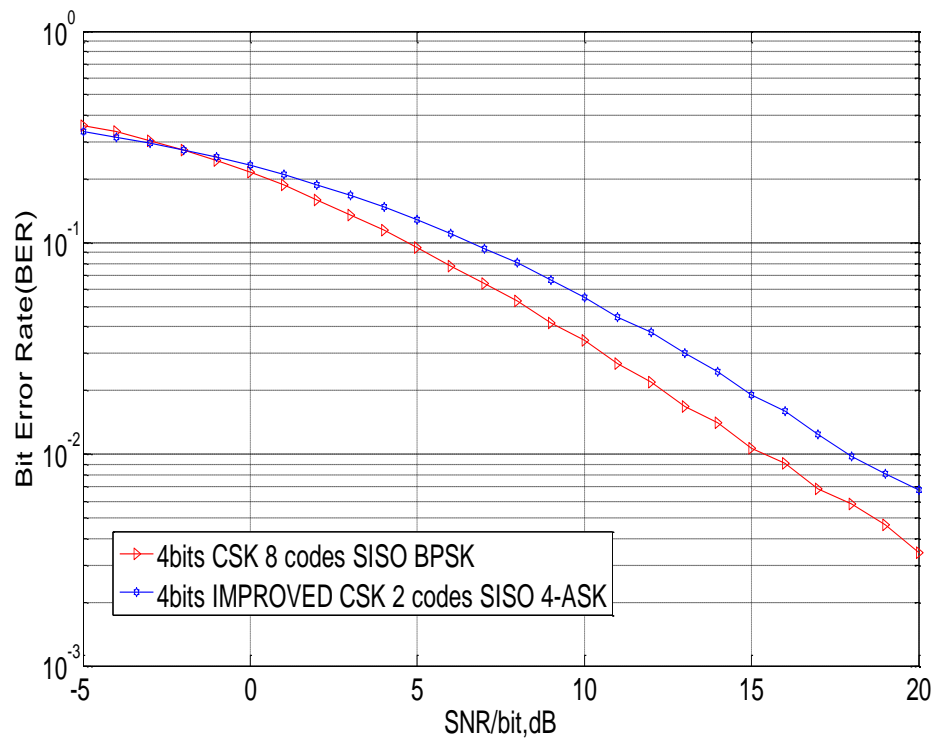


Fig. 3.16 Performance comparison between the Improved and the conventional CSK when transmission rate is 4 bits per period of interest. Number of receive antennas is one in both systems

It can be seen that the Improved CSK in this scenario provides slightly worse performance and this is mainly attributed to the fact that 4-ASK symbols are more difficult to be estimated than the BPSK symbols. When SNR values are below 0 dB we can see that the two plots cross each other and the system in which two codes are available performs slightly better. The selection algorithm detects the signal with the greatest power and in such a noisy environment the estimation is more likely to be erroneous when more codes are available into the system.

By increasing the net spreading level of the proposed scheme performance is significantly enhanced and this can be seen in Fig. 3.17. The proposed scheme now has four receiver antennas and two spreading codes.

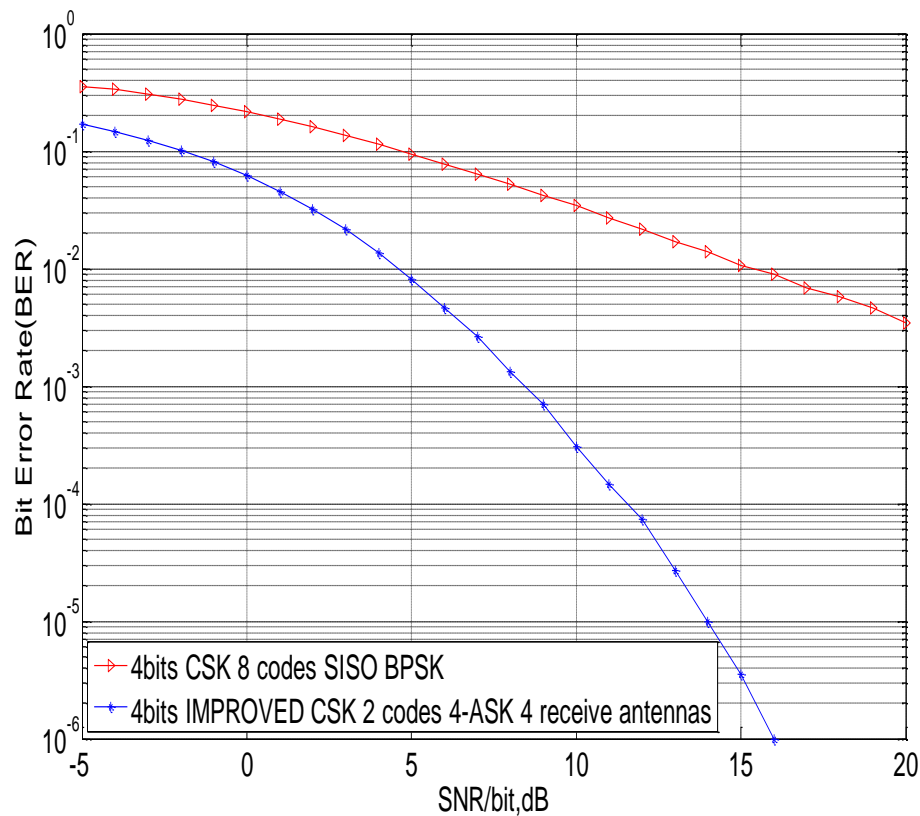


Fig. 3.17 Performance comparison between the Improved and the conventional CSK when transmission rate is 4 bits per period of interest

Throughput results of the proposed techniques are depicted in Fig. 3.18 and 3.19. Throughput is expressed as $T_r = (1-\text{BLER}) \cdot m \cdot N$ bits/channel use [31], where BLER is the block error rate, $m = 1$ bit/symbol for BPSK and $m = 2$ for QPSK. The block length used for these simulations is $N_f = 100$ symbols. In Fig. 3.18 the case of CSK in five bits transmission rate is shown. The channel is AWGN and the number of available spreading codes is 8 and 4 respectively.

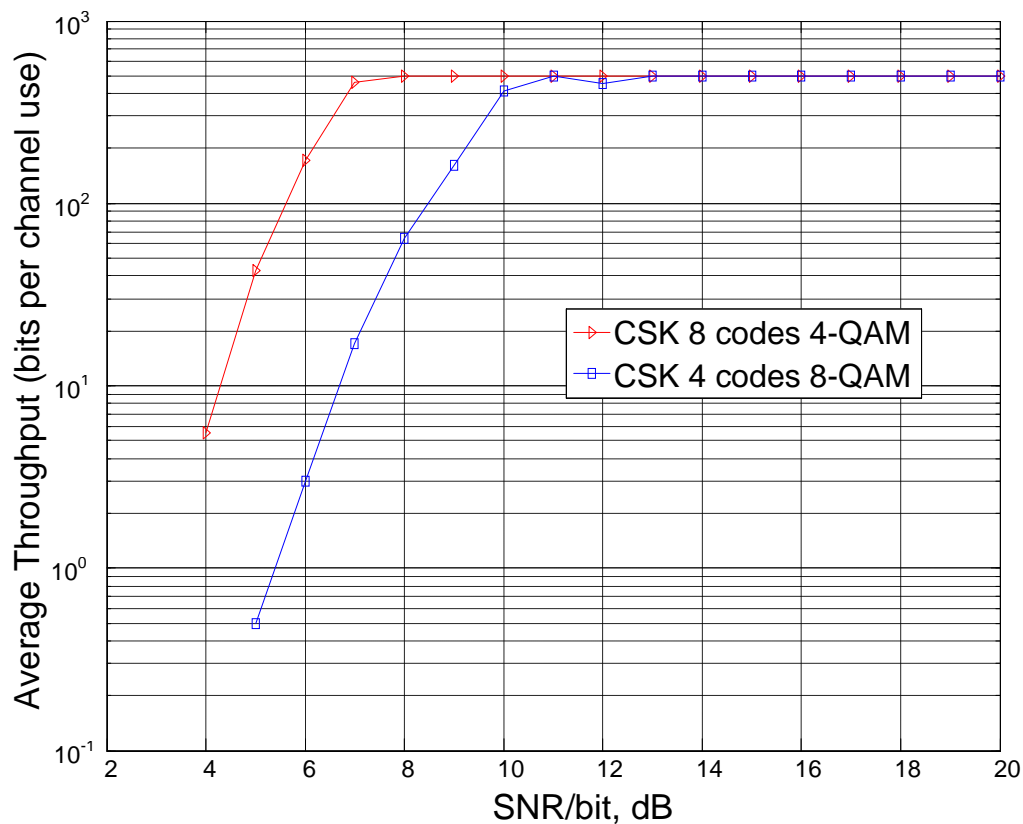


Fig. 3.18 Throughput results in CSK modulation when the number of available spreading codes is four and eight respectively in an ideal channel scenario

A constant transmit SNR gain of 2.5dB is observed when the number of the available spreading codes is 8. This is magnified to 3dB and it exists for up to 10dB SNR where both scenarios attain optimum performance.

In Fig. 3.19 the throughput of the proposed techniques is compared. The channel is flat Rayleigh fading and the number of available spreading codes is 4 (length four each) in the CSK and 2 (length 2 each). Therefore, the net-spreading of the Improved CSK is half the size of the conventional CSK. The Improved CSK attains better throughput results since it uses less number of

spreading codes and the symbol transmitted (2-ASK) provides the same levels of performance with BPSK.

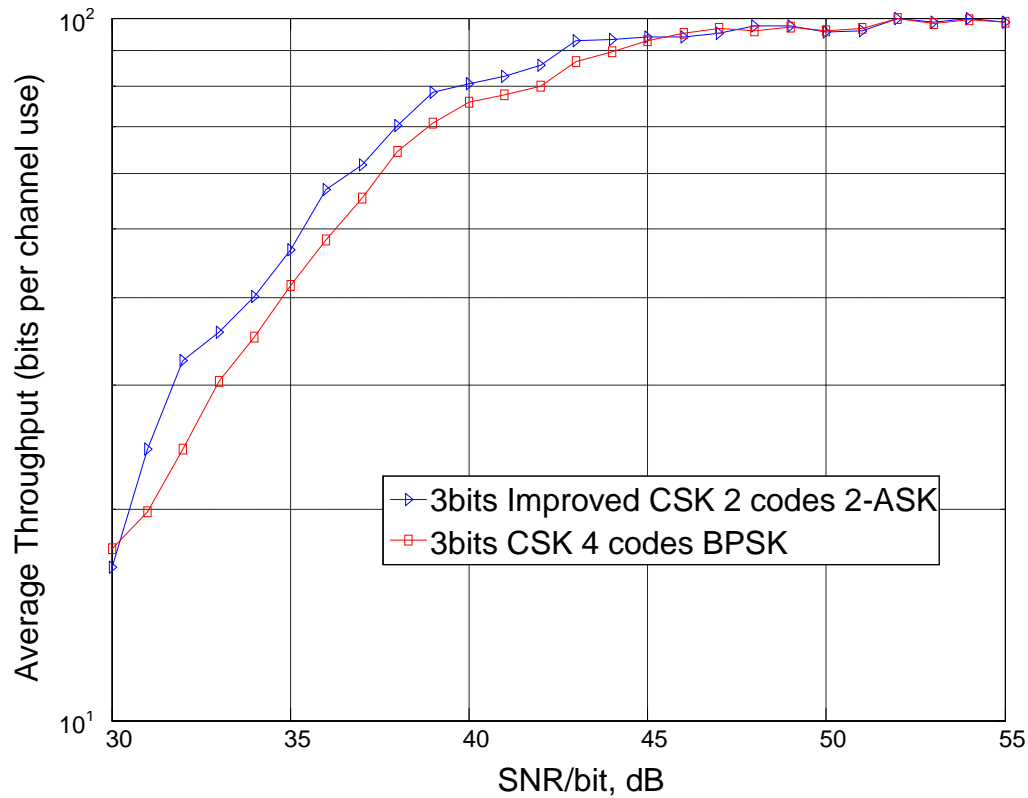


Fig. 3.19 Throughput results in CSK and Improved CSK modulation when the number of available spreading codes is 4 and 2 respectively in a flat Rayleigh fading channel scenario.

3.9 Summary

In this chapter CSK Modulation and Improved CSK Modulation have been presented. Namely, Walsh Hadamard orthogonal spreading codes and a symbol from a constellation diagram both convey information at the receiver. In CSK modulation the number of antennas is remarkably reduced at the cost

of increased bandwidth usage as orthogonal codes are employed to convey bit of information instead of antennas. Complexity is significantly reduced compared to conventional SM and the CSK shows improvements in BER performance compared to SM, MRRC and V-BLAST MMSE over a significant range of SNR values at the cost of increased bandwidth usage. This enhancement stems from the code selection algorithm that has been proposed. Two SIMO systems have also been introduced, while we maintain the net spreading level of the systems the same. Performance of these systems is significantly improved because of the exploitation of the existing high receive diversity order along with the orthogonality of the codes.

Chapter 4

Polarization Assisted Space Shift Keying Modulation

In conventional SM antenna index estimation errors can significantly degrade system performance and therefore, increased diversity at the receiver is normally used to minimise this problem. Moreover, this method can only work under normalised channel conditions. To overcome these drawbacks, in this chapter we consider exploiting the polarisation domain as a comparative study to SM. For the representation of information bits, a symbol from a signal constellation diagram and a polarisation from the polarisation domain are required. At the receiver estimation of the signal as well as the polarisation index occurs. For this purpose, a polarisation index detection algorithm is introduced. It will be shown that this alternative approach outperforms the conventional SM technique as well as MRRRC and V-BLAST MMSE schemes, in terms of BER performance, over a significant range of SNR values. Finally, it will be demonstrated that complexity of the system is halved.

4.1 Introduction

This chapter introduces a new scheme in which the antenna index estimation is not needed. Also in this approach we overcome SM's biggest drawback which is its inability to perform in conventional channel conditions. The method proposed is referred as Polarisation Assisted Space Shift Keying (PASSK) Modulation. Each of the two available polarisations is used to convey information bits at the destination, along with the transmitted symbol. One polarisation is used in each time slot. The ideal case of dual-polarised antennas is discussed here in which the level of cross polarisation effects is zero. During reception the system estimates which polarised receiver antenna has received the signal and then the corresponding polarisation is classified as the active one. We show that PASSK technique performs better over a significant range of SNR values. Finally, it is demonstrated that the system's complexity is halved compared to conventional SM. The proposed technique stems its idea from [12] where the performance of multiantenna signalling techniques in the presence of polarisation diversity is investigated. These techniques are mainly preferred when large antenna spacing, which is required to achieve significant diversity, is not desirable by the size of the transmitter and receiver devices. The richness of scattering is also an important factor that contributes to the performance of a MIMO system and dual polarised antennas are mainly preferred when the channel is not sufficiently rich in scattering [12].

The rest of the chapter is organised as follows, in Section 4.2 the PASSK technique is illustrated in details. Moreover, a complexity analysis for the proposed technique follows in section 4.3. Finally in section 4.4 and 4.5 simulation results and conclusion are introduced, respectively.

4.2 Basics of the PASSK Technique

In this section we describe the new technique that employs dual polarised antennas to convey information at the receiver. The polarisation domain is exploited and each antenna polarisation is used to convey information bits at the receiver. The system consists of one transmitter dual polarised antenna and multiple dual polarised antenna receivers. The total bit rate is distributed over the two available polarisations and the symbol that is chosen from a constellation signal. In practice, two polarisation schemes are typically used: horizontal/vertical ($0^\circ / 90^\circ$) or slanted ($45^\circ / -45^\circ$). Therefore, for a fixed bit rate transmission the two polarisations will represent one bit of information and the rest will be mapped into a symbol from a constellation diagram. When the transmission rate is three bits per period then each of the two polarisations will forward a QPSK symbol at the destination (see TABLE 7). At the receiver the polarisation index along with the transmitted symbol will determine the total number of information bits.

TABLE 7 MAPPING TABLE FOR POLARISATION ASSISTED SHIFT
KEYING MODULATION

Input Bits	2 Polarisations , QPSK	
	Polarisations	Transmitted Symbol
000	Horizontal	$1+j$
001	Horizontal	$1-j$
010	Horizontal	$-1+j$
011	Horizontal	$-1-j$
100	Vertical	$1+j$
101	Vertical	$1-j$
110	Vertical	$-1+j$
111	Vertical	$-1-j$

4.2.1 Polarisation Index Estimation

In a MIMO system, where PASSK is applied, the corresponding polarisation that has been active needs to be identified. Therefore, a novel polarisation estimation algorithm is proposed. For the sake of simplicity, and without loss of generality, the system consists of one transmitter dual polarised antenna and one receiver dual polarised antenna (see Fig. 4.1). The paths with the black solid lines in Fig. 4.1 are the auto-polarisation paths that connect the antenna elements with the same polarisation.

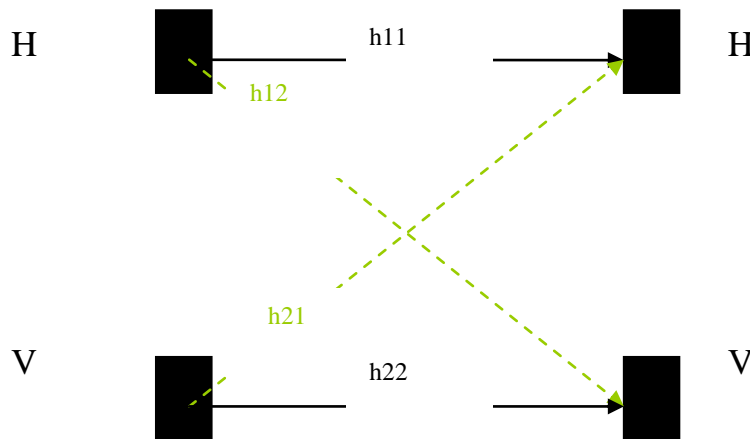


Fig. 4.1 2x2 MIMO system consisted of one dual polarised transmitter antenna and one dual polarised receiver antenna (H: horizontally, V: vertically polarised)

The green dotted line paths in Fig. 4.1 are the cross-polarisation paths and in our case they are assumed to be zero as the antennas are perfectly polarised. Assuming that, the horizontal (H) polarisation has been employed in this time, the received signal can be described as follows:

$$\mathbf{r} = x[|h_{11}|^2, |h_{12}|^2] + [n_1, n_2] \quad (4.1)$$

$$\mathbf{r} = x[|h_{11}|^2 + n_1, n_2] \quad (4.2)$$

where h_{11} is the path that connects the horizontal polarised transmitter antenna with the horizontal polarised receiver antenna and h_{12} is the path that connects the horizontal transmitter antenna with the vertical receiver antenna because of the cross-polarisation effects (see Fig. 4.1). In the ideal case the latter path is zero and thus the vertical receiver antenna receives no signal. Eventually, the detection algorithm will identify which of the two polarisations at the receiver has received the signal with the greatest power.

$$\mathbf{r} = [r_1 \quad r_2] \quad (4.3)$$

$$\tilde{l} = \arg \max_j |\mathbf{r}|. \quad (4.4)$$

In the case of physical antennas this cannot be applied because each antenna receives signals from the transmitter that have on average the same power.

4.2.2 Case study

To clarify the working principle of the proposed we consider the case of 3 bits PASSK modulation using 1x2 antenna configuration. The mapping table for 3 bits transmission using dual polarised antenna devices and QPSK modulation is shown in TABLE 7. Assuming that the bits to be transmitted are $\mathbf{q}(k)=[1,0,0]$, from the mapping table we can map this sequence to $x=1+j$ and the active polarisation will be the vertical one. The MIMO channel configuration will be

$$\mathbf{H} = \begin{bmatrix} -1.4594 - 1.0562j & 0.3677 - 2.5214j & 1.3326 - 0.7319j & -0.4760 + 0.063j \\ 0.0192 + 0.3273j & -0.9709 + 0.2732j & -0.2320 - 0.3939j & 1.1499 - 0.7499j \end{bmatrix}.$$

The SNR in this example is 8dB. Thus the symbol will be forwarded through the channel \mathbf{H} at the destination and the received signal will be

$$\mathbf{r} = [0.1762 + 0.1278j \quad -0.9830 - 0.3806j \quad -0.1460 + 0.0957j \quad 1.4548 + 0.1809j].$$

The polarisation index estimation algorithm is considered in the following and the channel is assumed to be known at the receiver. The first and third element of the signal \mathbf{r} is the signal received in the Horizontal receive antennas and the second and forth element is the signal received in the vertically polarised receive antennas respectively. Applying the estimation algorithm to the received vector results in

$$\mathbf{P} = [0.0778 \quad 3.2604].$$

By observing the vector \mathbf{P} , we see that $\mathbf{P}(2)$ is the largest element. From this element we are able to estimate that vertical polarisation has been employed as this represents the power of the received signal. Moreover, once the polarisation has been identified the in-phase received signal is

$$\mathbf{r} = 2.3877 + 1.9370j$$

and therefore the received symbol $\bar{x} = 1 + j$ have been employed. From the estimated polarisation and symbol we can retrieve the initial sequence of bits $\bar{\mathbf{q}}(k) = [1, 0, 0]$, which exactly corresponds to the transmitted bits.

The estimation of the transmitted bits is based on the power at the received polarised antennas and not the cross correlation of the different channels like in conventional SM.

4.3 Complexity Estimation

It is shown [27] that the number of multiplications when the system uses conventional SM is

$$\delta_{SM} = 2N_r N_t + N_t \quad (4.5)$$

where N_r is the number of receive antennas and N_t is the number of transmit antennas. In the case of the proposed approach we can likewise view that we have N_r multiplications when the received signal is formed. During reception we have 2 comparisons once the two different polarisations are investigated in order to detect which one has received the signal. Finally, once estimation of the polarisation has occurred we perform N_r calculations so as to retrieve the signal transmitted. Therefore, the total number of multiplications is

$$\delta_{PASSK} = 2N_r + 2 \quad (4.6)$$

where N_r is the number of receiver antennas in the dual MIMO system. Assuming that the net-spreading levels of the systems remain the same, we can see that in a 2x4 MIMO system that employs SM we have 20 calculations and in the alternative 1x2 dual MIMO system (2x4 virtual) that employs the PASSK technique we have only 6 calculations. This leads to a remarkable reduction in system's complexity.

4.4 Numerical Simulation

In this section we validate the proposed approach by means of simulation results for various scenarios. In the simulations either a flat Rayleigh or Rician fading channel is assumed. The channel is assumed to be known at the receiver. The Monte Carlo technique (see Appendix A.4.3) is applied for the estimation of the Bit Error Rate. The SNR is defined as $\frac{P}{\sigma^2}$, where P is the total transmit power, which is the same for all transmission, and σ^2 is the noise variance. Finally, the variance of the fading channel paths is 1.

Fig. 4.2 introduces the performance in terms of the bit error rate. Transmission rate is 3 bits per symbol. The system consists of one transmitter dual polarised antenna and two receiver dual polarised antenna elements (2x4 MIMO channels). For the sake of easier comparison, in Fig. 4.2 is also plotted the conventional SM method in a 2x4 MIMO system and 3 bits transmission rate along with the MMRC and V-BLAST schemes.

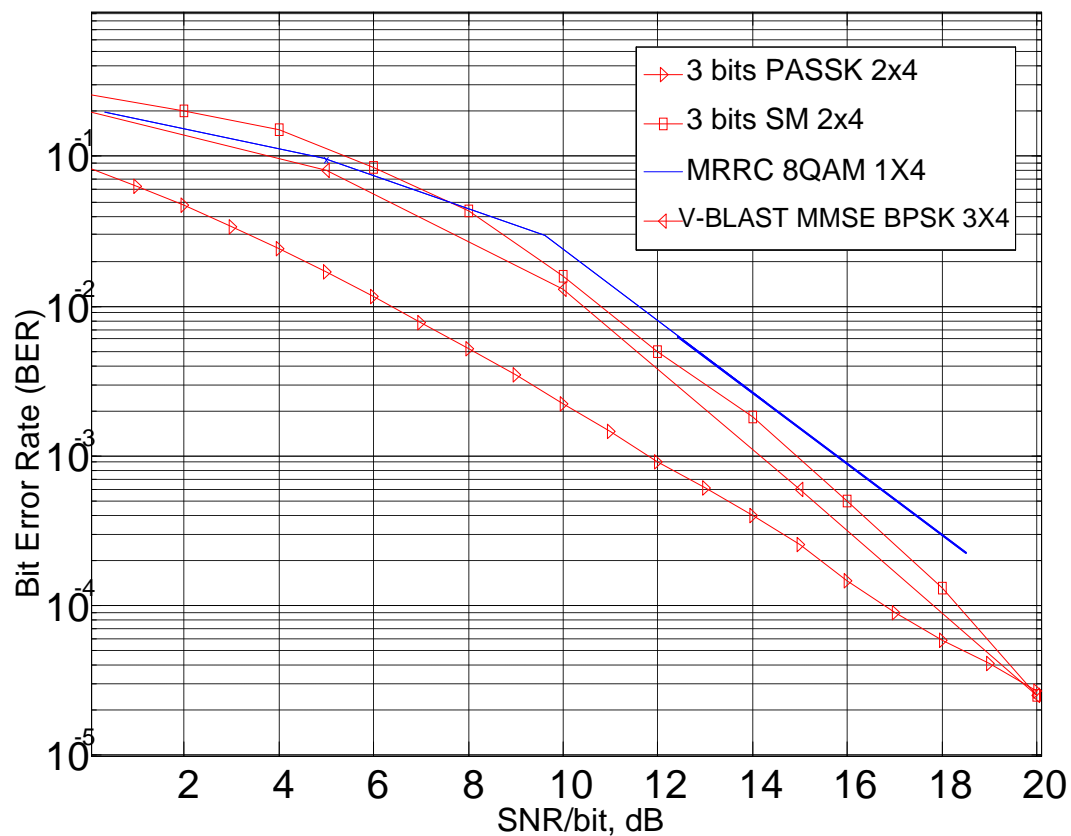


Fig. 4.2 Performance comparison between the proposed and SM when transmission rate is 3 bits per symbol

In the above scenario we can see the superiority of the new approach that employs polarisations. This enhancement relies on the fact that the detection algorithm of the PASSK scheme performs better than the antenna detection algorithm at the conventional SM, since we assumed that the level of cross polarisation effects is zero. The two figures cross each other when SNR is 20dB because in dual polarised antennas diversity is not fully exploited, once only half of them receive as opposed to conventional SM that fully exploits receive diversity.

In Fig. 4.3 it is attempted to compare the performance of the proposed technique for various numbers of bits per period of interest. Namely, the transmission rate is 3 and 4 bits per period respectively and the number of available polarisations is 2. In the case of 3 bits, each polarisation will forward a QPSK symbol and when the number of the bits is 4 then each polarisation will forward an 8-QAM symbol. The channel paths are Rayleigh fading coefficients.

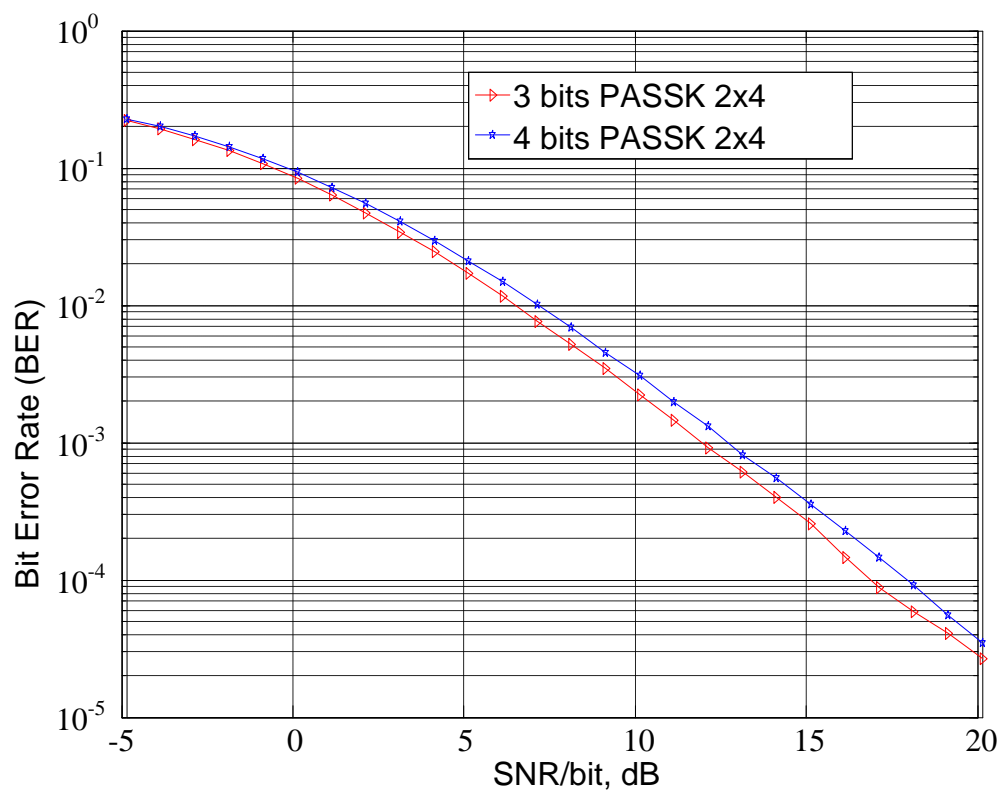


Fig. 4.3 Performance comparison in PASSK when the number of available polarisations is 2 and the transmission rate varies in a Flat Rayleigh fading channel scenario

It is easily noticeable from Fig. 4.3 that the system, in which transmission bit rate is 4, performs slightly worse than the corresponding one where transmission rate is 3 bits. This is attributed to the fact that in an environment of 4 bits transmission rate, where two orthogonal polarisations are available,

each polarisation will forward an 8-QAM symbol. On the other hand, when transmission rate is 3 bits each polarisation will forward a QPSK symbol.

Figure 4.4 depicts the same scenario as in fig. 4.3 apart from the fact that the channel paths are now Rician fading. In Rician fading there is always a dominant line of sight and thus performance of the system is significantly enhanced.

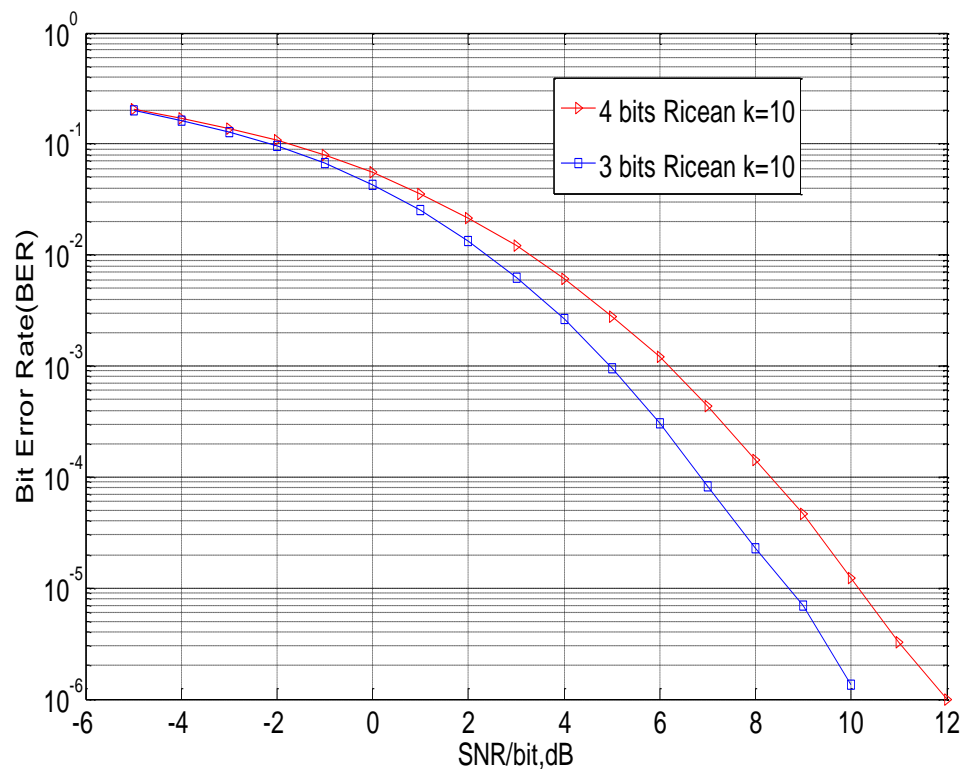


Fig. 4.4 Performance comparison in PASSK when the transmission bit rate number varies and the available polarisations are 2 in a Rician channel scenario and $K=10$

It is obvious from the above figure (see Fig. 4.4) that the difference in performance is more significant compared to Fig. 4.3, once less channel imperfections occur in this type of channel.

Fig. 4.5 depicts the performance of the same system in the Rician channel scenario when the k -factor is 20.

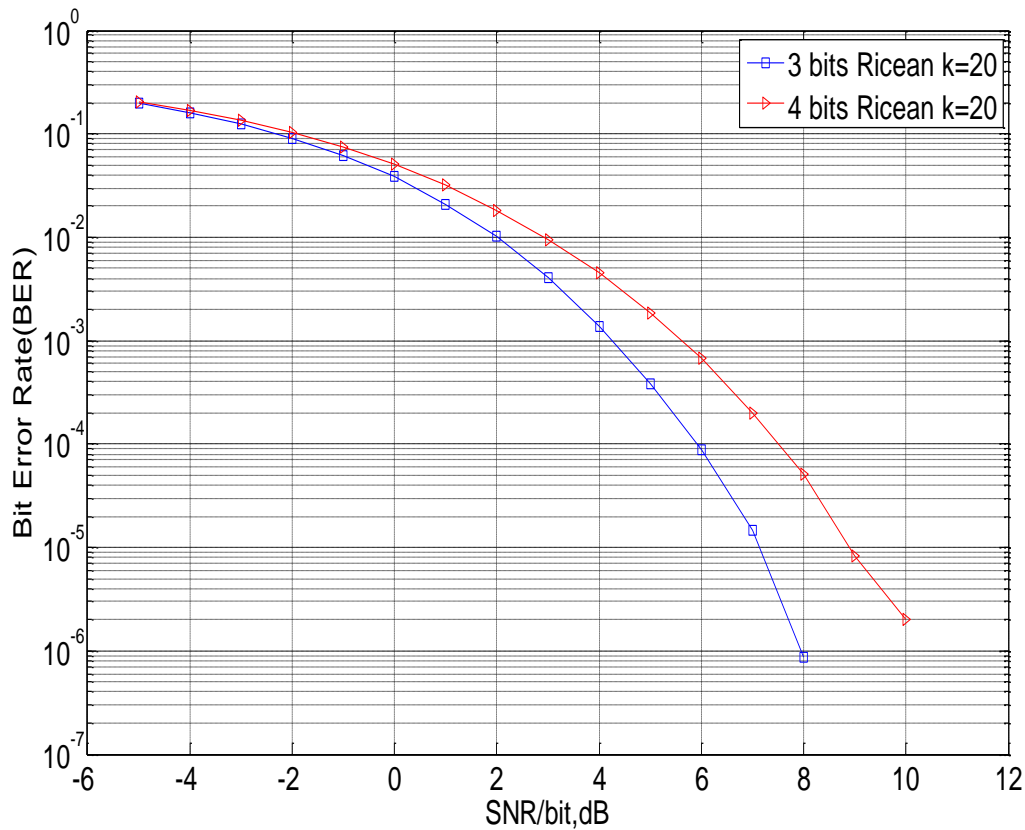


Fig. 4.5 Performance comparison between PASSK when the transmission rate varies and the available polarisations are 2 in a ricean channel scenario when the k-factor is 20

Performance is even further enhanced when k-factor is increased to 20. The dominant line of sight wave makes the channel more stable and with fewer imperfections. The more stable the channel the more visible the difference in performance because of the symbols transmitted through each polarisation.

So far, the ideal case of these antennas is discussed in this chapter where no cross-polarisation effects exist. In practice though, the dual polarised antenna devices experience cross coupling of the polarisation mainly due to the scattering of the channel environment. In such a scenario Fig. 4.6 introduces the performance of PASSK in three bits transmission rate for

different levels of cross polarisation effects. The system consists of one transmitter antenna element and two receiver antenna elements (2x4 MIMO). For the sake of easier comparison, in Fig. 4.6 is also depicted the conventional SM method in a 2x4 MIMO system and 3 bits transmission rate.

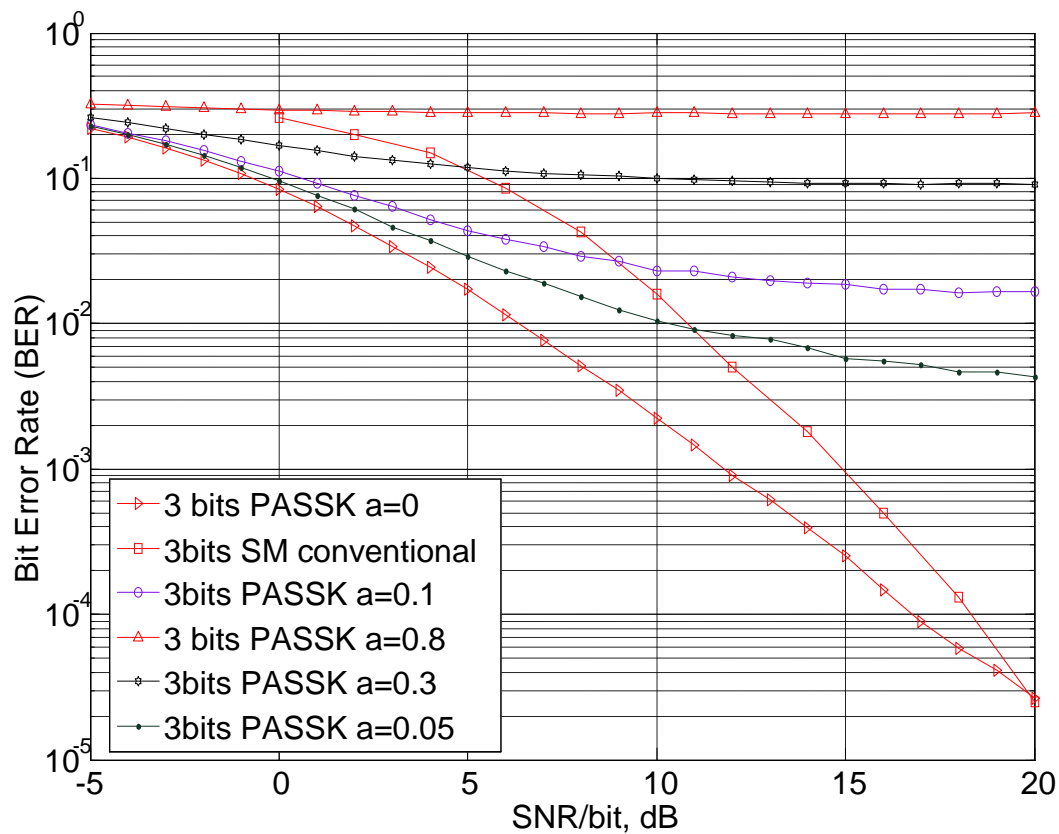


Fig. 4.6 Performance comparison between the PASSK and SM at different levels of cross-polarisation effects and when transmission rate is 3 bits per period of interest. The system is MIMO 2x4 in all cases

In Fig. 4.6 we can see the performance degradation under the existence of cross-polarisation effects. PASSK estimates erroneously the corresponding polarisation at the receiver once both antennas receive signal information. The higher the level of these effects (higher value of a), the worse the performance of the algorithm.

Throughput results of the proposed techniques are depicted in Fig. 4.7. Throughput is expressed as $T_r = (1-BLER) \cdot m \cdot N$ bits/channel use, where $BLER$ is the block error rate, $m = 1$ bit/symbol for BPSK and $m = 2$ for QPSK. The block length used for these simulations is $N_f = 100$ symbols. In Fig. 4.7 the case of PASSK is shown in three and four bits transmission respectively. The channel is 2x4 MIMO Rician with k-factor 20.

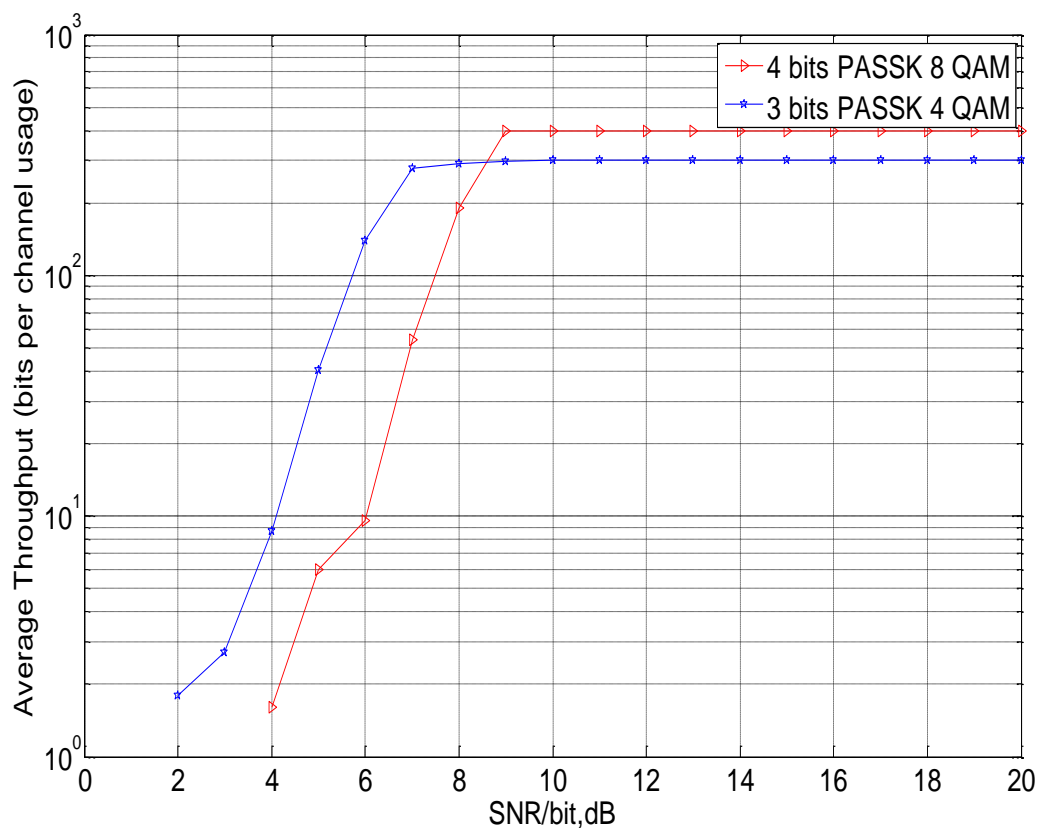


Fig. 4.7 Throughput results in PASSK modulation in three and four bit transmission rate when the channel is Rician ($K=20$)

A constant transmit SNR gain of 2 dB is observed when the number of bits is three and this is attributed to the fact that in three bits transmission the symbol to be identified is 4-QAM unlike the case of four bits where an 8-QAM symbol needs to be estimated. This exists for up to 9dB SNR where the four

bits scenario attains better performance since noise is negligible and symbol estimation more robust.

4.5 Summary

In this Chapter PASSK modulation with very low complexity has been introduced. Dual polarised antenna elements are deployed and the available polarisations convey information at the receiver. The ideal case of these antennas is discussed in this chapter where no cross-polarisation effects exist. The proposed method requires half the amount of calculations compared to the conventional SM and shows better BER performance in comparison with SM, MMRC and V-BLAST MMSE (below 20 dB SNR). This enhancement stems from the polarisation index selection algorithm that has been proposed. As future work the non-ideal case of these antennas could be a topic of analysis because system's performance is severely downgraded once the polarisation index estimation algorithm fails to identify the corresponding polarisation. Therefore it is worth attempting to either eliminate or exploit the existence of cross polarisation effects at the cost of slightly increased complexity.

Chapter 5

Precoded Polarization Assisted SSK

In PASSK Modulation, the existence of cross polarisation effects can significantly degrade the system's performance. In this chapter we consider either eliminating or exploiting these effects by precoding at the transmitter depending on some criterion that will be described later. The MIMO channel is assumed to be known at the transmitter, once precoding occurs. At the transmitter for the representation of information bits, a symbol from a signal constellation diagram and a polarisation from the polarisation domain are required. Similar to PASSK, at the receiver estimation of the signal as well as the polarisation index is needed. It will be shown that the proposed technique is able to exploit some of the cross polarisation effects and hence provide better performance over PASSK, conventional SM, MRRRC and V-BLAST MMSE.

5.1 Introduction

This Chapter introduces Precoded Polarisation Assisted Space Shift Keying (PPASSK) Modulation as a means to eliminate or exploit the cross-polarisation effects. The proposed technique will be shown to be most effective at the lower signal to noise (SNR) regions relative to PASSK. Similar to PASSK, each of the two available polarisations is used to convey information at the destination, along with the transmitted symbol. One polarisation is available at each time slot. At the transmitter this method knows which polarisation is active and thus with precoding is attempted to eliminate the cross-polarised channel effects. During reception, the system estimates which polarised receiver antenna has received the signal and then the corresponding polarisation is classified as the active one.

The rest of the Chapter is organised as follows, in Section 5.2 the PPASSK technique, in which the cross polarisation effects are either eliminated or exploited, is fully described. This is followed by a complexity analysis of the proposed technique in Section 5.3. In Section 5.4 we verify our results with an Signal to Interference Noise Ratio (SINR) analysis when the cross polarisation effects are eliminated or exploited. Finally in Section 5.5 and 5.6 simulation results and conclusion are presented, respectively.

5.2 The *PPASSK* Technique

In this section we describe the new technique that employs dual polarised antennas [12]. In this stage the cross polarisation effects of these antennas will be either eliminated or exploited. The system consists of one dual polarised transmit antenna and multiple dual polarised receive antennas. Similar to the conventional PASSK the detection algorithm has two steps. During the first step the system attempts to estimate the polarisation that has been employed and at the second step it attempts to identify the symbol transmitted. The cross polarisation effects can severely degrade performance at the first step of this technique. Therefore, precoding is employed at the transmitter. Similar to PASSK, the total bit rate is distributed over the two available polarisations and the symbol that is chosen from a constellation signal. In more detail, when the transmission rate is three bits per period then each of the two polarisations will forward a QPSK symbol [2] at the destination (see TABLE 8). At the receiver the polarisation index along with the transmitted symbol will determine the total number of information bits.

TABLE 8 MAPPING TABLE FOR PRECODED POLARISATION
ASSISTED SHIFT KEYING MODULATION

Input Bits	2 Polarisations	QPSK
	Polarisations	Transmitted Symbol
000	Horizontal	$1+j$
001	Horizontal	$1-j$
010	Horizontal	$-1+j$
011	Horizontal	$-1-j$
100	Vertical	$1+j$
101	Vertical	$1-j$
110	Vertical	$-1+j$
111	Vertical	$-1-j$

5.2.1 Polarisation Index Estimation

In a system, where PPASSK has been applied, the corresponding polarisation that has been active needs to be identified. Therefore a polarisation estimation algorithm, which stems its idea from PASSK, is first introduced. For the sake of simplicity, but without loss of generality, the system consists of one dual polarised transmit antenna and one dual polarised receive antenna (see Fig. 4.1). Assuming that the horizontal (H) polarisation has been employed in the 2x4 MIMO system (see Fig. 4.1), the paths with the black solid lines are the auto-polarisation paths that connect the antenna elements with the same polarisation.

The green line paths in Fig. 4.1 are the cross-polarisation paths. At the receiver and without precoding the signal is given as follows:

$$\mathbf{r} = x[h_{11} \quad h_{12}] \quad (5.1)$$

where x is the transmitted symbol, h_{11} is the path (black solid line in Fig. 4.1) connecting the horizontal transmitter antenna with the horizontal receiver antenna and finally h_{12} is the path (green line in Fig. 4.1) connecting the horizontal transmitter antenna with the vertical receiver antenna. Because of the cross-polarisation effects the latter path exists and therefore estimation of the polarisation index is severely degraded.

However, if we perform selective precoding at the transmitter then these effects can be potentially eliminated or even exploited. The precoded signal will be

$$\mathbf{a} = f\mathbf{T}s \quad (5.2)$$

where s the transmitted symbol, f is a normalisation factor that retains the energy of the signal at the same levels as the ones before precoding [14]

$$f = 1/\sqrt{((s^H \mathbf{T}^H \mathbf{T} s))} \quad (5.3)$$

and \mathbf{T} is the precoding vector

$$\mathbf{T} = [h_{11} \quad 0]^H. \quad (5.4)$$

The precoding vector \mathbf{T} stems its form from Eq. (5.1), so as to eventually eliminate or exploit the effects of the cross polarised path h_{12} . As we observe from Eq. (5.2), the precoded signal \mathbf{a} is a 1x2 vector. The second element of this vector is selected to be zero once the Vertical polarisation is idle at this time instant. Therefore, all the important information is stored in the first element of vector \mathbf{a} . At the transmitter each polarisation is assigned to a

different carrier frequency. Thus, each element of the precoded vector is sent through the channel from each polarisation using the two carrier frequencies. For the elimination of the cross polarisation effects at the receiver, an investigation in the power of the received signal is performed in the Horizontal receive antenna in carrier frequency f_1 and in the Vertical receive antenna carrier frequency f_2 (see TABLE 9). The antenna that has received the signal with the greatest power will be chosen and finally the corresponding polarisation was the one that has been employed.

The exploitation of the cross polarisation effects in this scheme occurs in a similar way as the elimination of these effects during the first step of the algorithm (polarisation index estimation). The signal that is a result of these effects in this scenario is located in either the Vertical receive antenna in f_1 or in the Horizontal receive antenna in f_2 (see TABLE 9). Therefore, for the exploitation of the cross polarisation effects at the receiver, an investigation in the power of the received signal is performed in the Horizontal and Vertical receive antenna in f_1 and f_2 (see TABLE 9). This is the part of the algorithm that differentiates the exploitation and the elimination schemes. The frequency that has received the signal with the greatest power will be chosen and finally the corresponding polarisation was the one that has been employed.

TABLE 9 POLARISATION INDEX ESTIMATION IN PRECODED
POLARISATION ASSISTED SPACE SHIFT KEYING MODULATION

Polarised Receive Antennas	No Precoding	Precoding	
	PASSK	f_1	f_2
Horizontal	sh_{11}	$s h_{11} ^2$	0
Vertical	sh_{12}	$sh_{11}^* h_{12}$	0

In TABLE 9 we show that the received signal is, either free from cross polarisation effects or these effects are exploited, since the Horizontal and Vertical polarised antennas in f_2 have received no signal. It is easily understandable now that the corresponding polarisation can be estimated. The above were discussed for the noiseless case for the purpose of clarity.

5.2.2 Example: 3 bits Elimination of Cross Polarisation Effects in PPASSK

The mapping table for 3 bits transmission using dual polarised antenna devices and QPSK modulation is shown in TABLE 8. Assuming that the bits to be transmitted are $\mathbf{q}(k)=[1,0,0]$, from the mapping table we can map this sequence to $x=1+j$ and the active polarisation will be the vertical one. The MIMO channel configuration will be

$$\mathbf{H} = \begin{bmatrix} 0.5224 - 0.6177j & 0.7121 + 0.3686j & 0.1478 + 0.3068j & 0.0867 - 0.2426j \\ -0.1775 + 1.0746j & -0.7639 - 0.9757j & 0.2874 - 0.6819j & -1.4197 - 0.2411j \end{bmatrix}.$$

The SNR in this example is 8dB. Thus the symbol will be forwarded through the channel \mathbf{H} at the destination and the received signal will be the following

$$\mathbf{r} = \begin{bmatrix} -0.1281 - 0.2375j & 0.4396 - 0.1981j & -0.0954 + 0.0546j & 0.7359 - 0.7690j \\ -0.1206 + 0.0396j & -0.1509 + 0.2078j & 0.0746 + 0.1389j & 0.1041 + 1.0968j \\ -0.1639 + 0.3718j & 0.0303 + 0.5803j & 0.1280 + 0.0452j & -0.5459 + 0.4378j \\ -0.1231 + 0.0716j & 0.2821 - 0.0664j & 0.2380 - 0.0689j & 1.2763 + 1.0596j \end{bmatrix}.$$

The first and third column of the received signal \mathbf{r} show the signal that has been received in the receive antennas in f_1 and the second and fourth column show the signal that has been received in the receive antennas in f_2 . The polarisation index estimation algorithm is considered when the channel is assumed to be known at the receiver. Applying the estimation algorithm to the received vector results in

$$\mathbf{P} = [0.0912 \quad 2.8176].$$

By observing the vector \mathbf{P} , we see that $\mathbf{P}(2)$ is the greatest element. From this element we are able to estimate that the Vertical Polarisation has been employed as this represents the Power of the received signal in the Vertical Polarisation domain. Moreover, once the polarisation has been identified the in-phase received signal is as follows

$$\mathbf{r} = 1.1254 + 1.2674j.$$

Therefore, the received symbol $\bar{x} = 1 + j$ has been employed. From the estimated polarisation and symbol we can retrieve the initial sequence of bits $\bar{\mathbf{q}}(k) = [1, 0, 0]$, which exactly correspond to the transmitted bits. The estimation of the transmitted bits is based on the power at the received polarised

antennas and not the cross correlation of the different channels like in conventional SM.

5.2.3 Example: 3 bits Exploitation of Cross Polarisation Effects

The mapping table for 3 bits transmission using dual polarised antenna devices and QPSK modulation is shown in TABLE 8. Assuming that the bits to be transmitted are $\mathbf{q}(k)=[1,0,0]$, from the mapping table we can map this sequence to $x=1+j$ and the active polarisation will be the vertical one. The MIMO channel configuration will be

$$\mathbf{H} = \begin{bmatrix} 1.1562 - 0.6475j & -0.6126 + 0.8089j & -0.3172 - 0.3436j & 0.6450 - 0.5090j \\ -0.1790 + 1.0691j & 0.1450 - 0.4164j & -0.4556 + 0.2950j & 0.8293 - 1.0501j \end{bmatrix}.$$

The SNR in this example is 8 dB. Thus the symbol will be forwarded through the channel \mathbf{H} at the destination and the received signal will be the following

$$\mathbf{r} = \begin{bmatrix} -0.0474 + 0.0352i & -0.4053 - 0.5081j & 0.1225 - 0.2575j & -0.8461 - 0.3878j \\ -0.3683 + 0.0475j & 0.5232 + 0.0565j & -0.0970 + 0.1564j & 0.2519 + 0.3504j \\ -0.1116 - 0.0386j & -0.1792 + 0.2177j & -0.1302 + 0.0513j & -0.0936 - 0.2858j \\ -0.0836 + 0.2877j & -0.1910 - 0.6163j & 0.0170 - 0.0066j & 0.7743 + 0.9959j \end{bmatrix}.$$

The first and third column of the received signal \mathbf{r} show the signal that has been received in the receive antennas in f_1 and the second and fourth

column show the signal that has been received in the receive antennas in f_2 . The polarisation index estimation algorithm is considered when the channel is assumed to be known at the receiver. Applying the estimation algorithm to the received vector results in

$$\mathbf{P} = [0.3659 \ 3.6636].$$

By observing the vector \mathbf{P} , we see that $\mathbf{P}(2)$ is the greatest element. From this element we are able to estimate that the vertical polarisation [12] has been employed as this represents the power of the received signal in the vertical polarisation domain. Moreover, once the polarisation has been identified the in-phase received signal is as follows

$$\mathbf{r} = 1.2975 + 1.0524j$$

and therefore the received symbol $x = 1 + j$ have been employed. From the estimated polarisation and symbol we can retrieve the initial sequence of bits $\mathbf{q}(k) = [1, 0, 0]$, which exactly corresponds to the transmitted bits. The estimation of the transmitted bits is based on the power at the received polarised antennas and not the cross correlation of the different channels like in conventional SM [27].

5.3 Complexity Estimation

In this section the complexity of the proposed algorithm is discussed and compared with the conventional SM technique. It is shown [27] that the number of multiplications when the system uses conventional SM is

$$\delta_{SM} = 2N_r N_t + N_t \quad (5.5)$$

where N_r is the number of receive antennas and N_t is the number of transmit antennas. In the case of the proposed approach we can likewise view that we have $2N_r$ multiplications when the received signal is formed. During reception we have 2 comparisons once the two different polarisations are investigated in order to detect which one has received the signal. Finally, once estimation of the polarisation has occurred we perform N_r calculations so as to retrieve the signal transmitted. Therefore, the total number of multiplications is

$$\delta_{PM} = 3N_r + 2 \quad (5.6)$$

where N_r is the number of the receiver antennas in the MIMO system [2]. Assuming that the net-spreading levels of the systems remain the same, we can see that in a 2x4 MIMO system that employs SM we have 20 calculations

and in the alternative 1x2 dual MIMO system (2x4 virtual) that employs the PPASSK technique we have only 14 calculations.

5.4 SINR of Precoded PASSK

In this section we calculate the SINR per received symbol in Precoded PASSK when the cross polarisation effects are eliminated or exploited. This serves as a qualitative measure of the expected experimental performance. A normalised uncorrelated Rayleigh flat fading channel such that $\|\mathbf{H}_u\|^2=1$ is assumed for the presented analysis, where \mathbf{H}_u denotes the u -th row of the channel matrix.

5.4.1 SINR for Elimination of Cross Polarisation Effects in Precoded Polarisation Assisted Space Shift Keying Modulation

According to TABLE 9 and under the assumption of statistically independent data the effective SINR per received symbol is

$$\gamma = \text{SINR} = \frac{E\{f_c^2\}[E_s E\{|h_{11}|^2\}]}{N_o/2} \quad (5.7)$$

where E_s is the average energy per symbol and $\sigma^2 = N_o/2$ is the AWGN variance, once complex-valued equivalent baseband signals are considered rather than passband signals and f_c is a normalisation factor that retains the signal energy at the transmitter.

In Eq. (5.7) the term $E\{|h_{11}|^2\}$ is 1 and thus Eq. (5.7) is

$$\gamma = SINR = \frac{E\{f_c^2\}E_s}{\sigma_n^2}. \quad (5.8)$$

The expectation of the scaling factor is well investigated [31] and it is shown that Eq. (5.8) is

$$\gamma = SINR = \frac{cE_s \int_{-\infty}^{+\infty} \frac{\beta^{N-2}}{(1+\beta)^{N+1}} d\beta}{\sigma_n^2}. \quad (5.9)$$

The integral in Eq. (5.9) is

$$\int_{-\infty}^{+\infty} \frac{\beta^{N-2}}{(1+\beta)^{N+1}} d\beta = N \frac{\beta^{N-1} {}_2F_1(N-1, N+1, N, -\beta)}{N-1} \quad (5.10)$$

where ${}_2F_1(X, Y, Z, Q)$ is the hyper geometric function. Details of this function can be found in [32]. A comparison of the analytical expression to simulation results can be found in the next section (see section 5.6).

5.4.2 SINR for Exploitation of Cross Polarisation Effects in Precoded Polarisation Assisted Space Shift Keying Modulation

According to TABLE 9 and under the assumption of statistically independent data the effective SINR per received symbol is

$$\gamma = SINR = \frac{E\{f_c^2\}[E_s E\{|h_{11}|^2\} + E\{A_c\}E_s E\{|\mathbf{h}_{un}^* \mathbf{h}_{um}|^2\}]}{N_o / 2}. \quad (5.11)$$

The term $E\{A_c\}$ in (5.11) denotes the number of the antennas that receive the signal from the other polarisation (cross polarisation effects) and in this system is $N_r/2$ where N_r is the number of the receive antennas. Thus Eq. (5.11) is

$$\gamma = SINR = \frac{E\{f_c^2\}E_s[1 + \frac{N_r}{2} E\{|\mathbf{h}_{un}^* \mathbf{h}_{um}|^2\}]}{N_o/2}. \quad (5.12)$$

In order to calculate the term $E\{|\mathbf{h}_{un}^* \mathbf{h}_{um}|\}$ we refer to the properties of the normalised uncorrelated Rayleigh channel. The variance of each element in the channel matrix is given as

$$\text{var}(h_{uk}) = \frac{1}{N_r} \quad (5.13)$$

It is well known that $E\{h_{un}^* h_{um}\} = 0$. Therefore

$$E\{|\mathbf{h}_{un}^* \mathbf{h}_{um}|^2\} = \text{var}\{\mathbf{h}_{un}^* \mathbf{h}_{um}\} = \text{var}\left\{\sum_{m=1}^{\frac{N_r}{2}} h_{un}^* h_{um}\right\} = \sum_{m=1}^{\frac{N_r}{2}} \text{var}\{h_{un}^* h_{um}\}.$$

For each element in the sum we have $\text{var}\{\mathbf{h}_{un}^* \mathbf{h}_{um}\} = \text{var}\{\mathbf{h}_{un}^*\} \text{var}\{\mathbf{h}_{um}\} = \frac{1}{N_r^2}$

since the channel paths are uncorrelated. Finally

$$E\{|\mathbf{h}_{u,n}^* \mathbf{h}_{u,m}|^2\} = \frac{N_r}{2N_r^2} = \frac{1}{2N_r}. \quad (5.14)$$

If we substitute in (5.13) the result in (5.14) then we have

$$\gamma = SINR = \frac{E\{f_c^2\}E_s[1+\frac{1}{4}]}{N_o/2}. \quad (5.15)$$

Now the expectation of the scaling factor from Section 5.5.1 is

$$E\{f_c^2\} = c \int_{-\infty}^{+\infty} \frac{\beta^{N_r-2}}{(1+\beta)^{N_r+1}} d\beta = N_r \frac{\beta^{N_r-1} {}_2F_1(N_r-1, N_r+1, N_r, -\beta)}{N_r-1}. \quad (5.16)$$

From the above, the overall SINR is

$$\gamma = SINR = \frac{N_r \beta^{N_r-1} {}_2F_1(N_r-1, N_r+1, N_r, -\beta) E_s[1+\frac{1}{4}]}{(N_r-1) N_o/2}. \quad (5.17)$$

A comparison of the analytical expression to simulation results can be found in the next section (see section 5.5).

5.5 Numerical Simulation

In this section we validate the proposed approach by means of simulation results for various scenarios. In the simulations a flat Rayleigh fading channel is assumed and Matlab software has been used to generate the results. The channel is assumed to be known at the transmitter. The Monte Carlo technique (see Appendix A.4.3) is applied for the estimation of the Bit Error Rate. The SNR is defined as $\frac{P}{\sigma^2}$, where P is the total transmit

power, which is the same for all transmission, and σ^2 is the noise variance. Finally the variance of the fading channel paths is 1.

In Fig. 5.1 it is attempted to compare the performance of the proposed precoding technique, in which the cross polarisation effects are eliminated, with the ideal PASSK and the conventional SM [27]. The channel paths are Rayleigh fading coefficients.

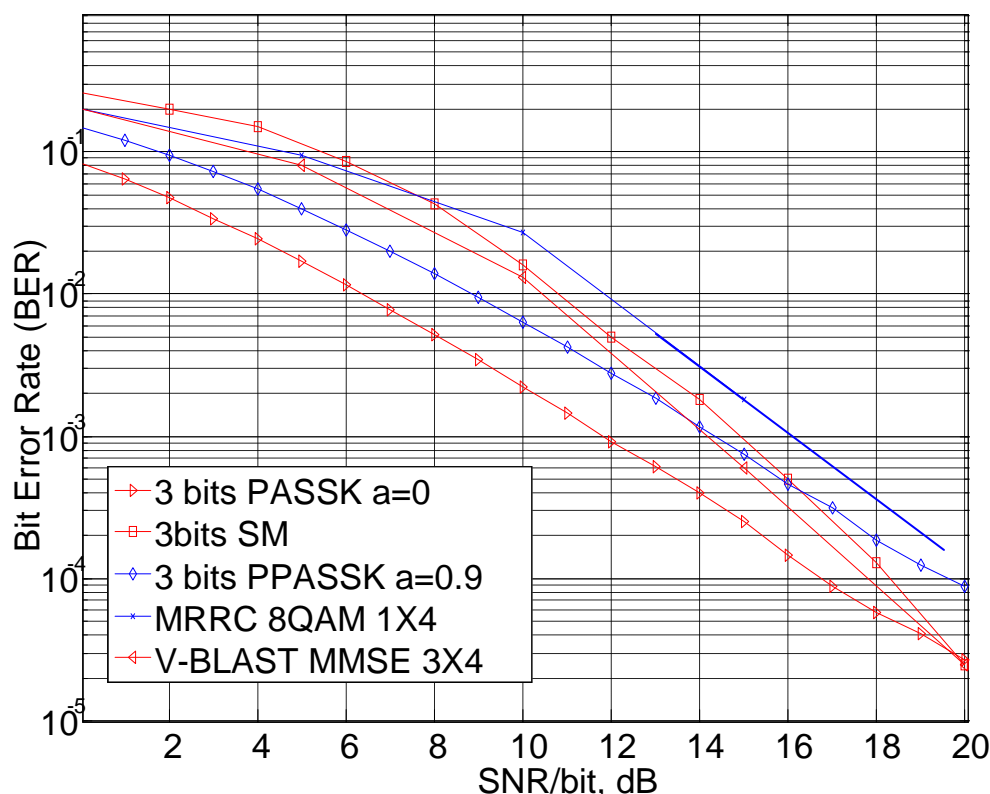


Fig. 5.1 Performance comparison between Precoded PASSK, PASSK, the conventional SM, MMRC and V-BLAST MMSE when the number of available polarisations is 2 and the transmission rate is 3 bits, in a Flat Rayleigh fading channel scenario. The MIMO system is 2x4 in all cases

It is easily noticeable from Fig. 5.1 the signal degradation in PPASSK that occurs, when normalising at the transmitter in order to retain the signal power at the same levels. However, this technique is still able to outperform the

conventional SM, MMRC and V-BLAST MMSE over a significant range of SNR values by providing performance improvements of about 2.5 dB over SM especially in small SNR values. In this scheme the number of antennas is halved, however there is an increase in bandwidth so as to be able to eliminate the cross polarisation effects.

Fig. 5.2 depicts the performance of the PPASSK compared to PASSK. It is assumed that the level of cross polarisation effects is 90% ($a=0.9$) in PPASSK and 10% ($a=0.1$) in PASSK. Transmission rate is 3 bits.

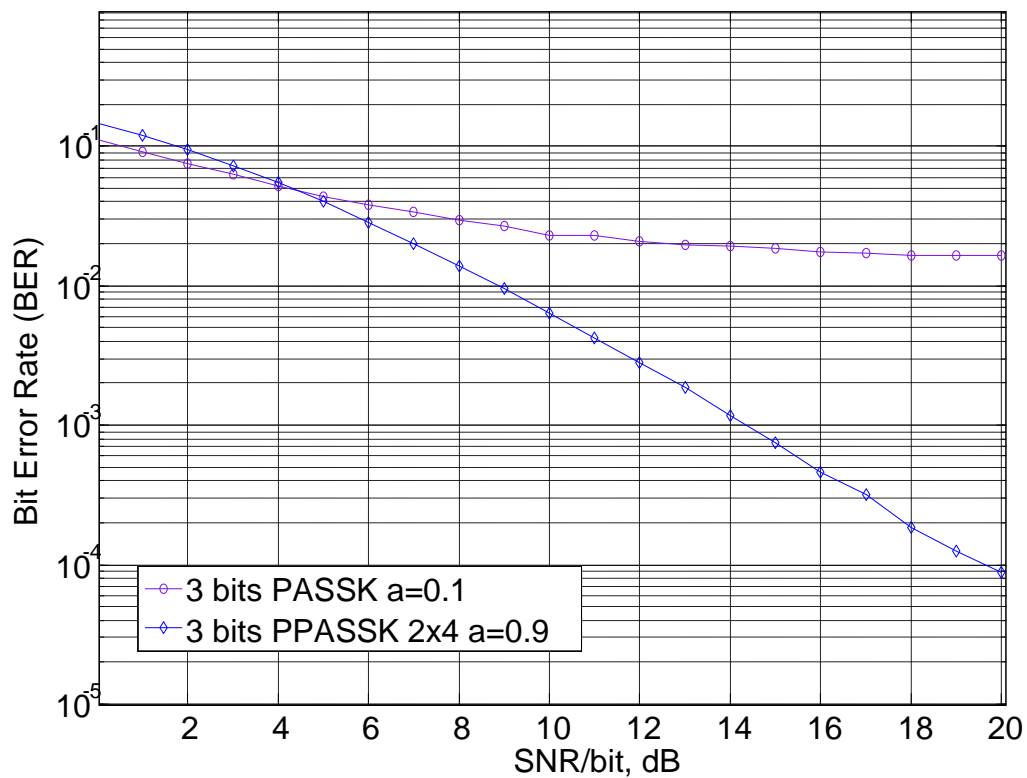


Fig. 5.2 Performance comparison between PPASSK and PASSK when a is 0.9 and 0.1 respectively.

It is obvious from Fig. 5.2 that the proposed technique when $a=0.9$ manages to entirely eliminate cross polarisation effects as opposed to PASSK and also even outperform PASSK when $a=0.1$.

Fig. 5.3 shows the performance of PPASSK in three bits rate in comparison with the five bits transmission rate case scenario. The cross polarisation effects are eliminated in this case. In three bits transmission rate the system employs QPSK constellation symbols, to completely represent the data, whereas in five bits transmission rate the system employs 16-QAM. Therefore, after the polarisation index estimation algorithm the system in three bits rate is left with the task of detecting a much simpler QPSK signal relative to the 16-QAM signal in five bits transmission rate.

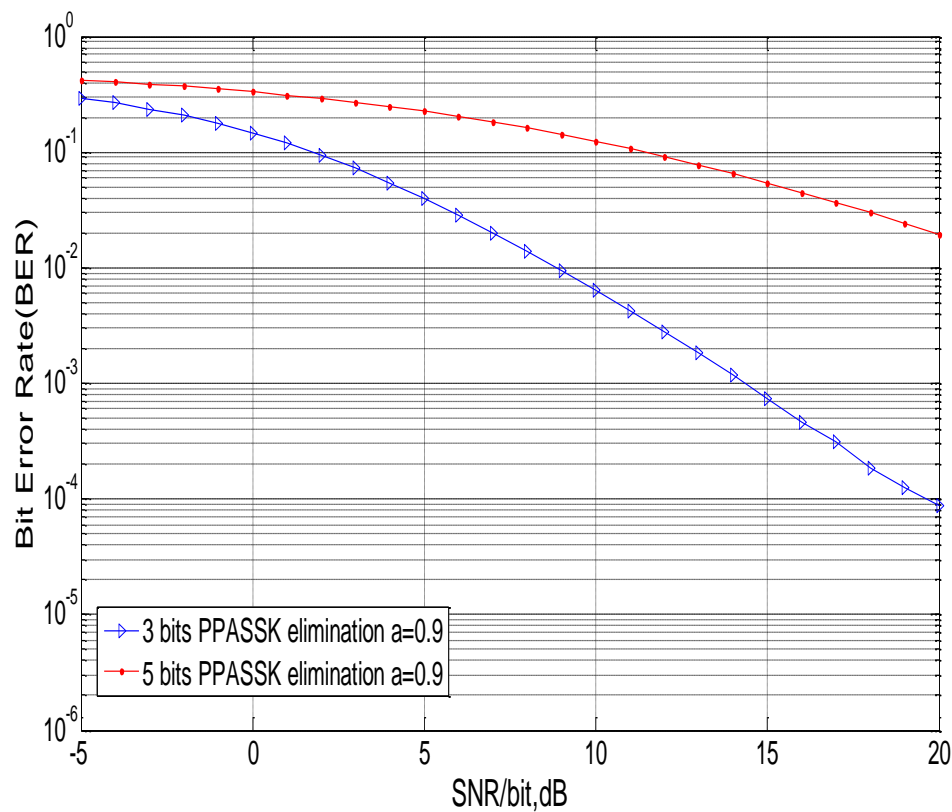


Fig. 5.3 Performance comparison between PPASSK when transmission rate is 3 and 5 bits respectively in a Flat Rayleigh Fading Channel. Cross-polarisation effects are eliminated.

In Fig. 5.4 it is attempted to compare the performance of the proposed precoding technique, in which the cross polarisation effects are exploited, with the ideal PASSK and the conventional SM [27]. The channel paths are Rayleigh fading coefficients [2].

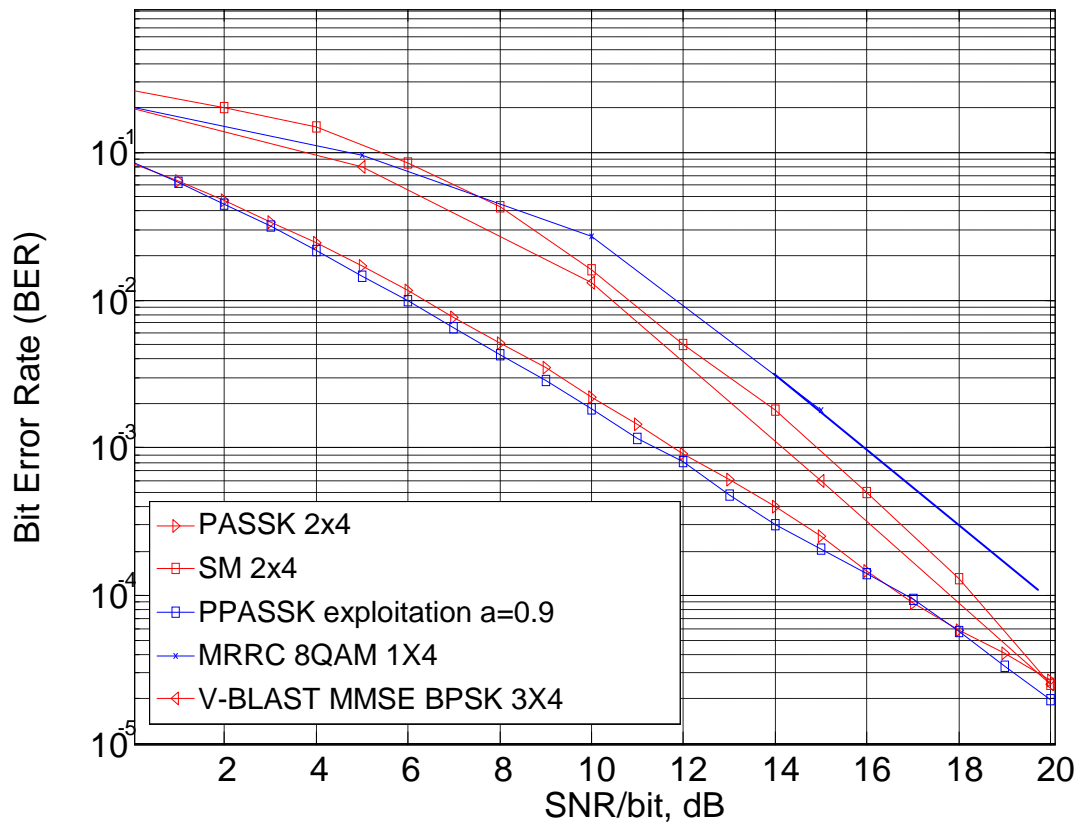


Fig. 5.4 Performance comparison between the proposed scheme and PASSK as well as the conventional SM, MRRC and V-BLAST MMSE. Transmission rate is 3 bits.

It is noticeable from Fig. 5.4 the signal enhancement that occurs in the proposed scheme whilst compared with PASSK. Moreover, the proposed technique outperforms conventional SM, MRRC and V-BLAST MMSE by about 4 dB especially in the low SNR region. The number of antennas is halved, however there is an increment in bandwidth so as to be able to exploit the cross polarisation effects.

In Fig. 5.5 it is attempted to compare the performance of the proposed precoding technique with the PPASSK that eliminates the cross polarisation effects as well as the conventional SM.

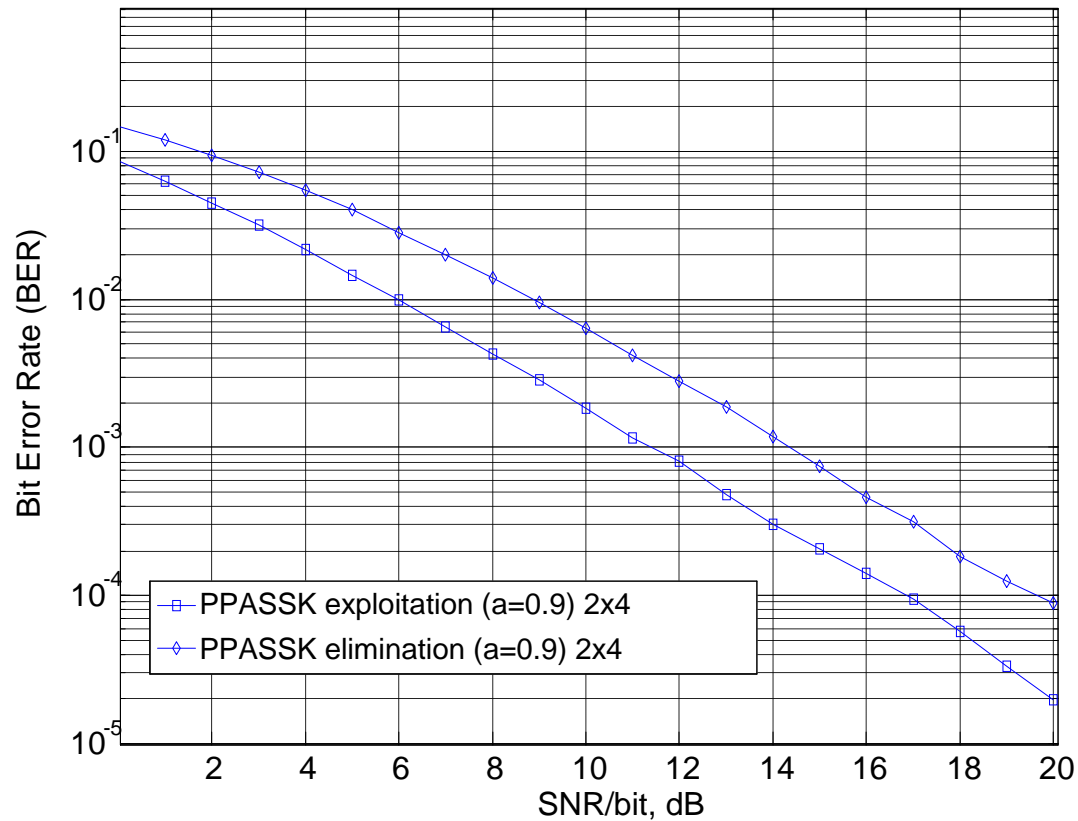


Fig. 5.5 Performance comparison between the proposed scheme when cross polarisation effects are either eliminated or exploited. Transmission rate is 3 bits

It is noticeable from Fig. 5.5 the signal enhancement that occurs in the proposed scheme whilst compared with the PPASSK. In more details, there is an improvement of about 3 dB in the new proposed scheme that exploits the cross polarisation effects at the receiver.

Fig. 5.6 depicts the performance of the proposed scheme for various values of alpha factor. The performance of the PPASSK is also plotted in the same figure.

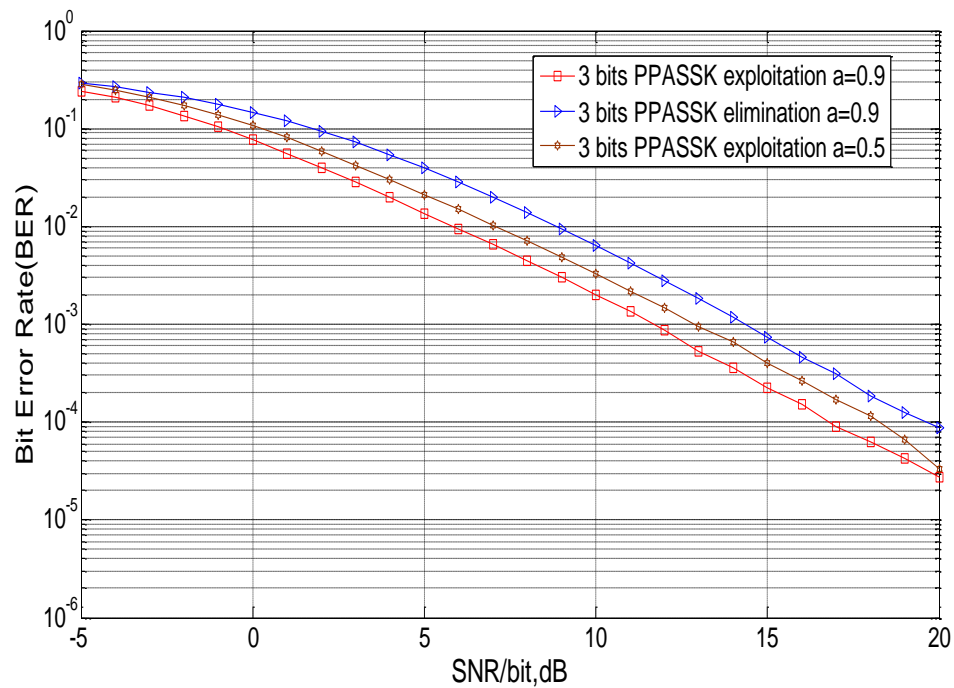


Fig. 5.6 Performance comparison of PPASSK for several values of the alpha factor

Fig. 5.7 shows the performance of the proposed scheme compared to PASSK in three bits transmission when α is 0.9.

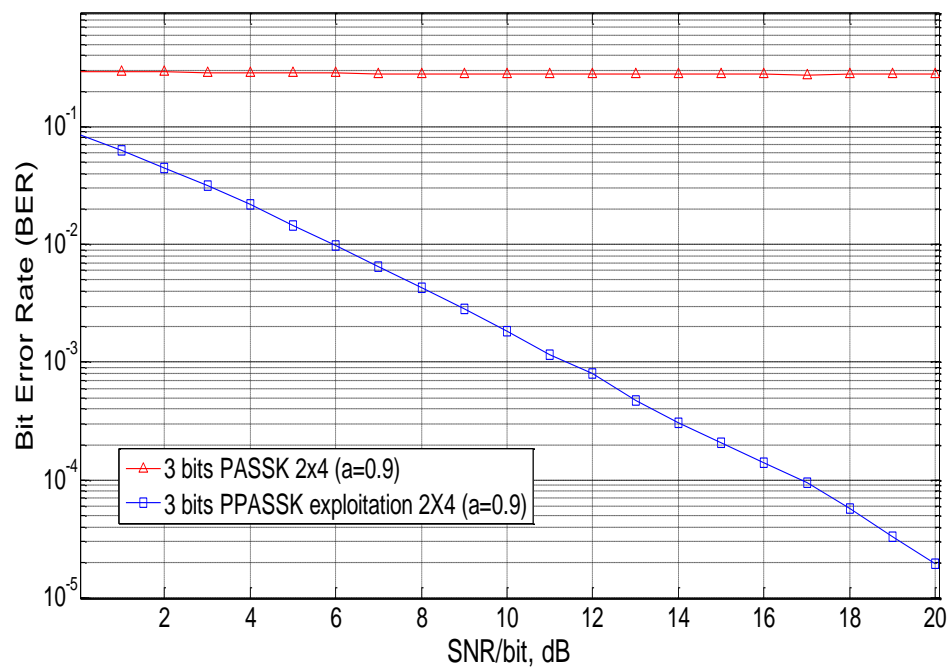


Fig. 5.7 Performance comparison between the proposed scheme and PASSK when the transmission rate is 3 bits.

It is clear from Fig. 5.7 that the proposed technique, when $a=0.9$, manages to entirely exploit cross polarisation effects as opposed to PASSK.

Figure 5.8 shows the superiority in performance of proposed scheme in three bits rate in comparison with the five bits transmission rate case scenario. In three bits transmission rate the system employs QPSK constellation symbols, to completely represent the data, whereas in five bits transmission rate the system employs 16-QAM. Therefore, after the polarisation index estimation algorithm the system in three bits rate is left with the task of detecting a much simpler QPSK signal relative to the 16-QAM signal in five bits transmission rate

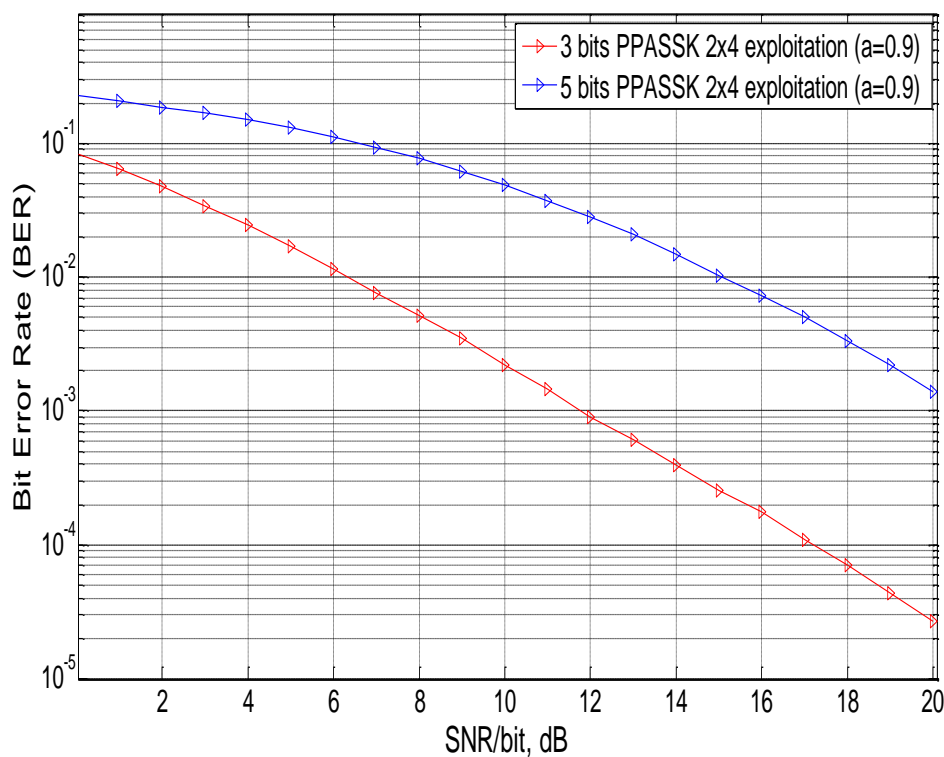


Fig. 5.8 Performance comparison of the proposed scheme when transmission rate is 3 and 5 bits respectively in a Flat Rayleigh Fading Channel.

Throughput results of the proposed techniques are depicted in Fig. 5.9. Throughput is expressed as $T_r = (1 - BLER)mN$ bits/channel use [31], where $BLER$ is the block error rate, $m = 1$ bit/symbol for BPSK and $m = 2$ for QPSK. The block length used for these simulations is $N_f = 100$ symbols. In more details, in Fig. 5.9 the case of PPASSK in which the cross polarisation effects are either eliminated or exploited. Transmission rate is three bits. The channel is flat Rayleigh fading.

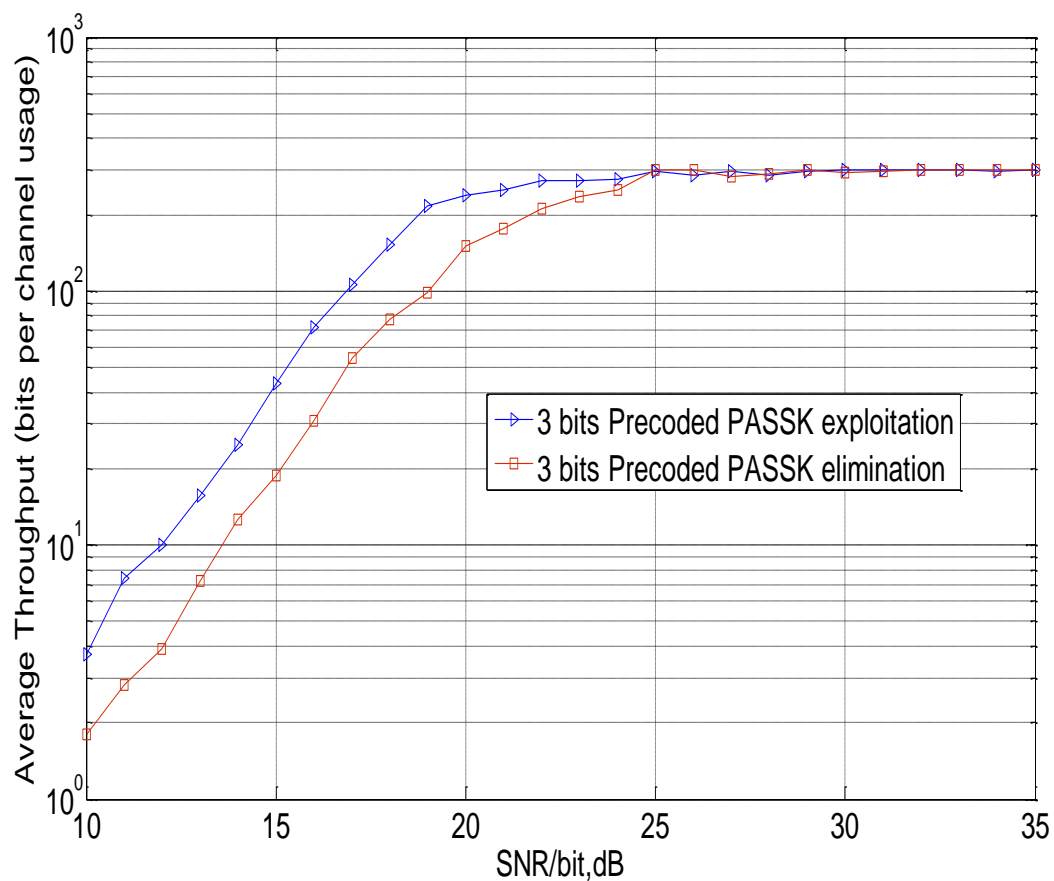


Fig. 5.9 Throughput results in Precoded PASSK modulation when the cross polarisation effects are either eliminated or exploited

A constant transmit SNR gain of 2 dB is observed when the cross polarisation effects are exploited during the polarisation index estimation process. This exists for up to 25 dB SNR where both scenarios attain optimum performance. The analysis carried out in section 5.5 is verified by simulations in Fig. 5.10 and Fig. 5.11. In a 2x2 MIMO system we plot the SINR per received symbol when the cross polarisation effects are either eliminated (see Fig. 5.10) or exploited (see Fig. 5.11). The transmission rate is 3 bits per symbol of interest and the channel is flat Rayleigh fading.

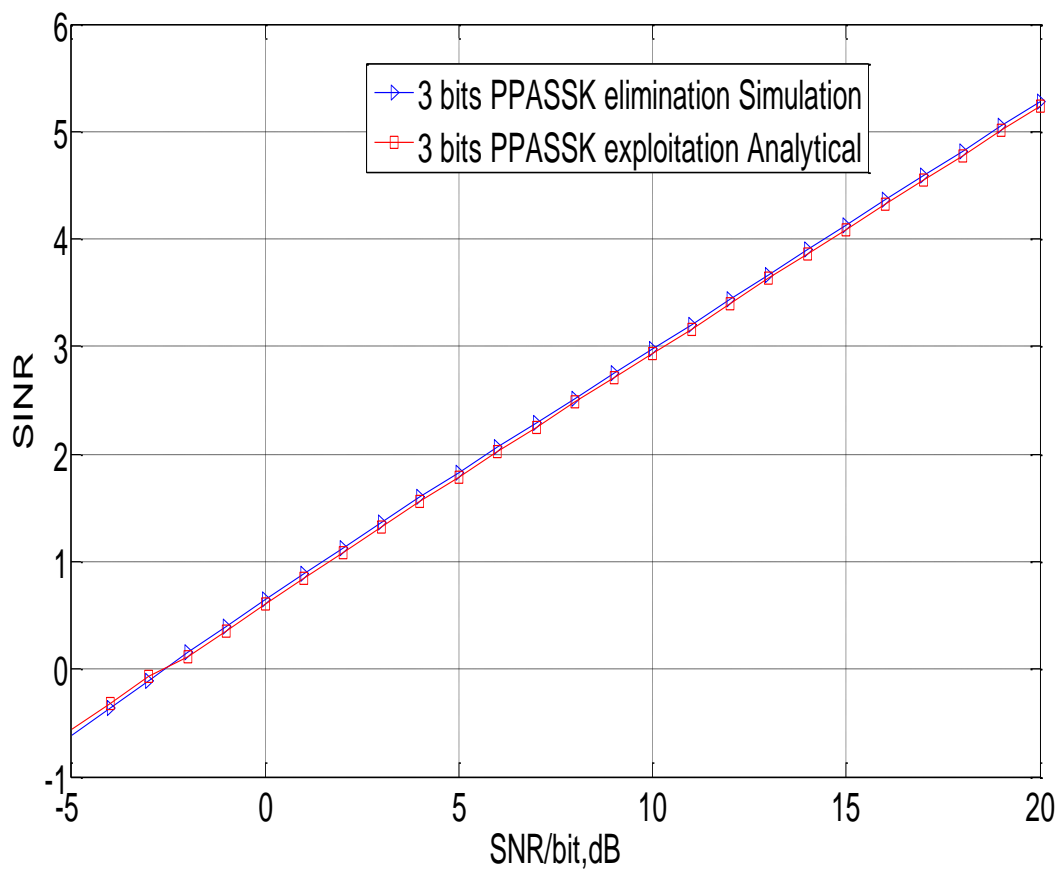


Fig. 5.10 SINR per received symbol in Precoded PASSK when cross polarisation effects are eliminated.

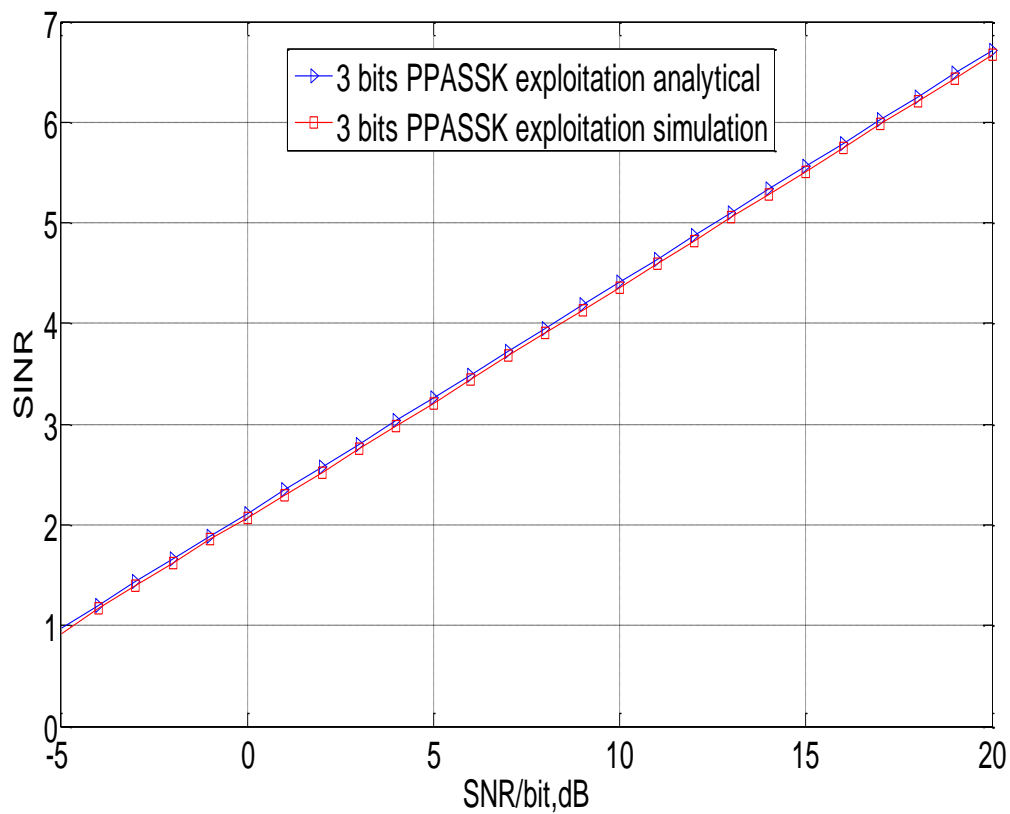


Fig. 5.11 SINR per received symbol in Precoded PASSK when cross polarisation effects are exploited.

5.6 Summary

In this Chapter a new simple linear precoding scheme that eliminates and exploits the existence of cross polarisation effects in dual polarised antennas has been presented. It is shown that the proposed scheme, in which the existence of cross polarisation effects is totally eliminated, introduces about 2.5 dB improvement in BER performance compared to conventional SM, MMRC and V-BLAST MMSE. In the case where the cross polarisation effects are exploited, the system introduces about 4 dB improvement in BER

performance compared to conventional SM, MRRC and V-BLAST MMSE, at the cost of extra bandwidth usage. It is also able to outperform PASSK for certain values of α , once the polarisation process estimation is more reliable. Moreover, the proposed technique offers similar levels of performance with PASSK when the antennas are ideally polarised. Complexity at the receiver is significantly low relative to PASSK since precoding occurs at the transmitter.

Chapter 6

Network Coding Techniques and Code Shift Keying Modulation

Robust communication as well as increased throughput over fading channels has always been a challenge for the designers of digital communication systems. The available frequencies for these systems amid increasing demands of modern applications are remarkably limited, and thus must be exploited optimally. A promising and efficient technique to help achieve optimisation of spectrum is Network Coding. It was first investigated in [1] and has thereafter encouraged great research efforts in the computer networking and communication communities.

In this chapter, two different approaches in Network Coding techniques will be discussed which aim to increase capacity as well as improve BER performance in systems employing distributed antennas as relay. It is assumed that there is no communication path between the users. The analysis will follow two branches with respect to the flat fading channel (see Appendix A.5) which is the one for *Rayleigh Fading + AWGN* and *AWGN*. We mainly deal with the case of two, three and five users that attempt to access the relay. It is shown that the proposed technique can accommodate them and mix their packets in an intelligent way in contrast to the conventional technique that accommodates only two users. Moreover, increased composite

rate per time slot is attained and thus less time slots are wasted in comparison with a loop coding scheme that attempts to increase capacity at the cost of employing more XOR-ed packets of bits.

6.1 Introduction

In this technique, information is not forwarded as it is but as a complex function of previously received data. This processing of the received information is the means to improve throughput and robustness, which is a characteristic of network coding techniques. Most pioneering work on network coding is theoretical and focuses on multicast traffic [33]. However, during the last ten years considerable work has been done to bridge the gap between theory and practice [60], [61], [62], [64]. They initially dealt with the scenario of two users [60] trying to communicate with each other, through a relay. It was assumed that there was no direct communication path between them, and packets from the two users are mixed at the relay using the XOR operation. The XOR-ed packet is forwarded to the destination and the destination can obtain the other user's packet by XOR-ing again with its own packet. The great advantage of this method is that the relay sends back half the amount of information that is needed in contrast to the case where no network coding is applied to the system [60].

In the case that more than 2 users want to access the relay and mix the received packets the whole technique fails to estimate the other users' bits. It is assumed [61], [33] that neighbouring users must overhear each other and when for example, 4 users are trying to access a relay the number of total transmissions is decreased from 8, that is required in a conventional

technique, to 5, because the relay sends back just one packet. It is easily justifiable that there is a significant coding gain of $\frac{8}{5}=1.6$. This scenario could be easily expanded to several users.

A new loop coding scheme has been presented [66], which is able to resolve the problem of more than 2 users who communicate with each other through a relay and without a user having to overhear the rest of them. Although, the number of XOR packets that are used is the same with the initial packets of bits that the relay would send if no network coding is incorporated into the system. The great advantage of this scheme is that the link loss rate is sharply decreased to less than 2% when the conventional network coding technique has loss rate 10%.

During the last seven years significant effort has been made in combining Network Coding and Cooperative Communications. A Cooperative Communication system can be viewed as a MIMO system and thus can provide a spatial diversity gain, also known as cooperative diversity, and is approximately the same with the space diversity that MIMO antennas can offer into a system. Therefore a combination of the two techniques [67], [68] could lead to better bandwidth efficiency and more robust communication due to increased throughput and diversity order correspondingly.

An Outage analysis has been proposed for Cooperative Communication systems that employ Network Coding [67] and has been proved that Outage probability can be reduced when Network Coding is combined with such systems.

In [69] the authors have introduced a diversity and multiplexing trade-off analysis of a Cooperative Network Coding System. This was for two users

that attempt to exchange bits among them, under the scenario that they can communicate directly as well as through the relay station. It was shown that a Cooperative Network Coding system improves both diversity and multiplexing gain, in comparison with a simple DAF transmission protocol.

This technique has also been applied to optical networks [20] as it can provide efficient and fault-tolerant communication through it. It is also denoted that the examples proposed in [20] show savings of up to 33% compared to conventional tail-end switching protection techniques. Other applications where this method has been proposed are presented in [71] and [74].

In this chapter we take Network Coding into a new direction where the focus is to increase capacity as well as exploit bandwidth. Firstly Collaborative Codes [78] are employed at the relay antenna and therefore we are able to accommodate more than two users at the same time and frequency. A simple encoding process takes place at the distributed antenna, which is based on the above codes and aims to mix the encoded packets. The mixed composite packet is then forwarded to all possible destinations. With this method we are able to increase throughput and capacity without having to waste time slots and available bandwidth. The second approach in Network Coding is when CSK Modulation is employed and at the relay antenna the orthogonal spreading codes as well as the transmitted symbol are XOR-ed. With this method, half of the amount of information is forwarded at the destination as in Conventional Network Coding technique. Moreover, with this technique BER performance improvement is attained because of the fact that when the antenna sources send the same orthogonal code then the relay is not necessary to forward the XOR-ed code but only the symbol transmitted

leading to less codes transmitted and therefore less chances for erroneous transmission.

6.2 Collaborative Codes

Collaborative Codes first appeared in 1978 [78] and they are popular for their increased throughput. When bandwidth is remarkably limited Collaborative Codes allow several numbers of users, without assigning frequencies or time-slots amongst them, to share a common channel. There are various Collaborative Codes that employ different number of users [83], [87], [89].

In this thesis Collaborative Codes are not used as a multiple access scheme but as a means to merge packets at the relay antenna. It is known that these codes are bandwidth efficient when are used in Collaborative Code Multiple Access (CCMA) scheme, although they suffer from synchronisation issues and makes the whole scheme somehow inefficient in the uplink compared to a CDMA one.

The main benefit of this family of codes is that transmission rate is greater than TDMA [89] namely the *3* and *5-user* codes. The *2-user* code cannot attain rates more than unity but it is the simplest case of this family of codes [90] [74].

The rate [89] for any constituent code C_i is given by

$$C_i = I/L \quad (6.1)$$

hence the total rate of a Collaborative Code is

$$C_{sum} = DC_i = D/L \quad (6.2)$$

where D is the number of users in this D -user code, and L is the codeword length. For example, in the 5-user case where the codeword length is $L=3$ the total rate is $C_{sum} = 5/3$.

For purposes of further understanding of this type of coding an example of a 3-user Collaborative Code is presented. This type of code has three constituent codewords so as users to send their “1” and “0”.

Specifically these codewords are the following $C_1 = \{00,11\}$, $C_2 = \{10,01\}$ and $C_3 = \{00,10\}$. For instance, if user 1 is assigned C_1 and wants to send a “0” then the pattern “00” is sent. TABLE 10 presents the three users and their corresponding codewords.

TABLE 10 CODEWORDS OF THREE-CODE CCMA SYSTEM

Code	0	1
	Binary	Binary
C_1	00	11
C_2	10	01
C_3	00	10

Under the assumption that C_1 is assigned to user 1, C_2 is assigned to user 2 and C_3 is assigned to user 3, thus TABLE 11 introduces all the possible combinations of codewords in the 3-user case.

TABLE 11 THREE USER CCMA SCHEME

User bits	Codewords			Output
123	C_1	C_2	C_3	
000	00	10	00	10
001	00	10	10	20
010	00	01	00	01
011	00	01	10	11
100	11	10	00	21
101	11	10	10	31
110	11	01	00	12
111	11	01	10	22

By better observing the above table, if the receiver receives the pattern “31” then it can be effortlessly unscrambled to the specified bits that have been sent from each distinct user. Hence, all the users are able to transmit their data simultaneously and with no ambiguities, providing that the codewords are employed suitably.

6.3 Existing Network Coding Technique and Proposed Modification

6.3.1 Loop Coding Scheme

The rationale is creating more XOR-packets at the relay [66]. For further understanding of this method it would be appropriate to introduce an example of three users (see Fig. 6.1) that cannot listen to each other directly but only through the relay link.

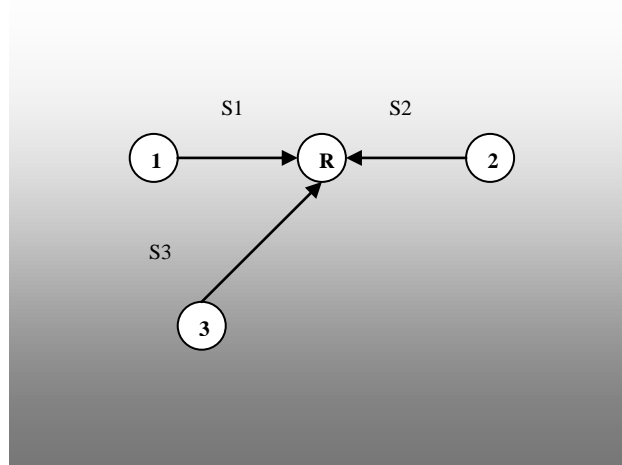


Fig. 6.1 Network coding when 3 users are attempting to access the relay.

In this example nodes 1/2/3 want to send packet $S1/S2/S3$ to other nodes. None of them is in the transmission range of each other. The relay can hear and be heard by everybody. This coding scheme introduces three XOR-packets, namely $S1 \oplus S2$, $S2 \oplus S3$, $S3 \oplus S1$. These packets are created at the relay and forwarded to all destinations. The motivation behind this increased number of packets transmission is that, if user 1 wants to send to user 2 and the packet $S1 \oplus S2$ will not arrive properly at the destination then there is another way to re-obtain user's 1 information at the destination (user-2) through the other two packets $S2 \oplus S3$, $S3 \oplus S1$. Although, with this scheme increased bandwidth is required once 3 packets are sent that is the same with the number of native packets, there is a potential which reduces the post-coding loss rate [66].

6.3.2 Proposed Approach based on Collaborative Codes

In the following a new approach in Network Coding will be presented, which exploits the properties of Collaborative Codes applies an intelligent packet mixing strategy.

This approach can be described in steps as follows:

- During the first step users send their bits at the relay either using a TDMA or CDMA scheme.
 - The relay then performs encoding operations so as to create the constituent codewords that are related to each user.
 - The codewords are added bit by bit and the result is then a distinct composite codeword.
 - With this codeword as referred above it is simply re-obtainable the triplet of bits in the case that three users are accessing the relay.
- The same operation takes place when five users are attempting to access the relay.

The way that the triplet of bits is retrieved from the composite codeword can be described as follows. Let us assume that all the possible noiseless composite codewords are given as

$$\mathbf{a}_i = \mathbf{s}_i \mathbf{h} \quad \mathbf{i} = 1, \dots, 8 \quad (6.3)$$

where \mathbf{s}_i is each possible composite codeword and \mathbf{h} is the Flat Rayleigh fading channel that connects the destination with the relay antenna. The received composite codeword is

$$\mathbf{r} = \mathbf{s}\mathbf{h} + \mathbf{n} \quad (6.4)$$

where \mathbf{s} is the received composite codeword and \mathbf{n} is White Gaussian Noise. Maximum Likelihood soft decision decoding can be performed [89] by calculating the distances between the received codeword and all the admissible noiseless codewords.

$$\min \|\mathbf{d}_i\| = \min(\mathbf{r} - \mathbf{a}_i). \quad (6.5)$$

The codeword with minimum distance is chosen as the received codeword. Subject to the fact that codewords are equally likely, with Maximum Likelihood we reach optimality [89] in the sense that errors are minimised at the receiver.

With this approach increased throughput can be achieved once more than one bit per time slot is sent to the destinations, namely 1.5 bits/slot when three users are employed and 1.67 bits/slot in the case of five users, once the composite packets are consisted of 2 and 3 symbols respectively. Each symbol requires one time slot to be sent and thus we are able to sent information of 3 users in 2 slots and information of 5 users in 3 time slots (see TABLE 13). The Loop Coding Scheme attains unity rates because 3 XOR-packets are sent through the relay which is the same with the number of initial packets before Network Coding being applied. The pioneering network coding scheme [60] attains rates of 2 bits/slot, in the case of 2 users but it is not applicable when more than 2 users are applied, and they are out of the transmission range of each other. As stated above, it could be applied in the

scenario that users could hear each other directly and based on this information the sent bits could have been recovered from the mixed packet that is sent in each different case. In this assumption we can achieve composite rates of 3 bits/slot and 5 bits/slot when 3 and 5 users are employed respectively, so as to share a common relay.

TABLE 12 THROUGHPUT FOR VARIOUS NUMBERS OF USERS

Method	Number of users		
	2	3	5
TDMA	1 bit/slot	1 bit/slot	1 bit/slot
Conventional	2 bits/slot	Not applicable	Not applicable
Loop coding scheme	2 bits/slot	1 bit/slot	1 bit/slot
Proposed	1 bit/slot	1.5 bits/slot	1.67 bits/slot

In TABLE 13 we can notice that the proposed technique consumes 2 and 3 slots, when 3 and 5 users are accommodated into a relay antenna, so as for the whole information to be forwarded properly, while the loop coding scheme [66] requires 3 and 5 slots respectively.

TABLE 13 TIME SLOTS CONSUMED FOR VARIOUS NUMBERS OF USERS WHEN RELAY FORWARDS INFORMATION AT THE DESTINATIONS

Method	Number of users		
	2	3	5
TDMA	2 slots	3 slots	5 slots
Conventional	1 slot	Not applicable	Not applicable
Loop coding scheme	1 slot	3 slots	5 slots
Proposed	2 slots	2 slots	3 slots

It could be claimed that the above method is time efficient, because the composite codewords are sent in less time slots once we attain composite rates more than unity compared to a conventional TDMA as stated above. This family of codes into a system is the best way to increase the number of users with somewhat small added complexity and interference [80].

6.4 Outage analysis

6.4.1 Outage Analysis of three users without network coding

An outage event is characterised when data from the three sources cannot be fully recovered at the specified destinations. In the scenario where the three users want to exchange their bits through the relay the probability of outage is P_s . We focus on the second step of the whole process when the relays forward the received information at the destinations. We assume the SER of the channels that connect the assisting antennas with the destinations are p_1, p_2, p_3 . The probability of outage can be computed as follows:

$$P_s = p_1 p_2 p_3 + p_1 p_2 (1 - p_3) + p_1 (1 - p_2) p_3 + p_1 (1 - p_2) (1 - p_3) + (1 - p_1) p_2 p_3 + (1 - p_1) p_2 (1 - p_3) + (1 - p_1) (1 - p_2) p_3. \quad (6.6)$$

After the appropriate substitutions the above equation results to the following one:

$$P_s = p_1 + p_2 + p_3 - p_1 p_2 - p_3 p_1 - p_3 p_2 + p_1 p_2 p_3. \quad (6.7)$$

Assuming that the system power is E_T then the three relays equally share the total amount of the available power E_T .

$$E_1 = \frac{E_T}{3} \quad (6.8)$$

$$E_2 = \frac{E_T}{3} \quad (6.9)$$

$$E_3 = \frac{E_T}{3}. \quad (6.10)$$

Under the assumption that the relay-destination channels are Flat Rayleigh fading and the modulation signal that is used is BPSK then the SER of such channels is written as, [3]:

$$p_e \approx \frac{1}{4SNR}. \quad (6.11)$$

Thus the outage probability can be written as follows:

$$P_s = \frac{1}{4SNR_1} + \frac{1}{4SNR_2} + \frac{1}{4SNR_3} - \frac{1}{4SNR_1 4SNR_2} - \frac{1}{4SNR_3 4SNR_1} - \frac{1}{4SNR_3 4SNR_2} + \frac{1}{4SNR_1 4SNR_2 4SNR_3} \quad (6.12)$$

$$P_s = \frac{N_o}{4E_1} + \frac{N_o}{4E_2} + \frac{N_o}{4E_3} - \frac{N_o N_o}{4E_1 4E_2} - \frac{N_o N_o}{4E_3 4E_1} - \frac{N_o N_o}{4E_3 4E_2} + \frac{N_o N_o N_o}{4E_1 4E_2 4E_3}. \quad (6.13)$$

Based on (6.10), (6.11) and (6.12) we have the following:

$$P_s = \frac{N_o 3}{4E_T} + \frac{N_o 3}{4E_T} + \frac{N_o 3}{4E_T} - \frac{N_o 3 N_o 3}{4E_T 4E_T} - \frac{N_o 3 N_o 3}{4E_T 4E_T} - \frac{N_o 3 N_o 3}{4E_T 4E_T} + \frac{N_o 3 N_o 3 N_o 3}{4E_T 4E_T 4E_T} \quad (6.14)$$

$$P_s = \frac{9}{4SNR} - \frac{27}{16SNR^2} + \frac{27}{64SNR^3}. \quad (6.15)$$

6.4.2 Outage Analysis of three users with network coding

In this scenario only one relay is employed. Fig. 6.2 depicts this scenario

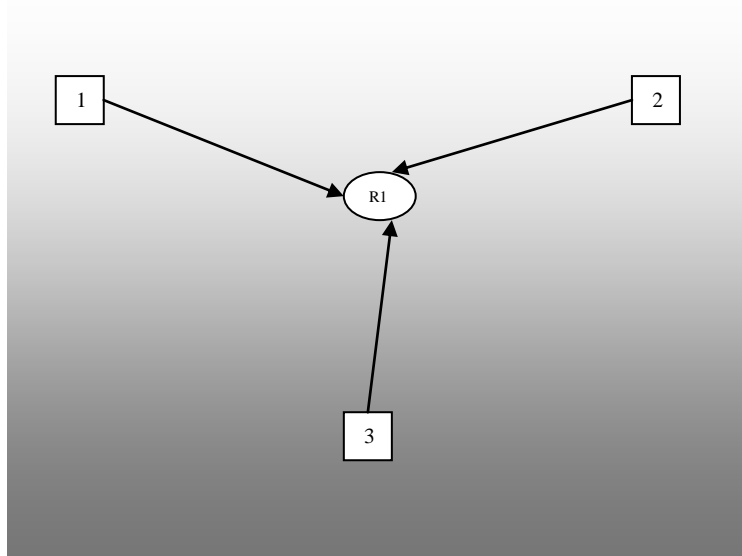


Fig. 6.2 When 3 users are trying to access the relay using network coding. No other communication path exists but through the relay station

The relay is overheard by all the destinations. Once it has received the information from the three sources it sends just one common packet to all destinations that can hear it. Thus the probability of outage of the system during the second phase (relay – destinations information forwarding) can be written

$$P_s = p_R. \quad (6.16)$$

In this method collaborative codes are used and the relay forwards packets of 4-ASK symbols at the specified destinations. Moreover, assuming again that the channels that connect the relay with the destinations are Flat Rayleigh fading it is appropriate to proceed with a SER analysis in Flat Rayleigh conditions of the 4-ASK constellation.

TABLE 14 THREE USER CCMA SCHEME

User bits	Codewords			Output
123	C_1	C_2	C_3	
000	00	10	00	1 3
001	00	10	10	-1 3
010	00	01	00	3 1
011	00	01	10	1 1
100	11	10	00	-1 1
101	11	10	10	-3 1
110	11	01	00	1 -1
111	11	01	10	-1 -1

Assigning bits to BPSK symbols ($1 \rightarrow -1, 0 \rightarrow 1$) we can see the output, by adding these codewords symbol by symbol, in TABLE 14.

Considering all the possible bits that the three sources are sending to the relay then we can conclude that symbol 3 has a probability $\frac{3}{16}, 1 \rightarrow \frac{7}{16}$

, $-1 \rightarrow \frac{5}{16}$ and $-3 \rightarrow \frac{1}{16}$.

A SER analysis for 4-ASK in AWGN is depicting the SER probability as, [3]:

$$P_{e,ASK} = \frac{1}{16}Q\left(\sqrt{\frac{2d^2}{N_o}}\right) + \frac{5}{16}2Q\left(\sqrt{\frac{2d^2}{N_o}}\right) + \frac{7}{16}2Q\left(\sqrt{\frac{2d^2}{N_o}}\right) + \frac{3}{16}Q\left(\sqrt{\frac{2d^2}{N_o}}\right) \quad (6.17)$$

$$P_{e,ASK} = \frac{28}{16}Q\left(\sqrt{\frac{2d^2}{N_o}}\right) \quad (6.18)$$

where d is the distance from the ideal symbol that is a decision threshold and Q is the Q -function (see Appendix A.3). In our case $d=1$.

Hence we can write $P_{e,ASK}$ in terms of average energy per symbol

$$E_s = \frac{1}{16}(-3)^2 + \frac{5}{16}(-1)^2 + \frac{7}{16}(1)^2 + \frac{3}{16}(3)^2 \quad (6.19)$$

$$E_s = \frac{1}{16}9d^2 + \frac{5}{16}1d^2 + \frac{7}{16}1d^2 + \frac{3}{16}9d^2 \quad (6.20)$$

$$E_s = 3d^2 \quad (6.21)$$

$$d^2 = \frac{1}{3}E_s. \quad (6.22)$$

Based on (6.24) the SER probability of the ASK constellation is

$$P_{e,ASK} = \frac{28}{16}Q\left(\sqrt{\frac{2\frac{1}{3}E_s}{N_o}}\right) = \frac{28}{16}Q\left(\sqrt{\frac{2}{3}SNR}\right). \quad (6.23)$$

Thus for any given value of \mathbf{h} we have that the SER probability is

$$P_{e,ASK} = \int_0^\infty \frac{7}{4} \frac{1}{2} \operatorname{erfc}\left(\sqrt{|\mathbf{h}|^2 \frac{2}{3} SNR \frac{1}{2}}\right) p(\gamma) d\gamma = \int_0^\infty \frac{7}{4} \frac{1}{2} \operatorname{erfc}(\sqrt{\bar{\gamma}}) p(\gamma) d\gamma \quad (6.24)$$

where $p(\gamma) = \frac{1}{\bar{\gamma}} e^{-\frac{\gamma}{\bar{\gamma}}}, \gamma \geq 0$, $\gamma = |\mathbf{h}|^2 \frac{1}{3} SNR$, $\bar{\gamma} = \frac{1}{3} SNR$ and $\operatorname{erfc}(\cdot)$ is the complementary Gauss error function.

Thus the above equation (6.24) is similar to the equation for the derivation of the BER for BPSK in Rayleigh fading [2] (see Appendix A.4).

$$P_{e,ASK} = \frac{7}{8\bar{\gamma}} [\bar{\gamma} \operatorname{erfc}(\sqrt{\bar{\gamma}}) e^{-\frac{\bar{\gamma}}{\bar{\gamma}}} + \bar{\gamma} \sqrt{\frac{\bar{\gamma}}{\bar{\gamma}+1}} \operatorname{erf}\left(\sqrt{\frac{\bar{\gamma}}{\bar{\gamma}+1}} \sqrt{\bar{\gamma}}\right)]_0^\infty \quad (6.25)$$

$$P_{e,ASK} = \frac{7}{8\bar{\gamma}} [\bar{\gamma} + 0 + 0 - \bar{\gamma} \sqrt{\frac{\bar{\gamma}}{\bar{\gamma}+1}}] = \frac{7}{8} [1 - \sqrt{\frac{\bar{\gamma}}{\bar{\gamma}+1}}] \quad (6.26)$$

and because $\bar{\gamma} = \frac{1}{3} SNR$ then the above is

$$P_{e,ASK} = \frac{7}{8} \left[1 - \sqrt{\frac{\frac{1}{3} SNR}{\frac{1}{3} SNR + 1}}\right] = \frac{7}{8} \left[1 - \sqrt{\frac{SNR}{SNR + 3}}\right]. \quad (6.27)$$

6.5 Network Coding and Code Shift Keying Modulation

In this section we introduce a new approach in Network Coding in which BER performance is improved as well as the throughput. There are two users

who are attempting to communicate with each other using a Relay node (see Fig. 6.3). CSK Modulation is employed for transmission.

At the relay antenna, Network Coding is applied when both users have forwarded their bits. When CSK Modulation is employed the sequence of bits is represented by orthogonal spreading codes as well as symbols from a constellation diagram. The main difference with the conventional Network Coding scheme is that we perform XOR not only in the bits that are transmitted but also in the orthogonal spreading codes. Therefore, the relay will send in only one time slot the XOR-ed code and XOR-ed symbol.

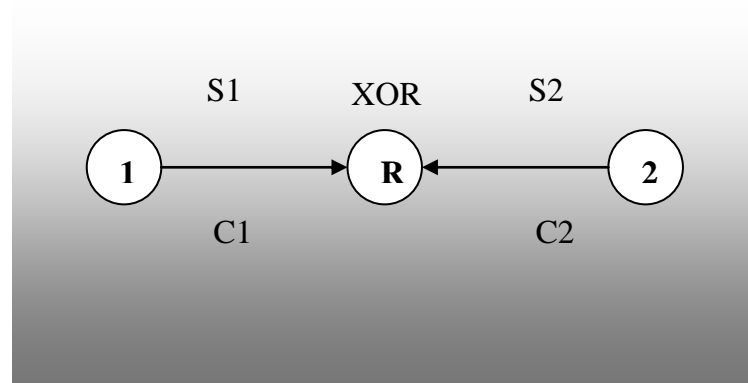


Fig. 6.3 Network Coding and CSK Modulation in an Ad-Hoc Network of two users and a relay antenna.

For the purpose of easier understanding and assimilating the whole process we examine the case of four orthogonal spreading codes available in three bits transmission rate.

6.5.1 Example of four Orthogonal Spreading Codes in three bits Transmission rate.

In this section we will present how the relay manages to XOR the orthogonal spreading codes as well as the symbols transmitted. The four spreading codes will be the following $\mathbf{c}_1 = [1, 1, 1, 1]$, $\mathbf{c}_2 = [1, -1, 1, -1]$, $\mathbf{c}_3 = [1, 1, -1, -1]$ and $\mathbf{c}_4 = [1, -1, -1, 1]$.

We first assume that user 1 and user 2 need to forward the following sequences of bits $\mathbf{q}_1(k) = [1, 0, 0]$ and $\mathbf{q}_2(k) = [0, 0, 1]$ respectively. From TABLE 5 in Chapter 3 we can see that user's 1 sequence of bits is mapped to spreading code $\mathbf{c}_3 = [1, 1, -1, -1]$ and BPSK symbol 1 whereas user's 2 sequence of bits is mapped to spreading code $\mathbf{c}_1 = [1, 1, 1, 1]$ and BPSK symbol -1.

For this example the relay antenna has received both users' information without errors. In order to XOR the spreading codes we first need to convert the chips 1 and -1 into 0 and 1 respectively. The same mapping applies for the users' symbols. Therefore $\mathbf{c}_3 = [0, 0, 1, 1]$ and $\mathbf{c}_1 = [0, 0, 0, 0]$ and the corresponding symbols will be $s_1 = 0$ and $s_2 = 1$, where s_1 and s_2 are user's 1 and 2 symbols.

If we perform the XOR operation in both the spreading codes as well as the transmitted symbols, the XOR-ed spreading code will be $\mathbf{c} = [0, 0, 1, 1]$ and the transmitted XOR-ed symbol will be $s = 1$. The de-mapping process will lead to $\mathbf{c} = [1, 1, -1, -1]$ and $s = -1$.

By employing CSK Modulation the relay transmits the XOR-ed symbol and orthogonal code. The mathematical model is similar to the one in Chapter 3 where CSK Modulation is illustrated in details.

At the destinations each user is performing the XOR operation between its data and the received data so as to retrieve the other user's data bits.

Another example that should be mentioned is when both users' bits are represented by the same spreading code. For example, the sequences of bits for user 1 and user 2 are $\mathbf{q}_1(k)=[1,0,0]$ and $\mathbf{q}_2(k)=[1,0,1]$. From TABLE 5 in Chapter 3 we can see that user's 1 sequence of bits is mapped to spreading code $\mathbf{c}_3=[1,1,-1,-1]$ and BPSK symbol 1 whereas user's 2 sequence of bits is mapped to spreading code $\mathbf{c}_3=[1,1,-1,-1]$ and BPSK symbol -1.

If we perform the XOR operation in both the spreading codes as well as the transmitted symbols, the XOR-ed spreading code will be $\mathbf{c}=[0,0,0,0]$ and the transmitted XOR-ed symbol will be $s=1$. The de-mapping process will lead to $\mathbf{c}=[1,1,1,1]$ and $s=-1$. In this case the spreading code is not necessary to be transmitted to the users since both users use the same code for the representation of their bits. Hence, the relay antenna has to forward only the XOR-ed symbol. This leads to less possible codes that are used for transmission without having to increase the modulation order and, therefore the code index estimation process offers better performance. This is verified in the Simulation Results in the following Section.

6.6 Numerical Simulation

In this section we validate the proposed approach by means of simulation results for various scenarios. In the simulations a flat Rayleigh fading channel is assumed. Matlab is used to generate all the results. The channel is assumed to be known at the transmitter. The SNR is defined as P/σ^2 , where P is the total transmit power, which is the same for all transmission, and σ^2 is the noise variance. Finally the variance of the fading channel paths is 1.

In Fig. 6.4 is made an effort to present the outage probability of a system that uses network coding and a system that does not use any kind of network coding technique. In this figure we plot the equations (6.15) and (6.27) respectively based on our analysis.

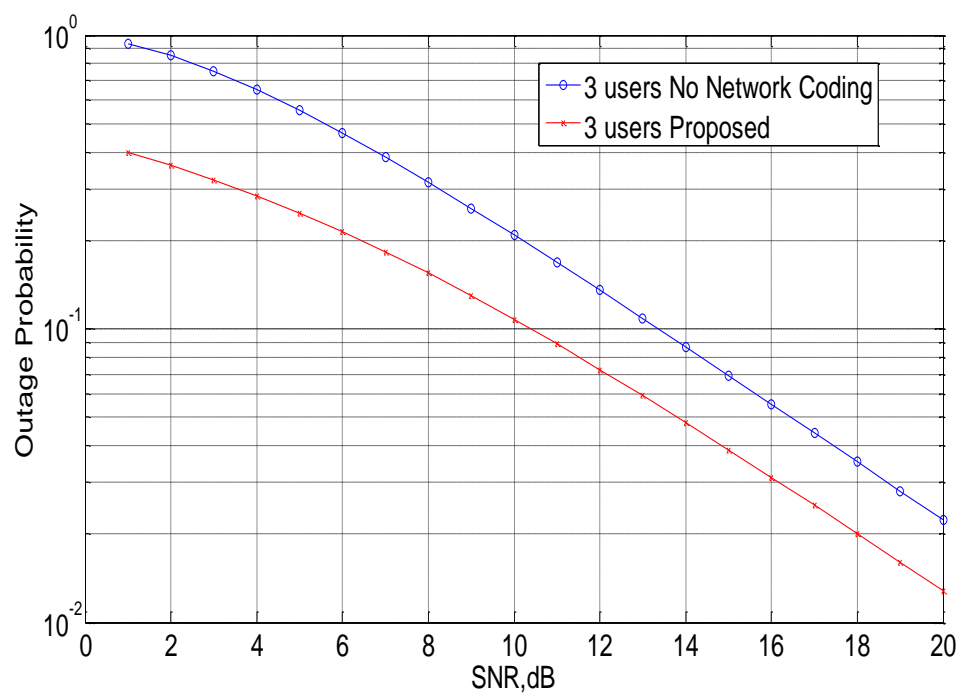


Fig. 6.4 Outage Probability when 3 users are trying to access the relay using network coding as well as using no network coding. No other communication path exists but through the relay station

It is easily conclusive that as in any network coding technique the outage probability is remarkably reduced if we employ collaborative codes so as to mix packets at the relay station.

Fig. 6.5 introduces the performance of the conventional network coding technique [60] that is presented in [68] in comparison with the performance of the proposed technique, as well as, a conventional TDMA system. A TDMA system happens to offer the same performance results with a CDMA scheme when the channels are Flat Fading and the spreading codes of the CDMA scheme are orthogonal. The system's performance [68] is using one relay so as to be accessed by the two users who cannot communicate with each other directly. However, there are various numbers of relays in [68] that are employed so as accommodate the pair of users but we mainly focus on the results provided using one relay.

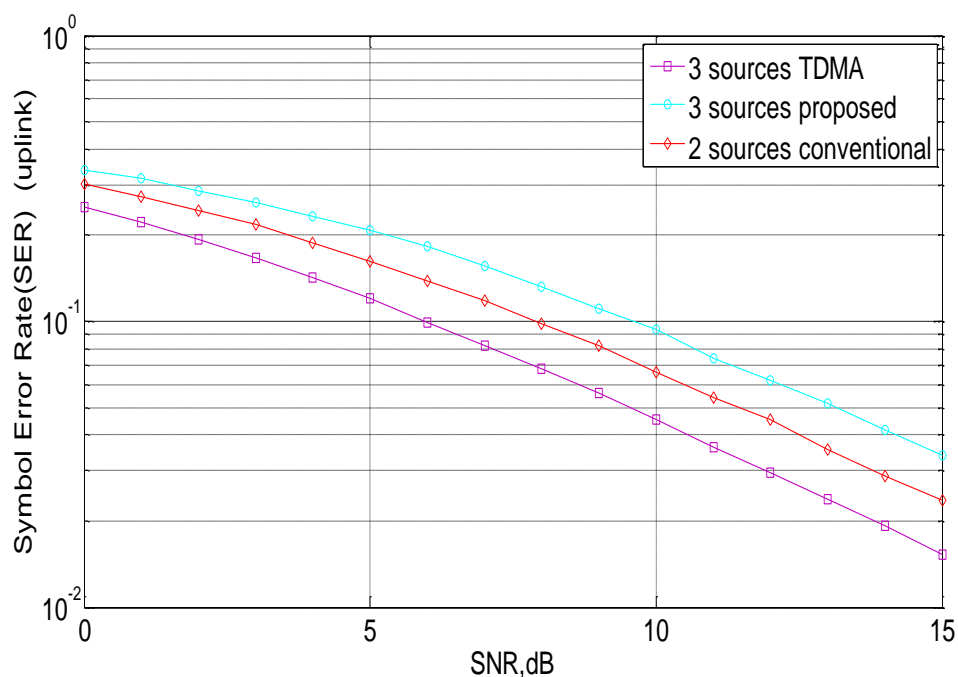


Fig. 6.5 Performance comparison using BPSK modulation

The square curve (one with the best performance) represents the case where 3 sources are using a conventional TDMA technique with no network coding applied at the relay. The triangle one represents the performance analysis of 2 users that are attempting to access a relay [68] using the conventional XOR-operation [60]. Finally the curve which has circles on it represents the case where 3 users are trying to access the relay and the relay mixes the packets based on the new approach of network coding. The transmission protocol that is used at the relay is a simple DAF one in all the three different cases.

It is conclusive that the 3 users' case provides slightly worse performance compared to the 2 users case because of higher levels of constellation signal (4-ASK) that is used when packets are mixed among them. On the other hand, it offers much higher throughput, once 3 users are employed, and the opportunity for the whole system to be applicable in sharp contrast to the conventional XOR-mixing technique [60] under the scenario that users are not hearing directly each other. Moreover, comparing this technique with the conventional TDMA method it would be appropriate to be referred that once packets are not mixed then interference tends to be even less and that is why we can see that performance is better than both methods of network coding. On the other hand, throughput is not increased (see TABLE 12) and bandwidth not used in the best way and that would be taken into deep consideration in a frequency limited environment.

In Fig. 6.6 it is made an effort to compare the performance of 3 and 5 users that are accommodated by one relay so as to mix packets.

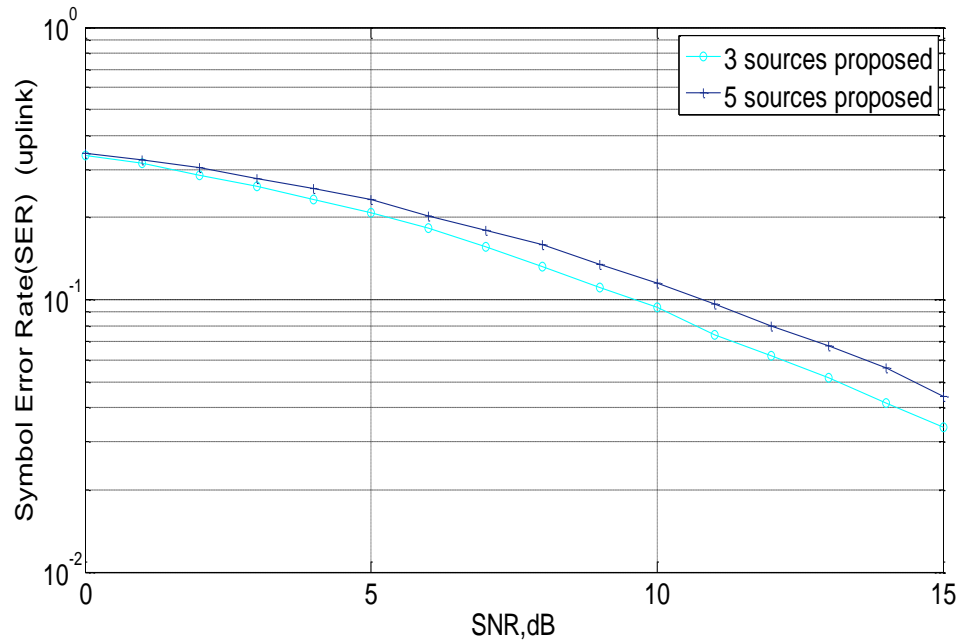


Fig. 6.6 Performance comparison using BPSK modulation of 3 and 5 users respectively that are managing to access the relay station

The curve with the circles on it represents the scenario of 5 users that are using the same relay at the same time whereas the curve with the stars shows the SER of 3 users that are attempting to access the relay station. At 10 dB SNR we attain 8.5% errors as can be seen in the 3 users' case and using one extra bit to accommodate 5 users we attain performance which is 11.5% due to increased interference when packets are combined together. On the other hand, throughput is almost doubled once 5 users' packets are mixed at the relay station.

In Fig. 6.7 we compare the AAF transmission protocol [70] with the DAF one when 3 sources are deployed so as to access the relay and then the relay mixes their information using the collaborative codes. It is always assumed that there is no other communication path between the sources but the relay.

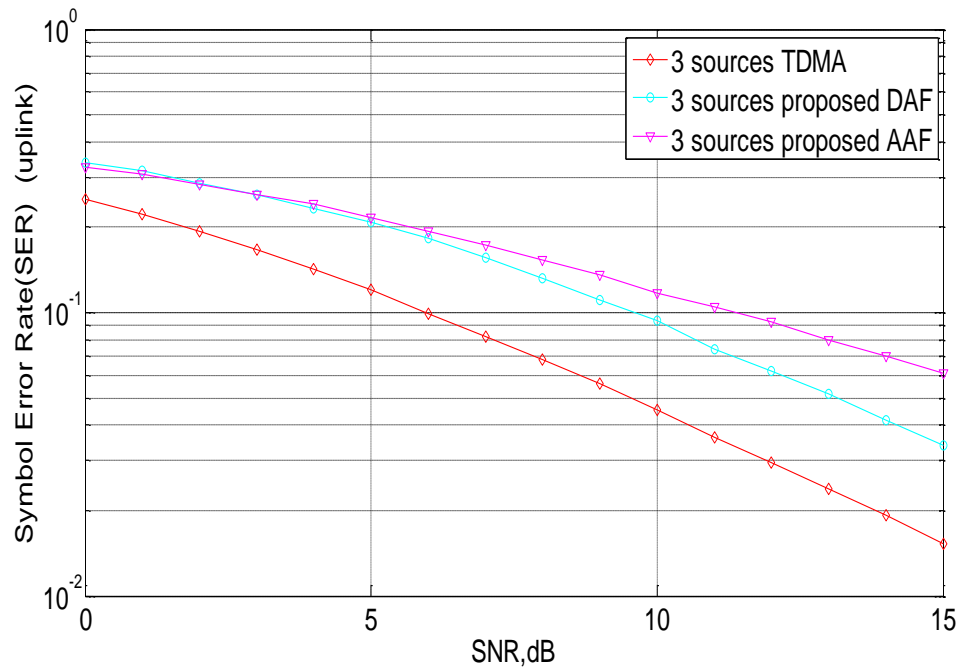


Fig. 6.7 Performance comparison using BPSK modulation of 3 users for Amplify and Forward as well as Decode and Forward Transmission protocol.

By observing the above picture (see Fig. 6.7) we are able to illustrate that performance of AAF is worse than that of DAF because noise is amplified when this protocol is applied at the relay and as already referred above this is a major impediment of this technique. The results comply with a similar comparison of another network coding technique [68].

In Fig. 6.8 we compare the BER performance of the Proposed Network Coding CSK scheme with the system that employs only CSK Modulation at the relay so as to forward the bits to the destinations.

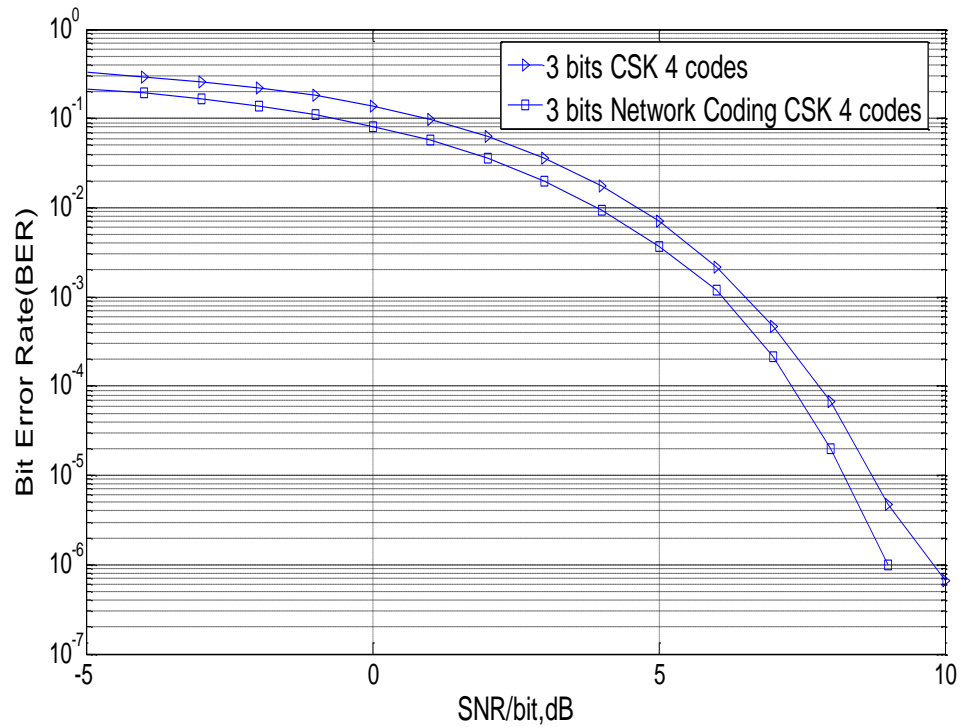


Fig. 6.8 Performance comparison of Network Coding CSK scheme with the simple CSK scheme that is employed at the relay station so as to forward the bits to the destinations.

As mentioned before, the proposed scheme occurs only in one time slot compared to the conventional CSK scheme that uses two slots so as to forward each user's data at the destination. This results to increased throughput at the relay station. Moreover, it is obvious the performance enhancement of the proposed scheme that manages to forward less number of spreading codes at the destinations and therefore the code index estimation process leads to better performance at about 2 dB in the low SNR region.

6.7 Summary

In this Chapter a different approach in network coding based on collaborative codes has been presented. It has also introduced a new Network Coding scheme that uses CSK modulation. The first scheme is shown that outperforms the pioneering conventional network coding technique [60], in terms of capacity, because the latter one fails to accommodate more than two users when they are out of the transmission range of each other. Moreover, increased throughput is accomplished and therefore less time slots are required in comparison with the existing loop coding scheme [66] that is able to solve the problem of more than two users so as to get connected through a relay and start swapping their bits. The second scheme is shown to improve performance in terms of BER as well as throughput when the bits are forwarded from the relay antenna to the destinations. A cooperative communication system can make use of the proposed technique at the relay station and that is a pledge for future work.

Chapter 7

Conclusions and Future work

7.1 Conclusions

The space effective scenario of employing spreading codes instead of antennas has been discussed in Chapter 3. With this scheme, the main two weaknesses of Conventional SM, which are the effects of channel correlation in estimating the antenna indices and the failure of SM to function in non normalised channel conditions, are overcome at the cost of decreased spectral efficiency. Besides this, an improved scheme that uses half the amount of spreading codes is also introduced, leading to significant performance improvement at the receiver as well as reduction in bandwidth usage.

In Chapter 4 and 5 it is discussed the employment of dual polarised antennas and how the two polarisations are able to convey information bits at the receiver. The existence of cross polarisation effects degrades performance of the overall system and therefore in Chapter 5 a simple linear precoding scheme manages to either eliminate or exploit them. Also, the proposed precoding scheme contributes towards the simplification of MU, since all the processing occurs at the Base Station.

The exploitation of these effects in Chapter 5 leads to further BER performance improvement at the receiver. In this scheme the number of

antennas is halved, at the cost of increased bandwidth usage. Moreover the main weaknesses of Conventional SM are again eliminated, due to reduced number of antennas employed and non reliance in antenna indices estimation errors due to channel correlation.

Finally in Chapter 6 it is discussed how Network Coding can be applied with CSK Modulation so as to increase throughput. It is shown that apart from the increased throughput that is attained, there is BER performance improvement at the receivers. Moreover, by introducing a new Network coding scheme based on Collaborative Codes we manage to increase capacity of a system that uses a distributed antenna system as the exclusive way for the sources to communicate amongst themselves. In this approach we increase the modulation order, so as to accumulate more bits at the relay at the same time slot. An outage analysis of this system has been introduced and we show that the outage probability of a system that employs Network Coding is smaller compared to a system that uses no Network Coding.

7.2 Future Work

This area of research is remarkably promising for further enhancements and as a future work it would be good to further optimise the CSK and PPASSK modulation in terms of computational complexity and system performance.

- An optimal detection technique for the CSK Modulation based on an *ML* approach could potentially improve performance even better at the cost of increased complexity.

- In the basic form of CSK, only one spreading code is employed at each symbol interval to represent bits of information. We could potentially use more than one spreading codes to transmit symbols simultaneously. This would increase spectral efficiency. At the receiver the detector that is employed will attempt to jointly estimate the transmitted symbols as well as the index of the spreading codes.
- It would worth mentioning the investigation of CSK and PPASSK in cooperative MIMO systems. How the various users would be able to send and detect orthogonal spreading codes and polarisations in an effective way so as to further improve performance as well as reduce complexity of the overall system.
- In CSK the number of spreading codes needs to be a power of two. It is worth investigating a generalised scheme that uses any number of orthogonal codes to represent the information bits.
- Like in any MIMO technique, the performance of SM is degraded in the presence of high channel correlation. Optical wireless communications in indoors environments is subject to high spatial correlation and low channel distinctness. Therefore it would be very interesting to evaluate the performance of CSK and PPASSK to this type of channel conditions.
- In several circumstances, channel fading might be sufficiently rapid to preclude the availability of the perfect knowledge of CSI at the receiver, and in particular, the estimation of a stable phase reference. Motivated by this consideration, it would be worth evaluating the performance of

the CSK as well as the PPASSK detector with unknown or partially unknown phase reference at the receiver.

- In PPASSK a trellis encoder could be incorporated into the system so as to exploit the benefits of both schemes resulting to potentially improved performance as well as reduced decoding complexity
- It would be very interesting to further investigate the system that uses both antennas and spreading codes at the same time to transmit information. In such a hybrid system we will be able to exploit the orthogonality of spreading codes along with the diversity that is offered, because of the employment of multiple receive antennas into the system. Results are well promising in terms of improvement in performance as well as complexity.
- An OFDMA system would serve to represent information along with the signal originated from a constellation structure. Potential new detection techniques will be introduced likewise so as to be able to overcome complexity issues and existing performance levels.

All the above would serve as a generalisation and comparison of the proposed schemes in the field called SM

References

- [1] R. Ahlswede, N. Cai, S.Y.R. Li, and RW Yeung, "Network information flow. IEEE Transactions on Information Theory", vol.46, no.4, pp.1204–1216, 2000.
- [2] John G. Proakis, Digital Communications, Electrical Engineering. McGraw-Hill,3rd edition, 1995.
- [3] T. S. Rappaport, "Wireless Communications: Principles and Practice", 2nd Edition, Prentice Hall PTR, 2002.
- [4] R. Y. Mesleh, et al., "Spatial Modulation", IEEE Trans. Veh. Technol., vol. 57, no. 4, pp. 2228–2241 , July 2008.
- [5] A. Goldsmith, S. Jafar, N. Jindal, and S. Vishwanath, "Capacity limits of MIMO channels," IEEE J. Sel. Areas Commun., vol. 21, no. 5, pp. 684–702, Jun. 2003.
- [6] M. Damen, A. Abdi, and M. Kaveh, "On the effect of correlated fading on several space-time coding and detection schemes," in Proc. IEEE 54th Veh. Technol. Conf., Oct. 7–11, 2001, vol. 1, pp. 13–16.
- [7] M. Chiani, M. Win, and A. Zanella, "On the capacity of spatially correlated MIMO Rayleigh-fading channels," IEEE Trans. Inf. Theory, vol. 49, no. 10, pp. 2363–2371, Oct. 2003.
- [8] T. Svantesson and A. Ranheim, "Mutual coupling effects on the capacity of multielement antenna systems," in Proc. IEEE ICASSP, May 7–11, 2001, vol. 4, pp. 2485–2488.
- [9] S. Ganesan, R. Mesleh, H. Haas, C. W. Ahn, and S. Yun, "On the performance of spatial modulation OFDM," in Proc. 40th Asilomar Conf. Signals, Syst. Comput., Oct. 29–Nov. 1, 2006, pp. 1825–1829.
- [10] R. Mesleh, H. Haas, C. W. Ahn, and S. Yun, "Spatial modulation—A new low-complexity spectral efficiency enhancing technique," in Proc. CHINACOM, Oct. 25–27, 2006, pp. 1–5.
- [11] A. ElKalagy, E. Alsusa, "A novel two-antenna spatial modulation technique with simultaneous transmission", in SoftCOM, 24-26 Sept. 2009
- [12] R. Nabar, H. Bolcskei, V. Erceg, D. Gesbert, and A. Paulraj, "Performance of multiantenna signaling techniques in the presence of polarization diversity," IEEE Transactions on Signal Processing, vol. 50, no. 10, pp. 2553–2562, Oct. 2002.

- [13] N.S. Kumar and K.R.S. Kumar, "A novel Symbol detection algorithm using V-BLAST/MAP for MIMO wireless channel", IJAEST, vol. 10, no. 2, pp. 353–379, 2011.
- [14] T. Haustein, C. von Helmolt, E. Jorswieck, V. Jungnickel, and V. Pohl, "Performance of MIMO systems with channel inversion," in Proc. 55th IEEE Veh. Technol. Conf., vol. 1, Birmingham, AL, May 2002, pp. 35–39.
- [15] C. Masouros, E. Alsusa, "Selective Channel Inversion Precoding for the Downlink of MIMO Wireless Systems," in Communications, 2009. ICC '09. IEEE International Conference on Issue Date: 14-18 June 2009, pp 1-5
- [16] A. Sendonaris, E. Erkip, and B. Aazhang, "User Cooperation Diversity Part I and Part II," IEEE Trans. Commun., vol. 51, no. 11, Nov. 2003, pp. 1927–48.
- [17] T. E. Hunter and A. Nosratinia, "Cooperative Diversity through Coding," Proc. IEEE ISIT, Laussane, Switzerland, July 2002, p. 220.
- [18] J. N. Laneman, D. N. C. Tse, and Gregory W. Wornell, Cooperative Diversity in Wireless Networks: Efficient Protocols and Outage Behaviour, 2002.
- [19] M. Yu and J. Li, "Is amplify-and-forward practically better than decode-and-forward or vice versa?" in Proc. IEEE Int. Conf. Acoustics, Speech, and Signal Processing (ICASSP), vol. 3, March 2005, pp. 365–368.
- [20] R. Menendez and J. Gannet, "Efficient, fault-tolerant all-optical multicast networks via network coding," in Conference on Optical Fiber communication/ National Fiber Optic Engineers Conference (OFC/NFOEC), February 2008, pp. 1–3.
- [21] W. W. Peterson and D. T. Brown (January 1961). "Cyclic Codes for Error Detection". Proceedings of the IRE 49 (1): 228-235. doi:10.1109/JRPROC.1961.287814.
- [22] A. Nosratinia, University of Texas, Dallas, Todd E. Hunter, Nortel Networks, Ahmadreza Hedayat, University of Texas, Dallas, Cooperative Communication in Wireless Networks, IEEE Communications Magazine • October 2004.
- [23] T. E. Hunter and A. Nosratinia, "Diversity through Coded Cooperation," submitted to IEEE Trans. Wireless Commun., 2004.

- [24] J. Hagenauer, "Rate-Compatible Punctured Convolutional Codes (RCPC Codes) and Their Applications," *IEEE Trans. Commun.*, vol. 36, no. 4, April 1988, pp. 389–400.
- [25] S. M. Alamouti, "A Simple Transmit Diversity Technique for Wireless Communications," *IEEE J. Sel. Areas Commun.*, vol. 16, pp. 1451–1458, October 1998.
- [26] P. Wolniansky, G. Foschini, G. Golden, and R. Valenzuela, "V-BLAST: an architecture for realizing very high data rates over the rich-scattering wireless channel," In *Proc. International Symposium on Signals, Systems, and Electronics (ISSSE'98)*, Pisa, Italy, pp. 295–300, Sept.-Oct. 1998.
- [27] J. Jeganathan, A. Ghayeb, and L. Szczecinski, "Spatial modulation: Optimal detection and performance analysis," *IEEE Commun. Lett.*, vol. 12, pp. 545–547, Aug. 2008.
- [28] Baidas, M.W.; O'Farrell, T.; , "The Performance of Coded Non-Coherent M-ary Orthogonal Keying Based OFDM Systems in a Frequency Selective and Fast Time-Varying Channel," *Communications*, 2007. ICC '07. IEEE International Conference on , vol., no., pp. 2930–2935, 24–28 June 2007.
- [29] M.-S. Alouini and A. Goldsmith, "A unified approach for calculating error rates of linearly modulated signals over generalized fading channels," *IEEE Trans. Commun.*, vol. 47, no. 9, pp. 1324–1334, Sep. 1999.
- [30] G. Casella and R. L. Berger, *Statistical Inference*, 2nd ed. ser. Duxbury Advanced. Pacific Grove, CA: Duxbury, 2002.
- [31] C. Masouros, "Investigation and Analysis of Interference Exploitation in Wireless Communication Systems", PhD thesis, University of Manchester, 2009.
- [32] M. Abramowitz and I. A. Stegun, *Handbook of Mathematical Functions: with Formulas, Graphics and Mathematical Tables*, Wiley and Sons, New York, 1972.
- [33] S. Katti, H. Rahul, W. Hu, D. Katabi, M. Médard, and J. Crowcroft. XORs in the air: practical wireless network coding. *Networking*, IEEE/ACM Transactions on Volume: 16, Issue: 3 Publication Year: 2008, Page(s): 497 – 510
- [34] R. Mesleh, H. Haas, C. W. Ahn, and S. Yun, "Spatial modulation–OFDM," in *Proc. 11th InOWo*, Aug. 30–31, 2006, pp. 288–292.

- [35] X. Shao, J. Yuan, Y. Shao, "Error performance analysis of linear zero forcing and MMSE precoders for MIMO broadcast channels", IET Commun, vol. 1, no.5, Oct. 2007
- [36] C. Masouros & E. Alsusa, "Dynamic Linear Precoding for the Exploitation of Known Interference in MIMO Broadcast Systems", IEEE Transactions on Wireless Communications, Vol. 8,(3) Publication Year: 2009 , Page(s): 1396 – 1404
- [37] P. Wolniansky, G. Foschini, G. Golden, and R. Valenzuela, "V-BLAST: An Architecture for Realizing very High Data Rates over the Rich- Scattering Wireless Channel," in URSI International Symposium on Signals, Systems, and Electronics (ISSSE '98.), pp. 295–300, 29 September-2 October 1998.
- [38] S. Verdu, Multiuser Detection, Cambridge, University Press 1998.
- [39] B. R. Vojcic and W. M. Jang, "Transmitter precoding in synchronous multiuser communications," IEEE Trans. on Communications, vol. 46, no. 10, pp. 1346– 1355, Oct. 1998.
- [40] D. Gesbert, D. Shiu, P. J. Smith, A. Naguib, "From theory to practice: an overview of MIMO space-time coded wireless systems", IEEE J. Sel. Areas Commun. Vol. 21, No. 3, pp. 281-302, Apr. 2003.
- [41] M. O. Damen, H. El Gamal, and G. Caire, "On maximum-likelihood detection and the search for the closest lattice point," IEEE Trans. Inf. Theory, vol. 49, pp. 2389–2402, Oct. 2003.
- [42] Marcus, M. and Minc, H. Introduction to Linear Algebra. New York: Dover, p.191, 1988.
- [43] T. Cover and J. Thomas, Elements of Information Theory. New York: Wiley, 1991.
- [44] G. E. Andrews, The Theory of Partitions (Encyclopaedia of Mathematics and its Applications), Cambridge University Press, 1984.
- [45] T. K. Y. Lo, "Maximum ratio transmission," IEEE Trans. Commun., vol. 47, no. 10, pp. 1458–1461, Oct 1999.
- [46] E. Biglieri, J. Proakis, and S. Shamai, "Fading channels: Information-theoretic and communications aspects," IEEE Trans. Inform. Theory, vol. 44, pp. 2619–2692, Oct. 1998.
- [47] C. B. Peel, Studies in multiple antenna wireless communications, PhD Thesis, Birgham Young University, 2004.
- [48] L. Garcia, A. Probability and Random Processes for Electrical Engineering, Addison-Wesley, Reading, MA, 1994

- [49] G. H. Golub and C. F. V. Loan, *Matrix Computations*, 3rd ed. Baltimore, Maryland: The Johns Hopkins University Press, 1996.
- [50] D. Coppersmith, S. Winograd, "Matrix multiplication via arithmetic progressions," *J. Symbolic Comput.* 9, p. 251-280, 1990
- [51] J. S. Lee, L. E. Miller, *CDMA System Engineering Handbook*, Artech House, London 1998.
- [52] R. C. Dixon, *Spread Spectrum Systems*, New York: Wiley Interscience, 1976.
- [53] S. Haykin *Communication systems*. Fourth ed, New York: Wiley; 2001.
- [54] F. H. Ali, I. Shakya and E. Stipidis, "User Cooperation Diversity for Multiuser CCMA", PIMRC '07, 2007 IEEE Symposium on Personal Indoor and Mobile Radio Communications, September, 2007
- [55] M. Gastpar and M. Vetterli. On the capacity of wireless networks: The relay case. In *Proceedings of IEEE INFOCOM*, 2002.
- [56] A. Scaglione, L. D. Goeckel, J. N. Laneman, "Cooperative Communications in Mobile Ad Hoc Networks", *IEEE Signal Processing Magazine* [19] September 2006
- [57] T. M. Cover and A. A. E. Gamal, "Capacity Theorems for the Relay Channel," *IEEE Trans. Info. Theory*, vol. 25, no. 5, Sept. 1979, pp. 572–84.
- [58] M. Janani et al., "Coded Cooperation in Wireless Communications: Space-Time Transmission and Iterative Decoding," *IEEE Trans. Sig. Proc.*, vol. 52, no. 2, Feb. 2004, pp. 362–71.
- [59] T. E. Hunter and A. Nosratinia, "Diversity through Coded Cooperation," submitted to *IEEE Trans. Wireless Commun.*, 2004.
- [60] Y. Wu, P. A. Chou, and S. Y. Kung. Information exchange in wireless networks with network coding and physical-layer broadcast. Technical Report MSR-TR-2004-78, Microsoft Research, 2004.
- [61] S. Katti, H. Rahul, W. Hu, D. Katabi, M. Médard, and J. Crowcroft. XORs in the air: practical wireless network coding. In *SIGCOMM '06: Proceedings of the 2006 conference on Applications, technologies, architectures, and protocols for computer communications*, pages 243–254, New York, NY, USA, 2006. ACM Press.
- [62] P. Larsson, N. Johansson, and K.-E. Sunell, "Coded bi-directional relaying," in *Proc. VTC'06*, vol. 2, pp. 851–855, 2006.

- [63] F.H. Ali, S. Chandler and S. Soysa, "Complex-valued Receiver for Multiuser Collaborative Coding Schemes", IEE Electronics Letter, 1995
- [64] P. Popovski and H. Yomo, "Wireless network coding by amplified-and forward for bi-directional traffic flows," IEEE Comm. Lett., vol. 11, no. 1, pp. 16–18, Jan. 2007.
- [65] J. Meel, "Spread Spectrum (SS)," Sirius Communications, Rostelaar, Belgium, ver.2 Dec. 99.
- [66] Q. Dong, J. Wu, W. Hu, and J. Crowcroft. Practical Network Coding in Wireless Networks. MOBICOM'07, short paper, 2007.
- [67] Y. Chen, S. Kishore, and J. Li, "Wireless diversity through network coding," in IEEE Wireless Commun. Networking Conf. (WCNC), vol. 3, Las Vegas, NV USA, Apr. 3–6, 2006, pp. 1681–1686
- [68] S. Fu, K. Lu, Y. Qian, and M. Varanasi, "Cooperative network coding for wireless ad-hoc networks," in IEEE Global Commun. Conf. (GLOBECOM), Washington, D.C., USA, Nov. 26–30, 2007, pp. 812–816.
- [69] Li-Chun Wang, Wei-Cheng Liu, and Sau-Hsuan Wu, Diversity-Multiplexing Tradeoff Analysis of a Cooperative Network Coding System. Sarnoff Symposium, 2009. SARNOFF '09. IEEE
- [70] K. S. Schneider, "Optimum Detection of Code Division Multiplexed Signals," IEEE Trans. Aerospace Elect. Sys., vol. AES-15, no., Jan. 1979, pp. 181-85.
- [71] L. Lima, M. Medard, and J. Barros. Random linear network coding: A free cypher? In IEEE Intl. Symp. Info. Theory ISIT, 2007.
- [72] P. B. Rapajic and D. K. Borah, "An Adaptive Maximum Likelihood Receiver for Asynchronous CDMA Systems," ISSSTA '98 Sun City, South Africa, Sept. 1998, pp. 671-675.
- [73] S. Chang, and E.J. Weldon: 'Coding for T-user multiple access channels', IEEE Trans. Inf: Theory, 1979, IT-25, pp. 684-691
- [74] J. P. Vilela, L. Lima, and J. Barros, "Lightweight Security for Network Coding," Proc. of the IEEE International Conference on Communications (ICC 2008), Beijing, China, May 2008.
- [75] M. K. Varanasi and B. Aazhang, "Multistage Detection in Asynchronous Code-Division Multiple-Access Communications," IEEE Trans. Commun., vol. 38, no. 4, pp. 509-519, Apr. 1990.
- [76] E. V. D. Meulen, "Three-terminal communication channels," Adv. Appl.Probability, vol. 3, pp. 120–154, 1971.

- [77] R. Esmailzadeh, M. Nakagawa, and E.A. Sourour, "Time-division duplex CDMA," *IEEE Personal Communications*, vol. 4, pp. 51–56, Apr. 1997.
- [78] Wolf, J.K.: 'Multi-user communication networks' in SKWIZYNSKI, J.K. (Ed.): 'Communication systems and random process theory' (Alphen aan den Rijn, The Netherlands, 1978), pp. 37-53.
- [79] Stallings, W., 2001. *Wireless Communications and Networks*. Upper Saddle River, New Jersey: Prentice Hall.
- [80] F.H. Ali, S. Soyas, Complex-valued collaborative coding multiple access for fading channels, *IEE Proceedings: Communications* 148 (5) (2001) 327–332.
- [81] R. Prasad, *CDMA for Wireless Personal Communications*, Artech, 1996.
- [82] S. Moshavi, "Survey of Multi-User Detection for DS-CDMA Systems," Bellcore pub., IM-555, Aug; 1996.
- [83] F.H. Ali, B. Honary, Low complexity soft decision decoding technique for collaborative coding multiple access channels, *Electronic Letters* 27 (13) (1991) 1167–1169.
- [84] Papathanasiou, M. Meurer, T. Weber, and P.W. Baier, "A novel multiuser transmission scheme requiring no channel estimation and no equalization at the mobile stations for the downlink of TD-CDMA operating in the TDD mode," *IEEE Vehicular Technology Conference Fall 2000*, pp. 203–210, 2000.
- [85] S. Verdu, "Multi-User Detection," *Advances in Statistical Signal Processing*, vol. 2, JAI Press 1993, pp. 369-409.
- [86] J. Jeganathan, A. Ghrayeb, and L. Szczecinski, "Space shift keying modulation for MIMO channels", *IEEE Trans. Wireless Commun.*, Jan. 2009. (accepted for publication). [Online]. Available:<http://users.encs.concordia.ca/~saghrayeb/Papers/SSK.pdf>
- [87] F.H. Ali, B. Honary, Collaborative coding and decoding for multiple access channel, *IEE Proceedings: Communications* 141 (2) (1994) 1167–1169.
- [88] R. Mesleh, S. Ganesan, H. Haas, "Impact of Channel Imperfections on Spatial Modulation OFDM", *The 18th Annual IEEE International Symposium on Personal, Indoor and Mobile Radio Communications (PIMRC'07)*, pp. 1–5, 3-7 September 2007.
- [89] A. Al-Sammak, Five-user collaborative code with rate of 1.67, *Electronics Letters* 37 (3) (2001) 183–184.

- [90] A. J. Al-Sammak. “New five-user collaborative codes with improved performance”, International Journal of Electronics and Telecommunications, www.elsevier.de/aeue, April 2009.
- [91] Y. Chau and S.–H. Yu, “Space modulation on wireless fading channels”, IEEE Veh. Technol. Conf. – Fall, vol. 3, pp. 1668–1671, Oct. 2001.
- [92] R.Y.Rubenstein, Simulation and the Monte Carlo Method, New York:Wiley,1981

Appendix

A.1 Gray Coding

A Gray code is an encoding of numbers so that adjacent numbers have a single digit differing by 1. The term Gray code is often used to refer to a "reflected" code, or more specifically still, the binary reflected Gray code. To convert a binary number $d_1d_2\dots d_n$ to its corresponding binary reflected Gray code, start at the right with the digit d_n (the n_{th} , or last, digit). If the d_{n-1} is 1, replace d_n by $1-d_n$; otherwise, leave it unchanged. Then proceed to d_{n-1} . Continue up to the first digit d_1 , which is kept the same since d_0 is assumed to be a 0. The resulting number $g_1g_2g_3\dots g_n$ is the reflected binary Gray code.

A.2 Useful Distributions

A.2.1 The Gaussian Distribution

It is an extremely important probability distribution that is also referred to as *Normal* (N). It models the statistics of thermal noise in receivers, known as AWGN. It is utilised in generation of fading envelopes. The pdf of a *Gaussian Distribution* is defined as

$$f_x(x) = \frac{1}{\sqrt{2\pi\sigma_x^2}} e^{-\frac{(x-\mu_x)^2}{2\sigma_x^2}} \quad (\text{A.1})$$

where μ is the mean and σ_x^2 is the variance (see Fig. A.1). The *Gaussian* pdf is a *bell-shaped* function. To indicate that a random variable X has a normal probability density function $f_x(x)$, we write $X \sim N(\mu_x, \sigma_x^2)$

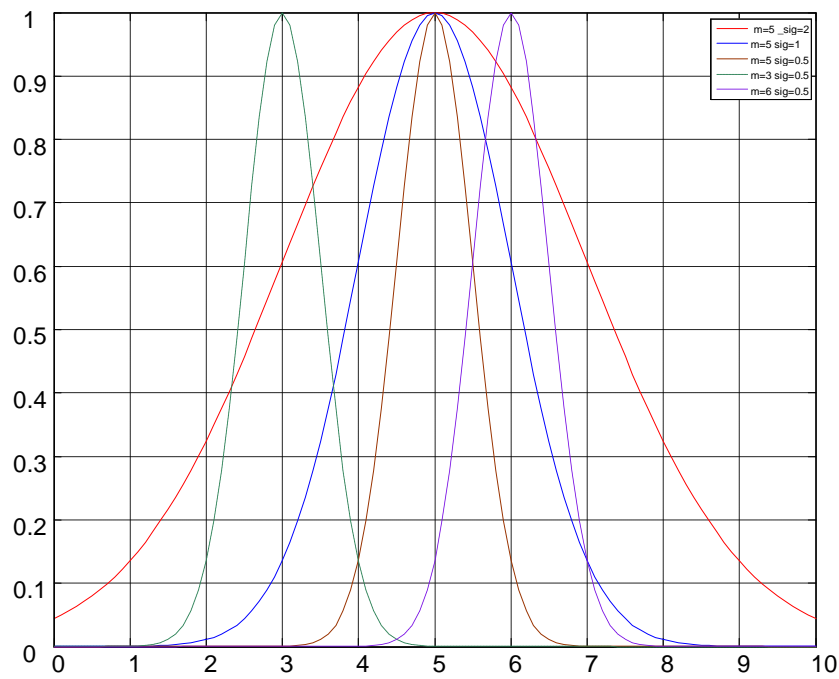


Fig A.1: Gaussian Distribution for various values of mean and variance.

A.2.2 The Rayleigh Distribution

Another useful distribution is the Rayleigh distribution, which is created by the magnitude of the variable $Y = X_1 + j * X_2$, where X_1 and X_2 are Gaussian random variables. This distribution is widely used in the modeling of the multipath channel. It is characterised by the pdf of

$$f_x(x) = \frac{1}{2\sigma_x^2} e^{\frac{-x}{2\sigma_x^2}}. \quad (A.2)$$

This is depicted in *Figure A.2*

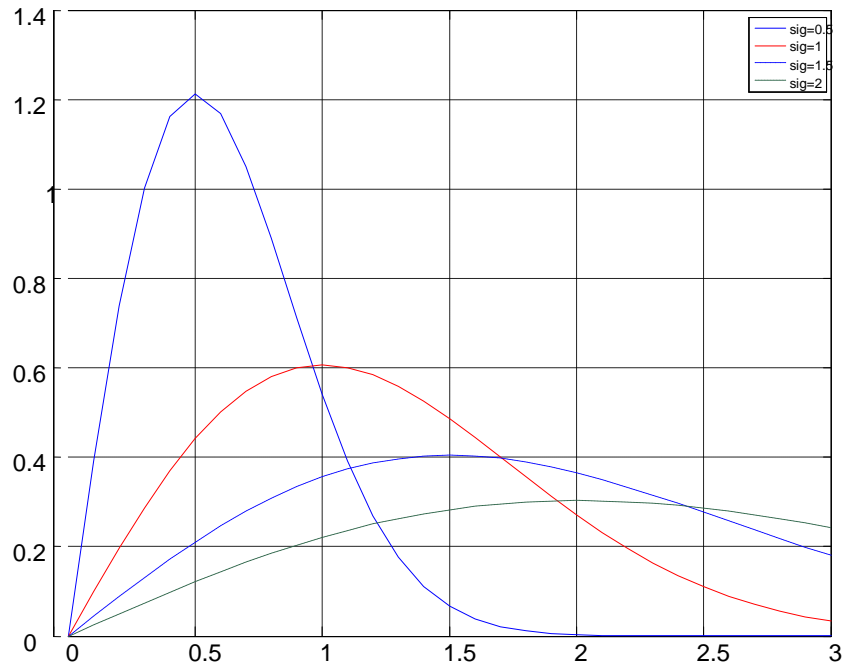


Fig A.2: Rayleigh Distribution for various values of variance.

A.3. The Q Function

In order to facilitate analysis of the probability of error of a communication system a commonly used function can be applied which is called the Q function [2]. Q function is the tail probability of the standard normal distribution. In other words, $Q(x)$ is the probability that a standard normal random variable will obtain a value greater than x . The mathematical formula is

$$Q(x) = \frac{1}{\sqrt{2\pi}} \int_x^{\infty} e^{-\frac{t^2}{2}} dt. \quad (A.3)$$

Figure A.3 depicts the Q function. It can be seen that is a monotonically decreasing function and that $Q(x) + Q(-x) = 1$.

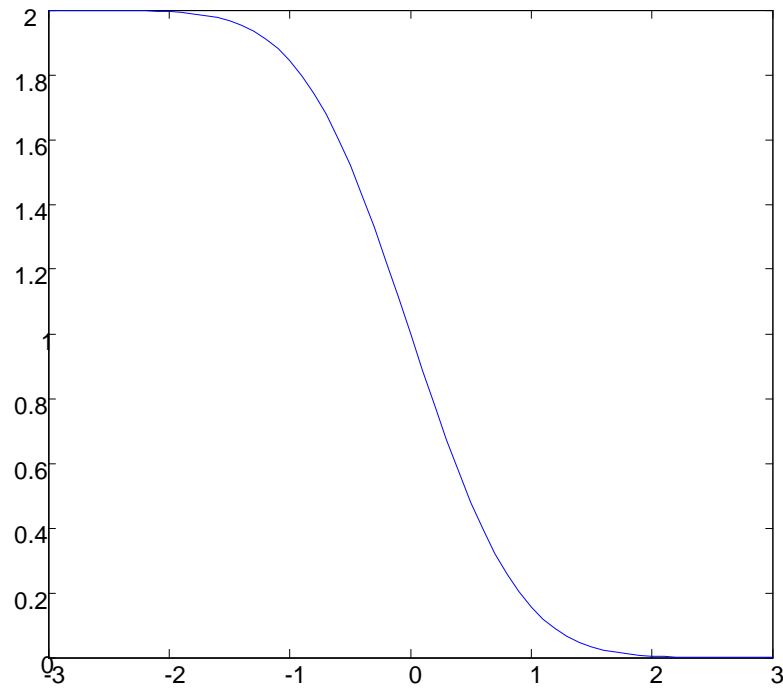


Fig A.3: The Q function

A.4 Bit Error Rate Analysis

A.4.1 Bit Error Rate Analysis for BPSK modulation in AWGN

The Gaussian pdf is defined as (see A.1):

$$f_x(x) = \frac{1}{\sqrt{2\pi}\sigma_x} e^{-\frac{(x-\mu_x)^2}{2\sigma_x^2}}. \quad (\text{A.4})$$

We assume that $\mu_x=0$ and $\sigma_x^2=\frac{N_0}{2}$. Moreover, in *BPSK* there are two different symbols (1 and -1). The received signal is $y=s_1+n$ or $y=s_0+n$ with the index 1 or 0 denoting the bit 1 or 0 that is mapped with the respective symbol [64b]. The conditional probability for the two cases is:

$$p(y|s_0)=\frac{1}{\sqrt{\pi N_0}} e^{-\frac{(y+\sqrt{E_b})^2}{N_0}} \quad (A.5)$$

$$p(y|s_1)=\frac{1}{\sqrt{\pi N_0}} e^{-\frac{(y-\sqrt{E_b})^2}{N_0}} \quad (A.6),$$

where $N_0=2\sigma_x^2$ and E_b is the Energy of the bit.

The following picture (see Fig. A.4) depicts the BPSK symbols, the conditional probability along with the transmission error (blue $p(e/-1)$ and green $p(e/1)$ shaded areas respectively).

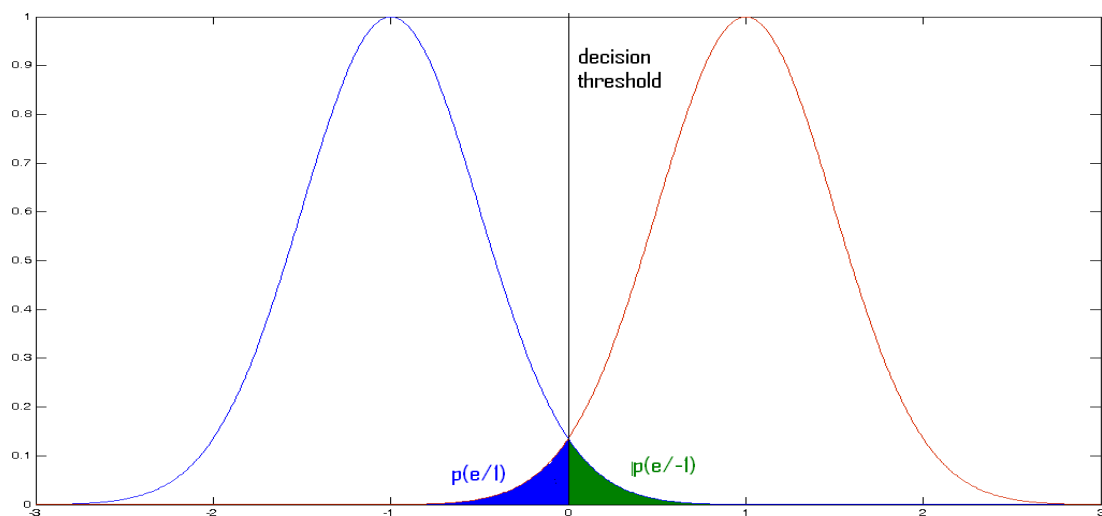


Fig. A.4: BPSK symbols and conditional probability in the existence of
AWGN

For decoding, a decision rule with threshold as 0 might be optimal. Hence, when the received signal is negative it can be assumed that s_0 is sent and when the received signal is positive then s_1 is sent. According to this decoding technique the probability of error given s_1 is defined as:

$$p(e | s_1) = \frac{1}{\sqrt{\pi N_0}} \int_{-\infty}^0 e^{-\frac{(y - \sqrt{E_b})^2}{N_0}} dy \quad (A.7),$$

This is depicted as the blue coloured area of the above graph (see Fig. A.4). After some math manipulations the final equation is

$$p(e | s_1) = \frac{1}{2} \operatorname{erfc}\left(\sqrt{\frac{E_b}{N_0}}\right). \quad (A.8)$$

Due to the symmetry of the system the error probability given s_0 leads to the same result

$$p(e | s_0) = \frac{1}{2} \operatorname{erfc}\left(\sqrt{\frac{E_b}{N_0}}\right). \quad (A.9)$$

Therefore assuming that symbols are equally probable, then

$$P_b = \frac{1}{2} \operatorname{erfc}\left(\sqrt{\frac{E_b}{N_0}}\right). \quad (A.10)$$

A.4.2 Bit Error Rate Analysis for BPSK modulation in Rayleigh

In the presence of channel \mathbf{h} , the effective Bit Energy to Noise Ratio is

$$\frac{|\mathbf{h}|^2 E_b}{N_0}. \quad (\text{A.11})$$

The BER for a given value of \mathbf{h} is

$$P_{b|h} = \frac{1}{2} \text{erfc}\left(\sqrt{\frac{|\mathbf{h}|^2 E_b}{N_0}}\right) = \frac{1}{2} \text{erfc}(\sqrt{\gamma}) \quad (\text{A.12})$$

where $\gamma = \frac{|\mathbf{h}|^2 E_b}{N_0}.$

The resulting BER in a communications system in the presence of channel \mathbf{h} , for any random values of $|\mathbf{h}|^2$, must be calculated evaluating the conditional probability density function over the probability density function of γ [60]. Thus, it can be expressed as:

$$P_b = \int_0^{\infty} \frac{1}{2} \text{erfc}(\sqrt{\gamma}) p(\gamma) d\gamma \quad (\text{A.13}),$$

where $p(\gamma) = \frac{1}{\gamma} e^{-\frac{\gamma}{\bar{\gamma}}}, \gamma \geq 0$ and $\bar{\gamma} = \frac{E_b}{N_0}.$

A.4.3 Monte Carlo Simulation of Communication Systems

Monte Carlo simulation [92] is a computerised mathematical technique that allows people to account for risk in quantitative analysis and decision making. The technique is used by professionals in such widely disparate fields as finance, project management, energy, manufacturing, engineering, research and development, insurance, oil & gas, transportation, and the environment.

Monte Carlo simulation furnishes the decision-maker with a range of possible outcomes and the probabilities they will occur for any choice of action. It shows the extreme possibilities—the outcomes of going for broke and for the most conservative decision—along with all possible consequences for middle-of-the-road decisions.

The technique was first used by scientists working on the atom bomb; it was named for Monte Carlo, the Monaco resort town renowned for its casinos. Since its introduction in World War II, Monte Carlo simulation has been used to model a variety of physical and conceptual systems.

Monte Carlo simulations require very little mathematical analysis and can be applied to any communication system for which the signal processing algorithm required to represent each functional block in the block diagram of the system is known. Monte Carlo is therefore a very general tool but is applied at the expense of very long simulation run times since a basic tradeoff exists between simulation accuracy and the time required to execute the simulation.

The Monte Carlo technique applied to the estimation of BER of a digital communication system, is implemented by passing N data symbols through a simulation model of the system and counting the number of errors that occur. Assuming that passing N symbols through the simulation model results in N_e errors, the estimate of the BER is

$$\hat{P}_e = \frac{N_e}{N} \quad (\text{A.14})$$

where \hat{P}_e is a random variable and accurate estimation of the BER is required that the estimator \hat{P}_e is unbiased and have small variance. Small variance requires that N be large and this in turn results in long computer run times.

Therefore, the main problem with Monte Carlo simulation is the large sample sizes required for estimating low error probabilities. Estimation of the error probability of the order of P_e , with a normalised estimation error less than $\frac{1}{3}$, requires a Monte Carlo simulation with a sample size of the order of $\frac{10}{P_e}$. A normalised estimation error of $\frac{1}{3}$ corresponds to a 95 percent confidence interval of $\left[\frac{1}{3}P_e, 1\frac{2}{3}P_e \right]$. With a typical error probability of, say, 10^{-6} , Monte Carlo requires 10^7 samples per simulation run, which is impractical.